To

DEPARTMENT OF ENERGY

WAVE ENERGY STEERING COMMITTEE

FINAL REPORT

ON

SUBMERGED CYLINDER

WAVE ENERGY DEVICE

Submitted by

Dr. T.L. Shaw, University of Bristol
Dr. D.V. Evans, University of Bristol
Sir Robert McAlpine & Sons Ltd.

OCTOBER 1979

C O N T E N T S

EXECUTIVE SUMMARY

A first overall assessment of the submerged cylinder device has been prepared, from which at outline design for the principal components has been produced. A budget estimate for this design has been made, including allowances for annual operation and maintenance charges.

The efficiency characteristics of the device have been determined from selected tank tests. With these efficiencies, the energy captured by each cylinder of an array has been estimated. Allowances have been made for the probable energy losses in each component through to the National network at Perth.

On the basis of the preliminary specification for the device agreed in June 1979, at the end of Stage 1 of this Contract, the price of electricity delivered to the network is estimated to be 11.4 p/kWh. This assumes a 5% discount rate and a 20 year operating life.

A number of improvements to the reference design are already clear. Principally its tuned frequency should be increased so that the efficiency characteristics match the wave spectrum more closely. This single improvement in gross output appears sufficient to reduce the unit cost to about 8.5 p/kWh because of the significance of annual maintenance charges on the net annual revenue from sales of electricity.

There is considerable scope to improve the design. Other power takeoff and energy transfer techniques deserve attention, and there is scope to rationalise the mooring and foundation arrangements. Because of the nature of its working environment, the same philosophy of using proven components or reasonable derivatives therefrom should be retained.

The stable behaviour of the device in all sea conditions studied, and its high efficiency in the more persistent waves, confirm that this further step towards a comprehensive design of the basically simple, efficient and robust system is justified.

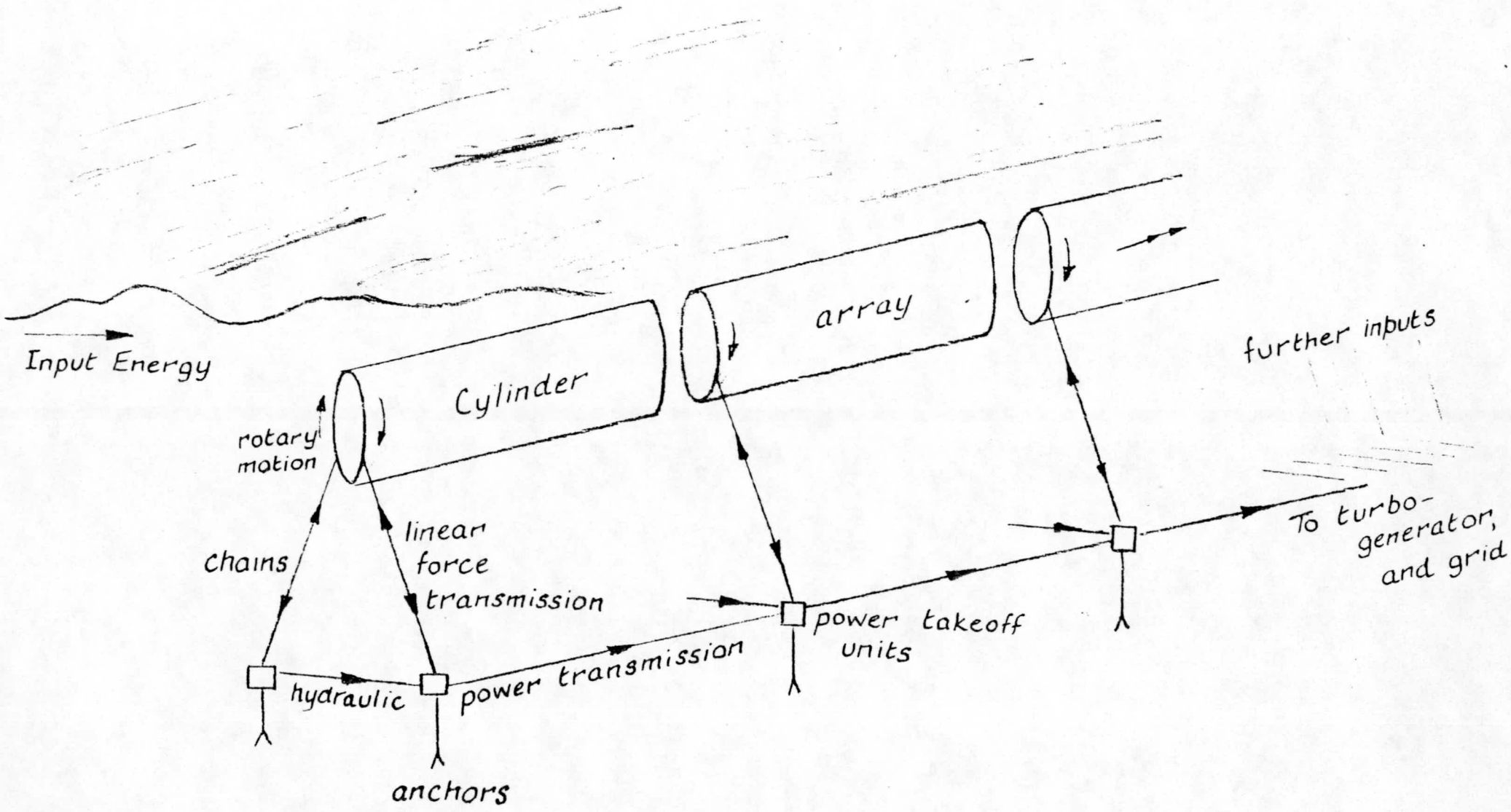
Input Energy
Cylinder
array
further inputs
rotary motion
chains
linear force transmission
To turbo-generator, and grid
power takeoff units
hydraulic
power transmission
anchors

of devices. The turbine would be mounted on a platform connected to shore by high voltage a.c. (or d.c.) lines. In view of the necessarily device specific nature of the power takeoff system, to suit the oscillatory motion of the rodes, and the more 'generic' nature of the landward and onshore transmission, it was decided that our studies should, for the present at least, terminate with the turbine, though costings would include the transmission estimates of others through to Perth.

The details of pumps given in Section 5 are therefore associated with the pipelines, turbine and platform foreseen as necessary for a nominal 200 MW string of cylinders. No attempt has yet been made to optimise the balance between the length of sea over which the devices are installed, the associated total length of pipework needed to minimise friction losses without an excessive number of pipes, the number of devices (sea length) connected to each turbine, and the number of cables for interconnection either at sea or ashore. These and other topics appear among Recommendations for the next phase of Study of the cylinder device listed in Section 8.

The important questions of costs, benefits and energy values are considered in two parts. With the information now available for the device, first cost estimates have been prepared. These are given in Section 7.2, for various possible cylinder and anchorage systems. Annual maintenance charges including the replacement of individual items at prescribed intervals are also quoted. These are compared with the estimated energy delivered by the devices and their transmission system to Perth over a lifetime taken here to be 20 years. The efficiency data determined from the Edinburgh tests (Section 2.2) have therefore been interpreted alongside the annual wave height/period scatter diagrams from the S. Uist offshore recorder, together with the anticipated efficiency for each element of the resource (Section 7.3). This information gives unit costs when the benefit is discounted back to the start of construction. Alternatively the percentage return on capital or the cost per kW of installed capacity may be quoted (Section 7.4).

For the real value of the resource to be judged, however, it has to be seen within the electrical system likely to exist during its lifetime. There are many difficulties to doing this, not least being that the timescale to the full installation of a wave power station is uncertain, as is the rate of build-up of the nuclear component. These will determine how readily wave energy may be integrated, hence its average unit value to the system. The parameters involved are considered in the Appendix to this Report.

It must be stressed that the objective of this Study has been to develop a feasible design for the cylinder and its power takeoff system but not an optimised design. This has been achieved. It is apparent that there is plenty of scope to improve the design. This is seen as work for a further stage of the Study.

The structural and mechanical engineering of the design has been deliberately kept within the limits of known technology, and established methods of construction have been used in the cost estimate. As the design has only been developed in outline the rates used in the preparation of the budget estimate are conservative and take account of current conditions and rates of pay within the industry. No allowances have been made for inflation.

SECTION 2

HYDRODYNAMIC PERFORMANCE OF SUBMERGED CYLINDER DEVICE

2.1 Behaviour of Cylinder in Waves

Like any floating, movable object, the circular cylinder wave energy device responds to the instantaneous (but changing) distribution of pressures about its outer profile. Because it is submerged, this distribution extends over its whole surface. In regular plane waves in deep water, the particle motion in the absence of the cylinder would be close to circular. This orbital amplitude decays exponentially with depth to only about 4% of that at the surface when the depth is equal to half a wavelength.

If a long prismatic cylinder, axis horizontal and parallel to the wave crests, is fully submerged within this rotating velocity field, it would, if of small diameter, neutrally buoyant and undamped, be moved as if part of the continuum water body. As the ratio of its diameter to the wavelength grows, the phase of its motion will increasingly differ from that of the wave. Also its orbital motion will be some amalgam of :

1. the integrated effect of the decaying wave-induced water motion over the volume displaced. For example, if the axis of the cylinder is at a depth equal to one-tenth of the wavelength and its diameter is equal to its depth, its orbit on this consideration alone would be at least 53% of wave amplitude and perhaps as much as 60%;
2. the effect of the rigid form of the cylinder on local water particle motions;
3. any external restraints applied to limit the orbit of the cylinder and the damping applied to its motion by the power takeoff system at the sea bed (Section 5).

Results from narrow tank tests at Bristol University for the interaction between wave height, cylinder submergence, damping and cylinder orbit are given here and in Section 2.3.

For full energy absorption the sum total of the component elements of wave motion and cylinder response must be such that the particle motion one wavelength downstream of the cylinder is destroyed. Any residual

motion is a measure of inefficiency according to the product of the square of orbital diameter and oscillatory period.

The converse of the above process is the classic mechanism whereby waves are generated when a submerged circular cylinder, axis horizontal, is moved in a circular orbit without rotating (Ref.1). For small cylinders the wave phase leads that of the cylinder by about 20°, but the angle is probably greater in the non-linear case of large cylinders.

It follows that if a wave train of the same amplitude and period approaches the cylinder in the same direction as the generated waves, but so phased as to cancel the generated motion, the cylinder will effectively absorb the incident train, leaving calm water 'behind' it. The phase relationship between incident waves and cylinder is then apparently different from that for the generating process considered previously. However, a cylinder doing work (generating) and one being driven (absorbing) will not necessarily be simply equal-and-opposite. This depends upon the 'damping' within each system, in the former case due to the mechanism by which energy is passed from cylinder to water, and in the latter due to the mechanical damping of the power takeoff arrangements.

To analyse and design the cylinder and its moorings and power takeoff to withstand the pressures and fatigue forces due to the most persistent waves, that is in all but breaking waves, it should be sufficient to base calculations on linear diffraction theory, or a variant such as Stokes 3rd Order, together with an expression such as Morison's Equation to convert oscillatory particle velocities into forces. To do this accurately requires that :

1. The velocity field local to the cylinder can be approximated;
2. The orbital motion of the cylinder is known;
3. The phase of cylinder motion relative to wave motion is known.

At the present stage it has to be assumed that the pressure field over the cylinder at any instant is due to the resultant of the particle accelerations that would, in its absence, occur at its centre together with its own motion, i.e., the net effect of the above three factors. Such calculations have now been made (Section 3.2) on the basis of relative cylinder motions and phases determined from two-dimensional

experiments in regular waves of varying steepness. The damping applied to the cylinder was varied from a minimum (not zero) to a maximum (not infinite). This range of damping was sufficient to reduce the ratio of cylinder orbital diameter to particle orbital diameter at the depth of the cylinder's centre from approximately 1.0 to an amount that depended on wave height (Figs. 2.1 a-d and 2.2). At the same time the phase lag of the zenith of the cylinder's orbit behind the crest of the wave increased from about 190° to about 230°. It should be noted that these results apply to a 12m diameter cylinder submerged by 3m below still water level, in waves of height 9m ($H_s \simeq 12.7$m).

The importance of submergence was also studied. The principal by which the device operates (absorption with neither transmission nor generation) suggests that this parameter should not be less than zero (otherwise it would tend to perform like a rather inefficient 'duck'). Resorting again to experiments for guidance over a range of damping factors, it is clear that even with zero submergence there is only a small exposure of the cylinder near to or after the trough of the wave has passed (lag increases with the damping) but before the principal increase in water level up to the crest occurs (Fig. 2.1). This is accompanied by a much less circular orbit than when the cylinder is more deeply submerged in waves of the same height and period. Furthermore, the motion is increasingly deformed in higher waves, though in up to 10m waves (the limit of testing so far) the fact that the orbit is then relatively flat and somewhat erratic does not imply that energy levels up to the limits chosen for the power takeoff device will not be transmitted to the sea bed via the 45° rodes (Section 5.1), though on grounds of maximising the capture efficiency it may be worth considering a more shallow rode angle in association with a power takeoff with higher rating (Section 8).

Zero submergence could therefore be chosen to coincide with lowest astronomical spring tide level.

2.2 Experimental Results from 'Edinburgh' Wide Tank

2.2a Introduction

A first assessment of the model studies carried out at Edinburgh in May 1979 was included in our Interim Report (June 1979). A full review is given here.

Fig. 2·1

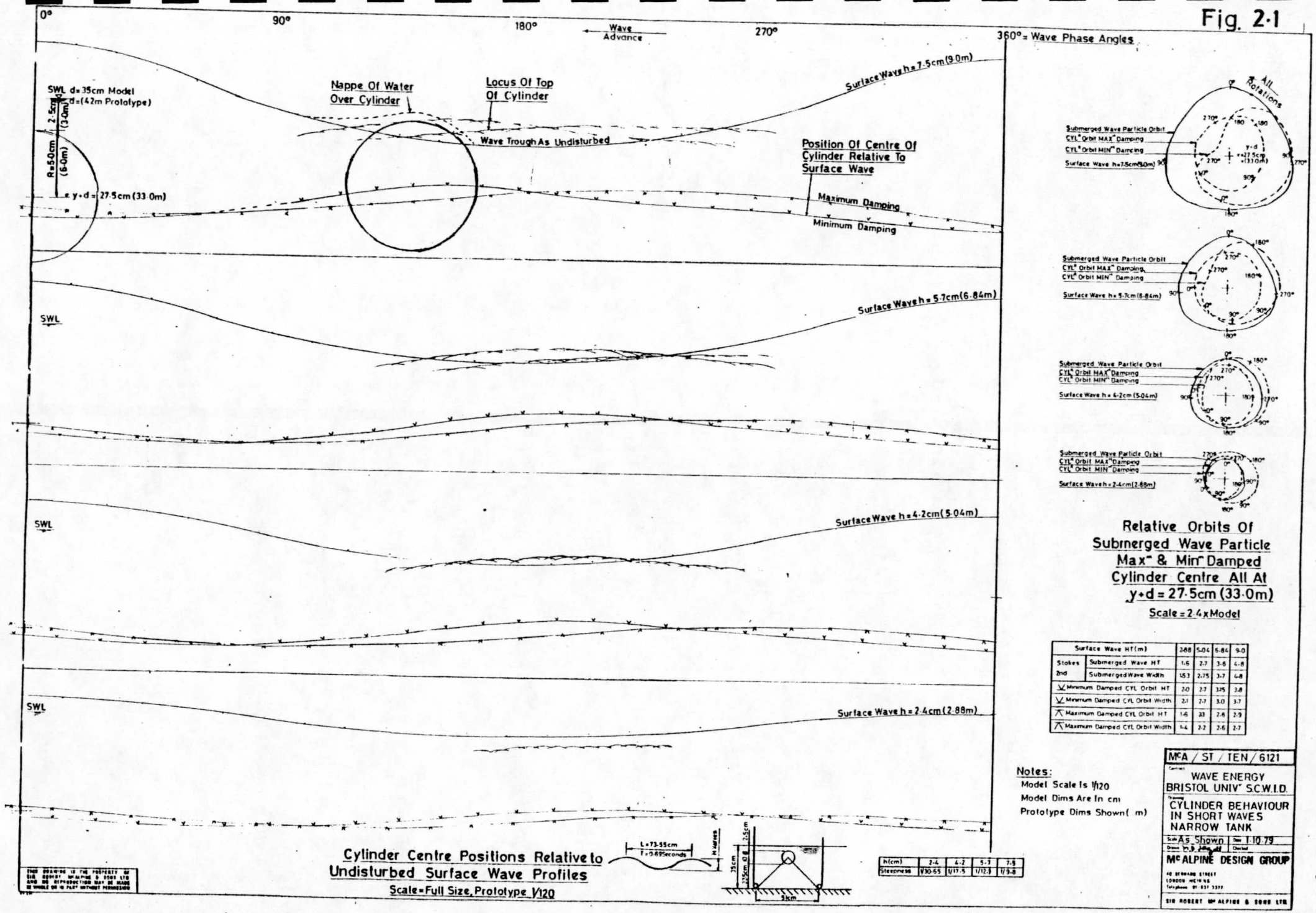

Relative Orbits Of Submerged Wave Particle Max^m & Min^m Damped Cylinder Centre All At y+d = 27·5cm (33·0m)

Scale = 2·4 x Model

Surface Wave HT (m)		2·88	5·04	6·84	9·0
Stokes 2nd	Submerged Wave HT	1·6	2·7	3·6	4·8
	Submerged Wave Width	1·53	2·75	3·7	4·8
⌄ Minimum Damped CYL Orbit HT		2·0	2·7	3·45	3·8
⌄ Minimum Damped CYL Orbit Width		2·1	2·7	3·0	3·7
⌃ Maximum Damped CYL Orbit HT		1·6	2·3	2·6	2·9
⌃ Maximum Damped CYL Orbit Width		1·4	2·2	2·6	2·7

Cylinder Centre Positions Relative to Undisturbed Surface Wave Profiles

Scale = Full Size, Prototype 1/120

h (cm)	2·4	4·2	5·7	7·5
Steepness	1/30·65	1/17·5	1/12·3	1/9·8

Notes:
Model Scale Is 1/120
Model Dims Are In cm
Prototype Dims Shown (m)

McA / ST / TEN / 6121

Contract: WAVE ENERGY BRISTOL UNIV° S.C.W.I.D.

Drawing: CYLINDER BEHAVIOUR IN SHORT WAVES NARROW TANK

Scale: As Shown | Date: 1.10.79

Drawn: | Checked:

McALPINE DESIGN GROUP

40 BERNARD STREET LONDON WC1N 1LB Telephone 01 837 3377

SIR ROBERT McALPINE & SONS LTD

THIS DRAWING IS THE PROPERTY OF SIR ROBERT McALPINE & SONS LTD AND NO REPRODUCTION MAY BE MADE IN WHOLE OR IN PART WITHOUT PERMISSION

FIGURE 2·1B

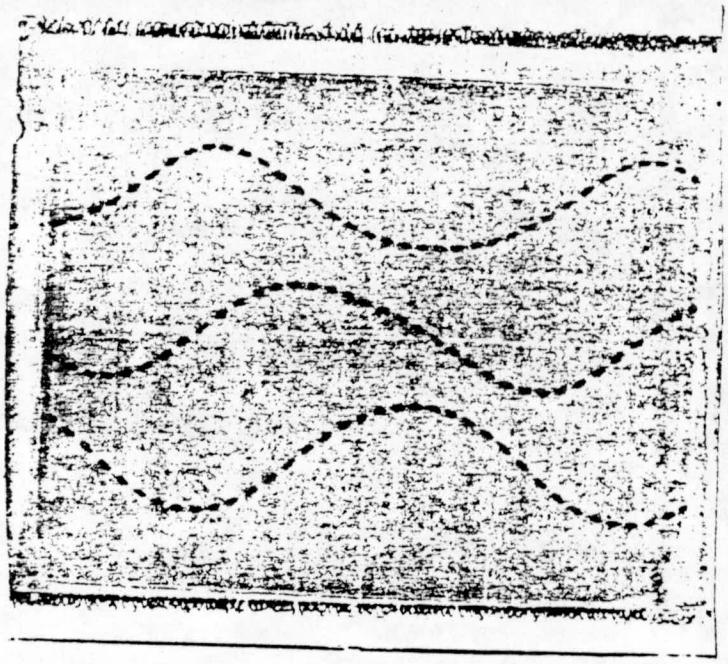

H = 9.0m MAX. DAMPING

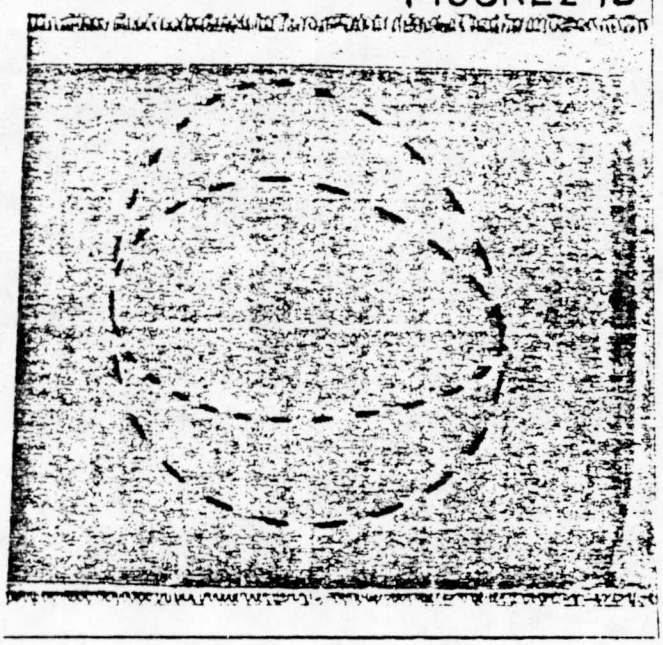

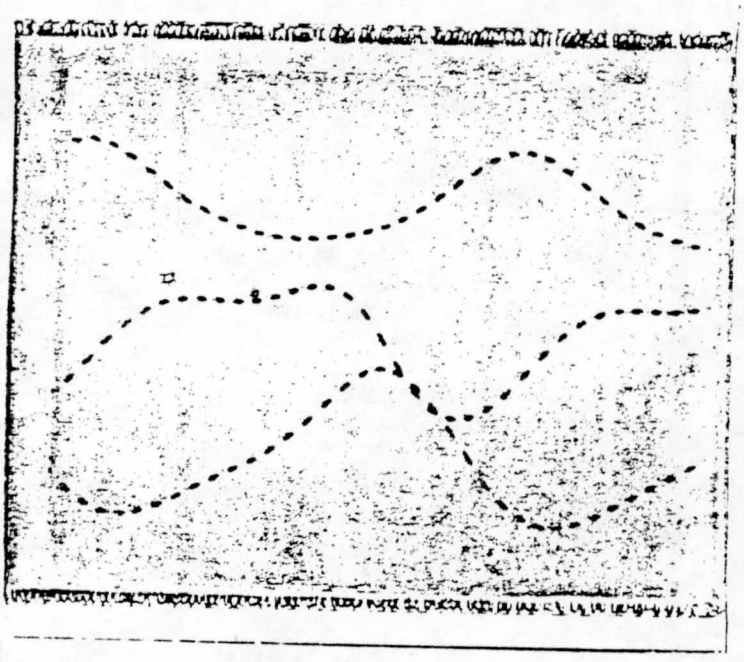

H = 9.0m MIN. DAMPING

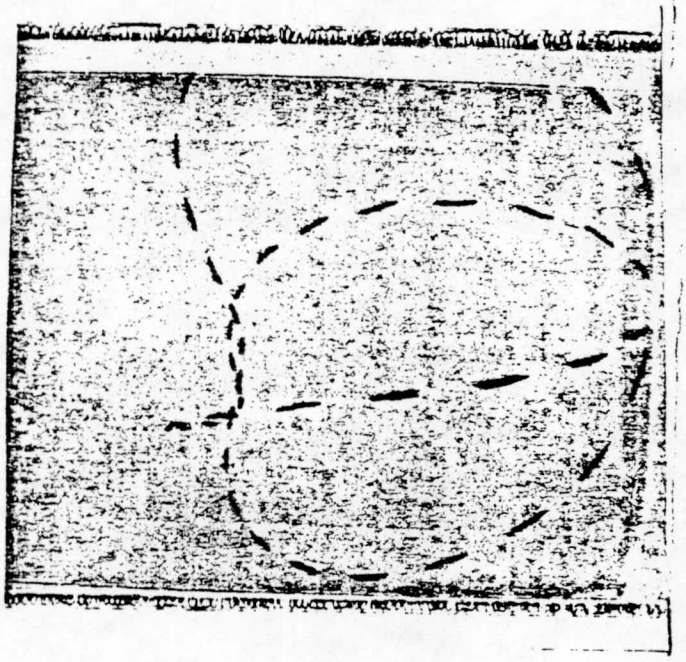

Each of 2 Figures:-

Surface Water Level
Fore Rode Movement
Aft. " "

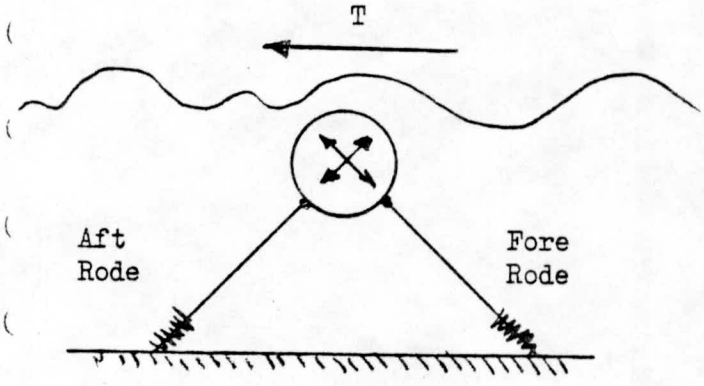

When Rode moves out,
its trace moves up.

Cylinder Orbit and Distorted
Surface Orbit.

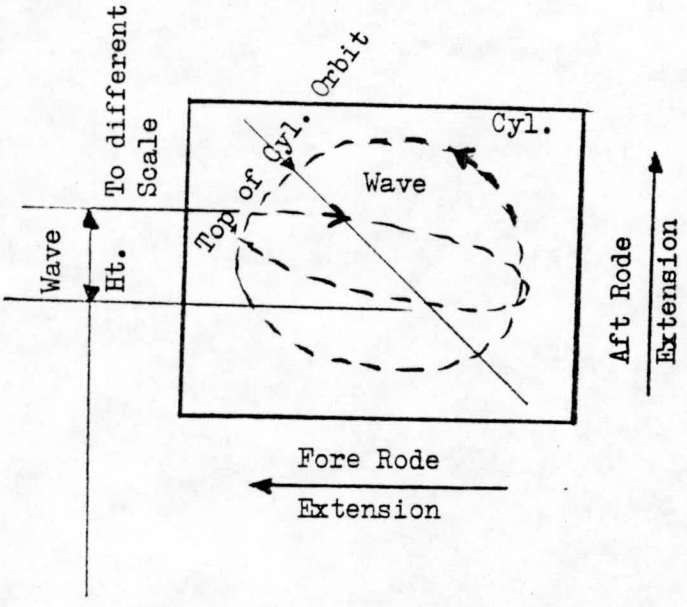

FIGURE 2·1C

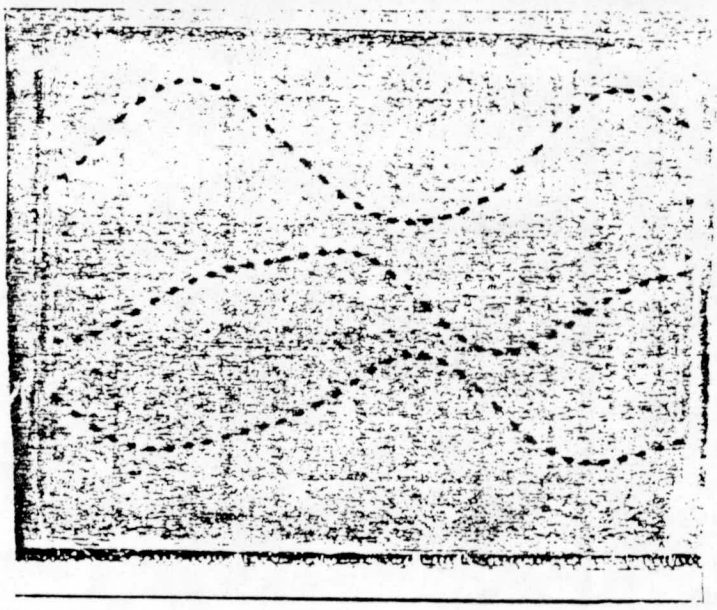

H = 5.04m MIN. DAMPING

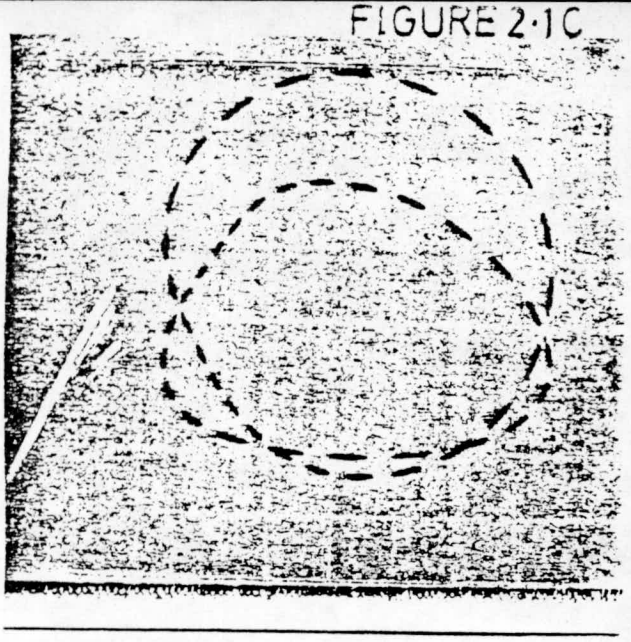

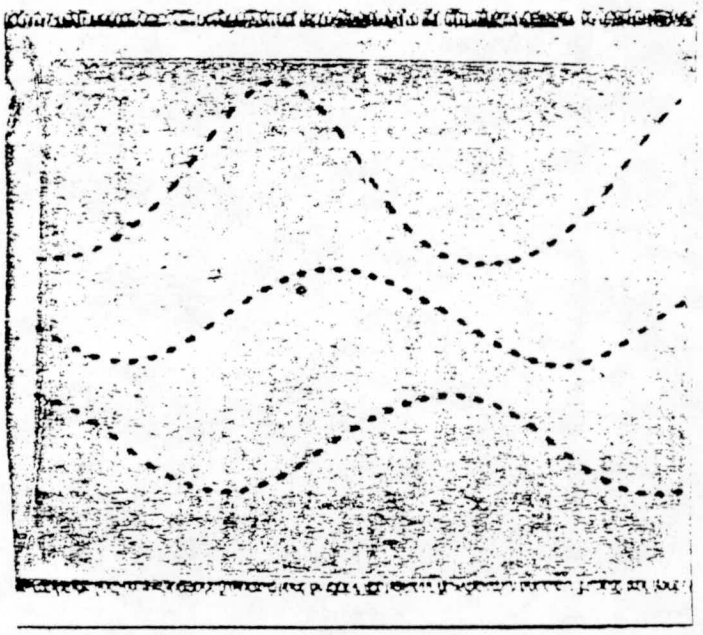

H = 6.84m MAX. DAMPING

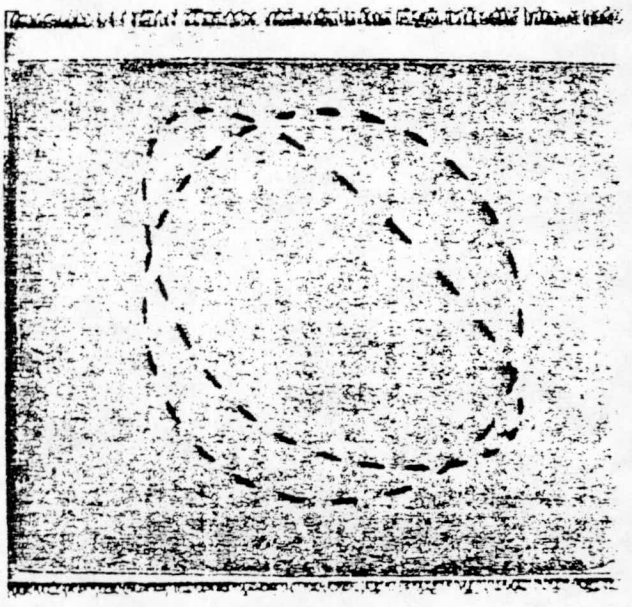

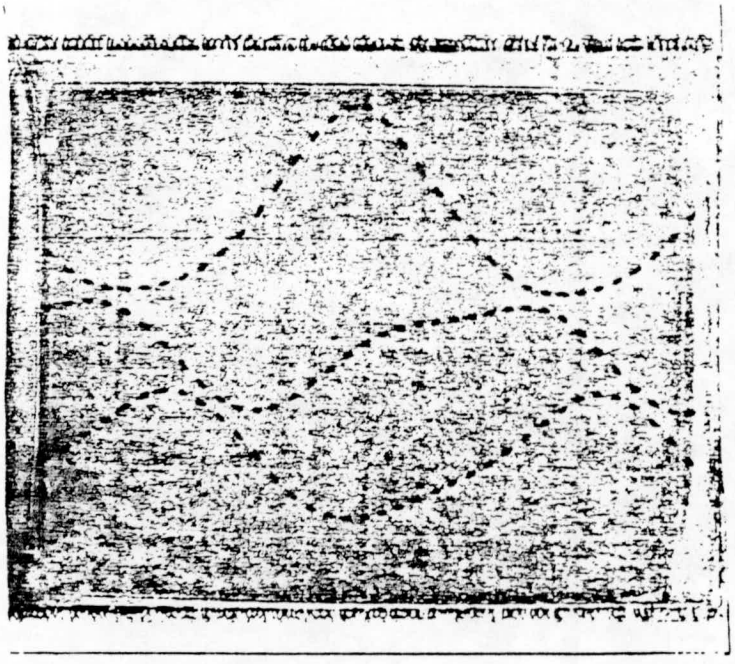

H = 6.84m Min. DAMPING

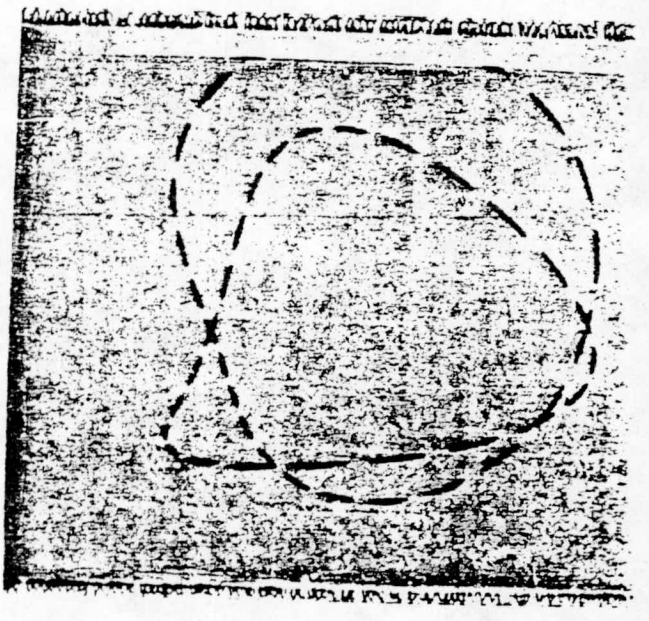

Surface Water Level

Fore Rode Movement

Aft. " "

Cylinder Orbit and
Distorted Surface Orbit.

FIGURE 2·1D

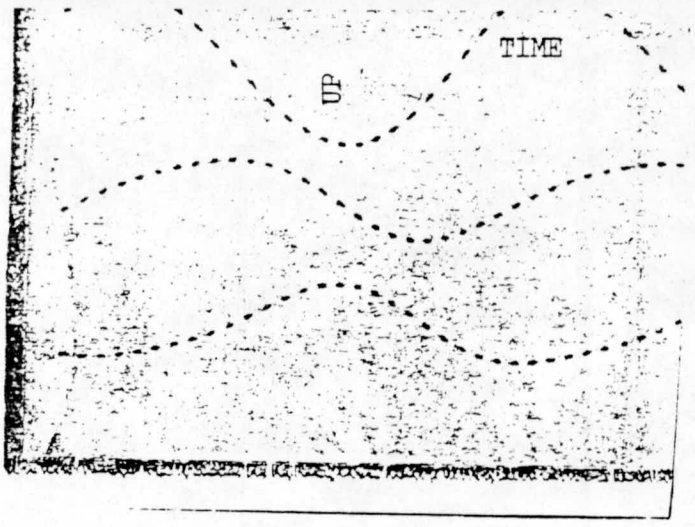

H = 2.88m MIN. DAMPING

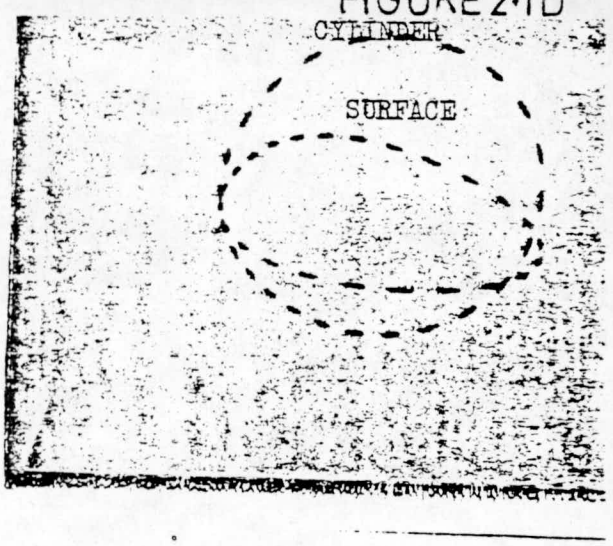

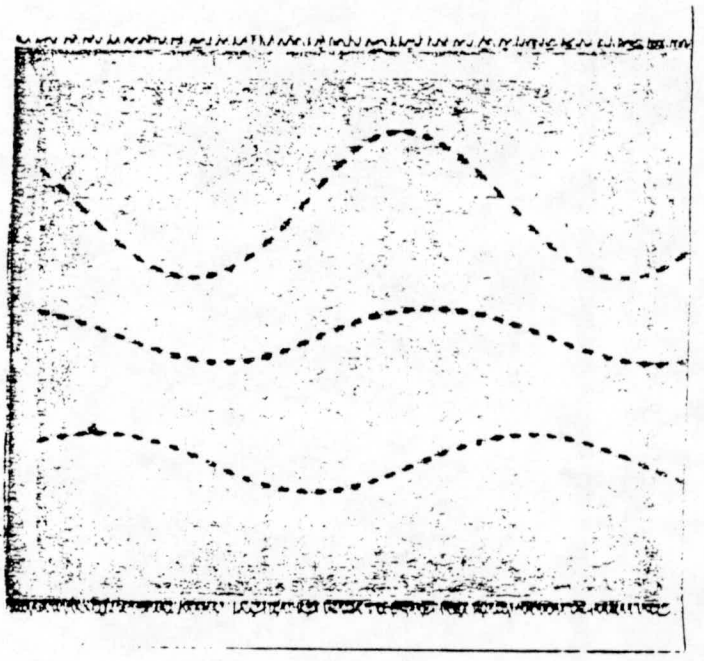

H = 2.88m MAX. DAMPING

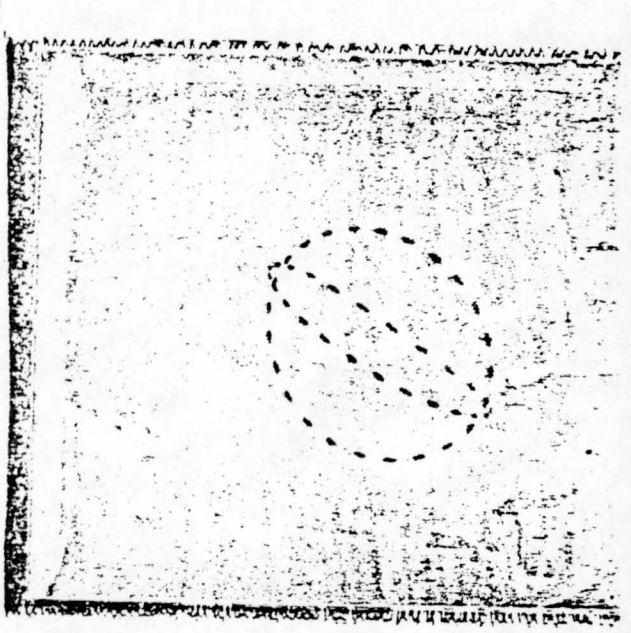

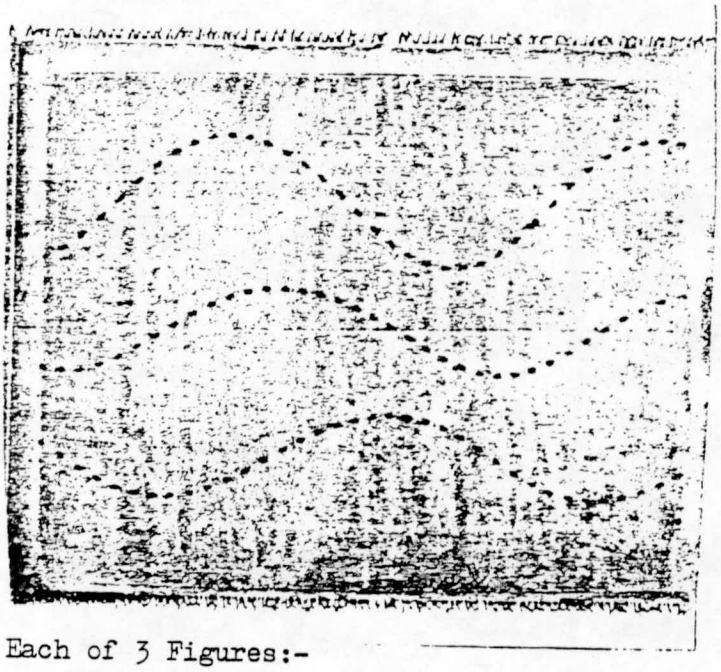

H = 5.04m MAX. DAMPING

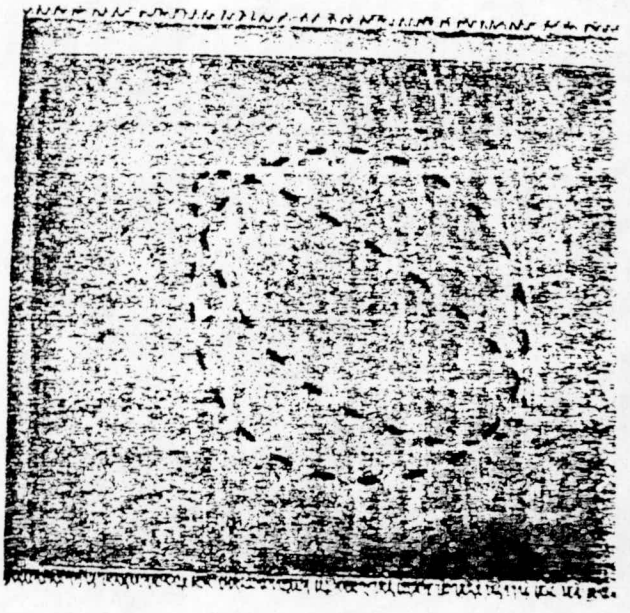

Each of 3 Figures:-

Surface Water Level
Fore Rode Movement
Aft. " "

Cylinder Orbit and
Distorted Surface Orbit

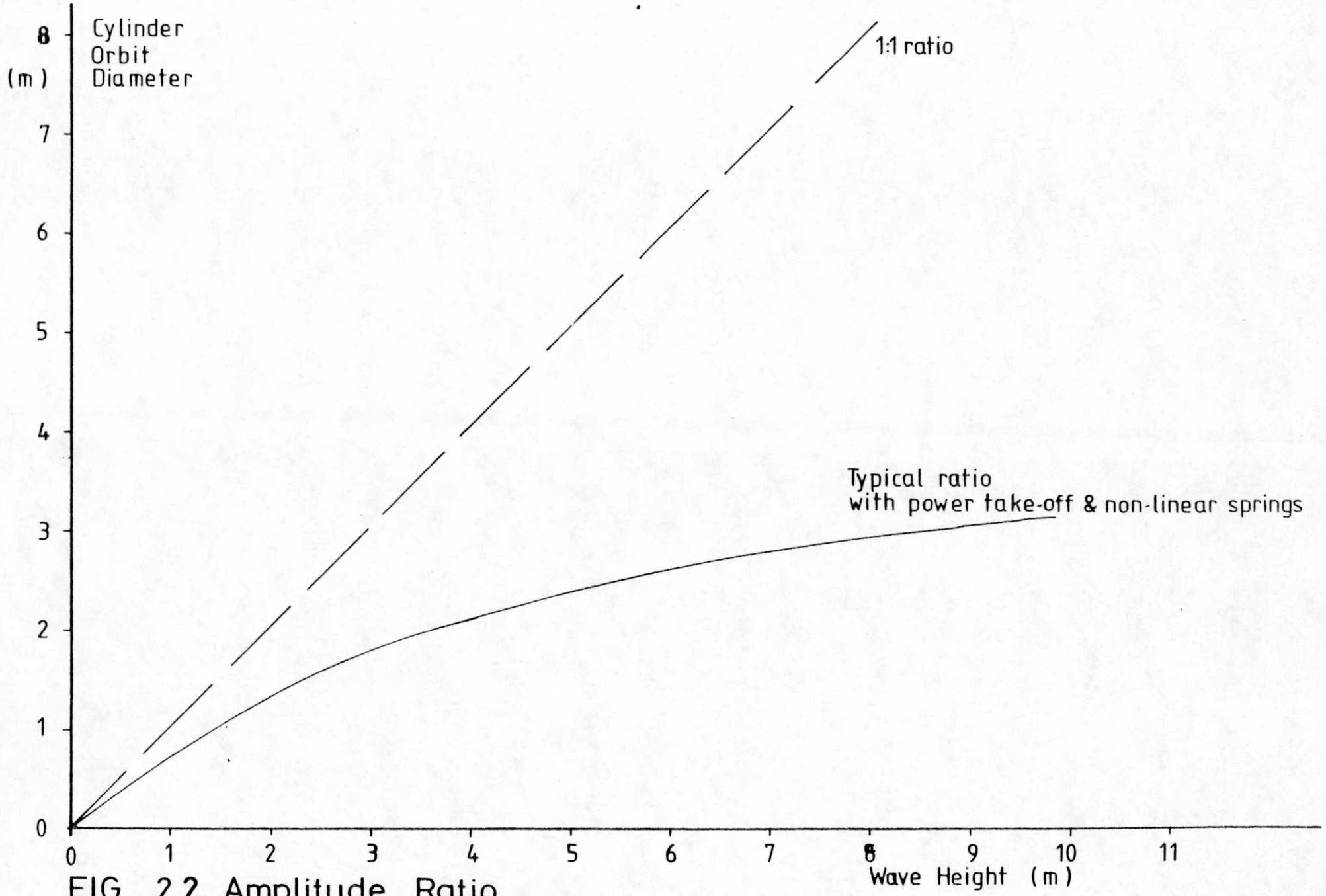

FIG. 2.2 Amplitude Ratio.

These tests (Table 2.1) were chosen to cover a broad spread of conditions sufficient to show the overall performance and stability of the device in more realistic waves than had thereto been possible. The total of 33 experiments included cylinders with aspect ratios (length : diameter) of 2:1, 4:1 and 6:1. The few data taken for the 2:1 cylinder were corrupted in the acquisition phase and cannot therefore be presented.

The 4:1 cylinder generally behaved best so it was chosen for more detailed study. All tests were recorded on film to facilitate subsequent analysis and judgement of overall performance.

2.2b The Rig

Some details of the rig were given in our Stage 1 Report, pp. 19-20. The dimensions of the model are interpreted, by a linear scale factor of 120:1, to represent a prototype cylinder 12m in diameter (the corresponding length should be 48m, but the addition of domed ends for reasons explained in Section 4 gives it a nominal overall length of 50m). However the model water depth then corresponds to about 144m rather than the favoured depth of 42m taken elsewhere through this Report. The principal findings of the laboratory tests will not be altered appreciably by this discrepancy, since the waves of interest lie in the length range 80-200m, i.e., the real effect on them of a water depth of 42m is small (though the actual wave climate at each depth off the S.Uist Islands may in some respects differ appreciably. Actual climates, especially the swell components, were not modelled).

2.2c Performance of Cylinder

The results for power capture in moderate seas (up to incident energy levels of 300 kW/m, e.g., waves with a significant height H_s of nearly 8m and 10 second period - Fig. 2.3) give an overview of cylinder performance. Most of these data apply to tuned conditions, with waves having an energy period of 8-10 seconds. The three points below the 25% efficiency line apply to a fully developed Pierson-Moskowitz (P-M) sea having an energy period of 11.6 secs, i.e., as a storm grows, the efficiency (though not necessarily the actual amount) of power capture drops off as both wave height and energy period increase.

The points which fall in the range of incident energy levels from 40-60 kW/m (say regular waves about 2.5m high with 8 second period, or 2m at 12 seconds - Fig. 2.3) give highest efficiencies, about 100%. Long-crested P-M seas come next, then short-crested P-M seas. The data for 45° regular waves are lower because the effective length of the

TABLE 2.1

EXPERIMENTAL DETAILS

CODE	SEA		Cylinder Used (see below)	Film	Experimental Data
F1	Head Sea Mod.	H=2cm(2.4m), T=0.91s(9.96s)	ABC	***	.**
F2	Head Sea Severe	H=8cm(9.6m), T=0.91s(9.96s)	ABC	***	.**
F3	Oblique Sea Mod.	H=2cm(2.4m), T=0.91s(9.96s)	ABC	***	..*
F4	Oblique Sea Severe	H=8cm(9.6m), T=0.91s(9.96s)	ABC	***	.**
F5	Beam Sea Mod.	H=2cm(2.4m), T=0.91s(9.96s)	ABC	***	...
F6	Beam Sea Severe	H≃7cm(8.4m), T=0.91s(9.96s)	ABC	***	.**
F7	P-M Sea with Mitsuyasu Spread (Short-Crested Mod.)				
		H_{rms}≃0.7cm(0.84m), T_e = 0.75 s(8.2s)	ABC	***	.**
F8	P-M/Mit.(Short-Crested Severe)				
		H_{rms} x 1.5cm(1.8m), T_e = 1.06s(11.6s)	ABC	***	.**
F9	P-M/Mit.1/8 Wave Angle Mult. (Long-Crested Mod.)				
		H_{rms} 0.7cm(0.84m), T_e = 0.75s(8.2s)	ABC	***	.**
F10	P-M/Mit.1/8 Wave Angle Mult. (Long-Crested Severe)				
		H_{rms}=1.5cm(1.8m), T_e=1.06s(11.6s)	ABC	***	.*.
F11	P-M/Mit. Oblique (Short-Crested Severe 45°)				
		H_{rms}=1.5cm(1.8m), T_e=1.06s(11.6s)	ABC	***	.**
R1(a)	Regular Period-Amplitude Sweep	H=1.0-6.0cm(1.2-7.2m)			
-R6(d)	Head Seas	T=1.11-0.62s(12.1-6.8s)	B		*
O1(a)	Regular Period-Amplitude Sweep	H=1.0-6.0cm(1.2-7.2m)			
-O4(d)	Oblique Seas	T=0.91-0.62s(9.96-6.8s)	B		*
PM1A	RM/Mit. Short-Crested Amplitude Sweep				
-PM1C	H_{rms}=0.71-1.23cm(0.85-1.47cm), T_e=0.74s(8.1s)		B		*
PM2A	P-M/Mit.1/4 Long-Crested Amplitude Sweep				
-PM2C	H_{rms}=0.75-1.5cm(0.9-1.8m), T_e=0.74s(8.1s)		B		*
SSS	P-M/Mit. Short-Crested Severe	H_{rms}=2.96cm(3.55m), T_e=0.82s	B		*
FW1	P-M/Mit.with Freak Wave Breaking on Cylinder		B	*	
FW2	T_e=1.06(11.6s) H_{rms}=1.0cm(1.2m) & 2.0cm(2.4m) with Freak Wave at Cylinder				

CYLINDERS USED

CODE	Model Size - Length x Dia.(mm)	Scale Size Length x Dia.(m)	Specific Gravity
A=2:1	200 x 100	24 x 12	0.6
B=4:1	400 x 100	48 x 12	0.6
C=6:1	600 x 100	72 x 12	0.8

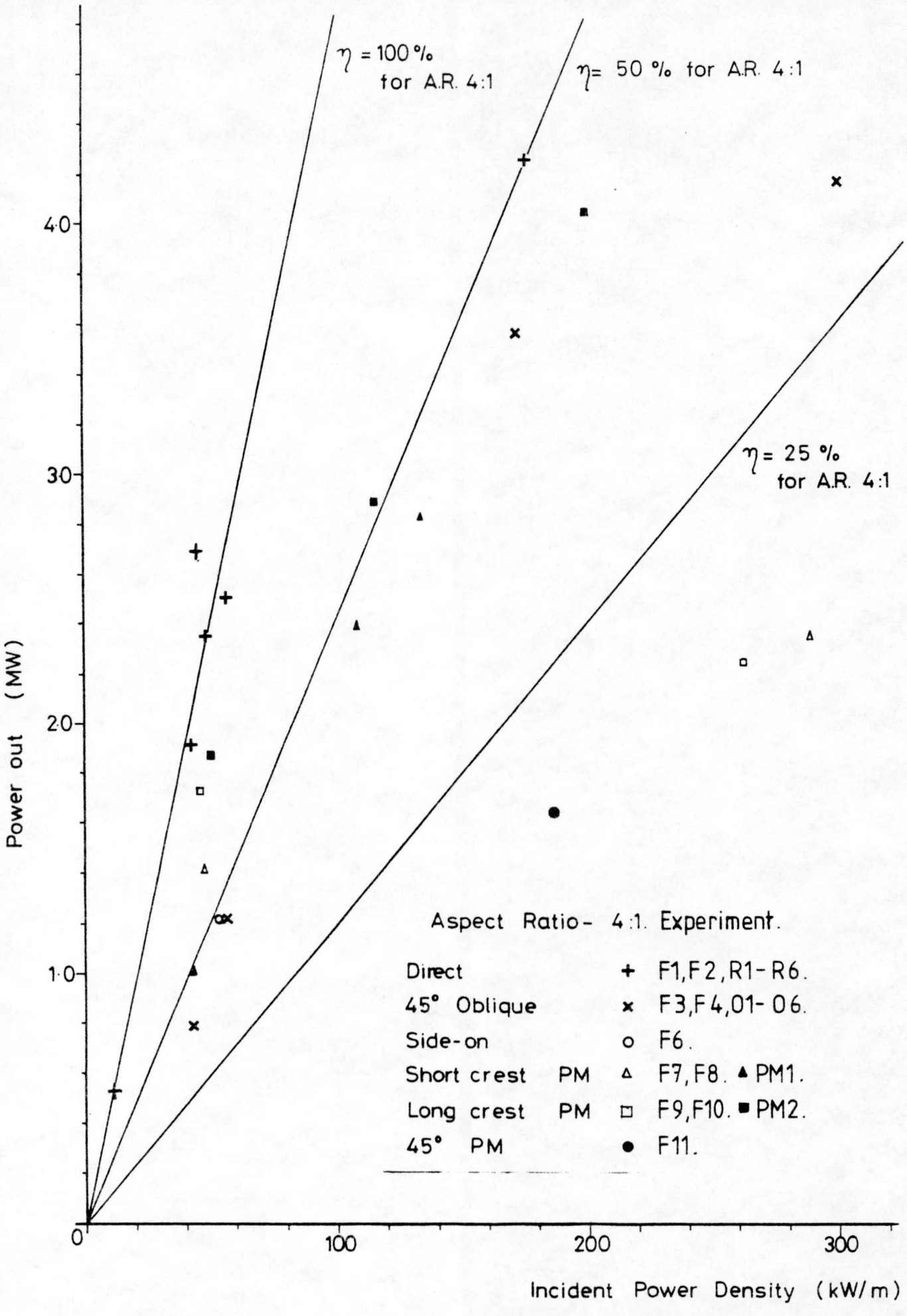

FIG. 2.3. Power Capture in Moderate Seas.

cylinder is then only $1/\sqrt{2}$ of its actual length (but see also Sections 2.2d and 7.3 because this reduction factor is open to some misinterpretation for the case of the cylinder in oblique waves).

Fig.2.4 is an extension of Fig. 2.3 to include severe seas. The upper limit of 0.8 MW/m shown for the x-axis infers, say, short-crested waves 12m high and 11 second period, giving nearly 40 MW over the length of the cylinder. The power captured by the model at this level was equivalent to 8MW, though as shown in Section 5 this depends on the orbital amplitude permitted. The remaining energy passes over the cylinder.

The results for the 6:1 tests are also shown on Fig. 2.4. Although from the short series of tests performed at Edinburgh the 4:1 cylinder appeared best as far as overall stability is concerned, the limited comparison possible from Fig. 2.4 does not fully confirm this. The film has greatly helped interpretation. It is important from many points of view that the optimum aspect ratio is identified; this must await further test data (Section 8).

The detailed efficiency curves for regular, oblique and short-crested seas (Figs. 2.5 - 2.7 resp.) were included in provisional form in the Interim Report. Fig. 2.5 shows the characteristic fall in efficiency with increasing wave height, though as mentioned above the actual power captured nevertheless goes up (Fig. 2.4). The dashed line in Fig. 2.5 is the appropriate theoretical curve for 2-D small amplitude waves. It may be coincidence that it appears to fit the data for 2.4m waves approaching normal to the axis of the cylinder, though the steepness of these waves, at 1:40, is sufficiently small for linear theory to be a not unreasonable approximation to this and to all less steep waves (further interpretations are made in Section 7.3).

The high frequency end of the 2.4m data in Fig. 2.5, also other data not plotted, suggest that the cylinder captures energy from beyond its own length. However, the extent of this cannot yet be specified. Clearly it could be an important feature of the cylinder device, allowing them to be spaced out without incurring a corresponding loss of energy. However, this is not a strong argument in favour of short cylinders (more ends per unit length of sea), nor is it clear how capture efficiency decays with distance beyond the cylinder hence how the energy not captured varies with gap between cylinders. Further tests are needed to clarify this (Section 8).

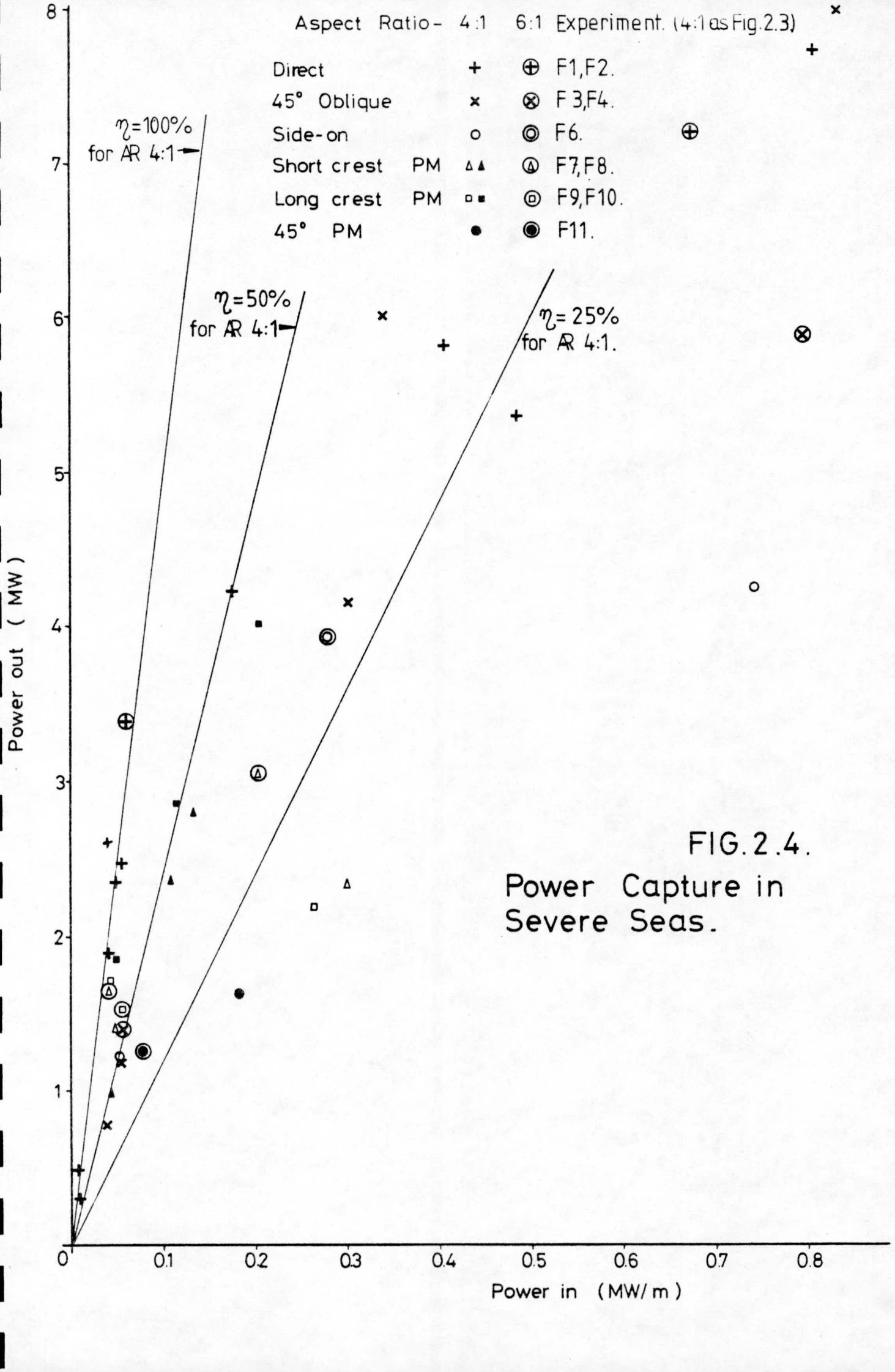

FIG. 2.4.
Power Capture in Severe Seas.

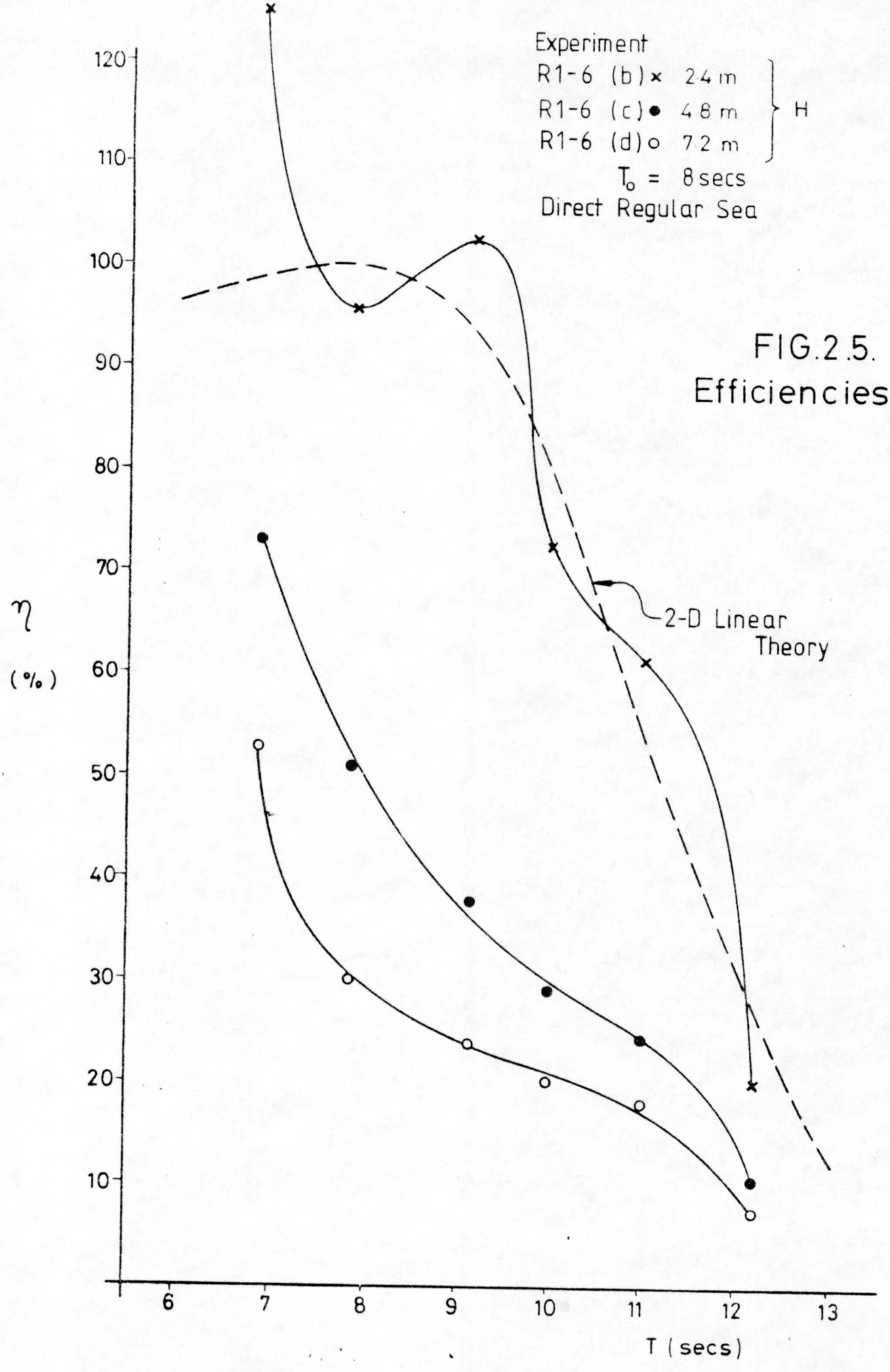

FIG.2.5.
Efficiencies.

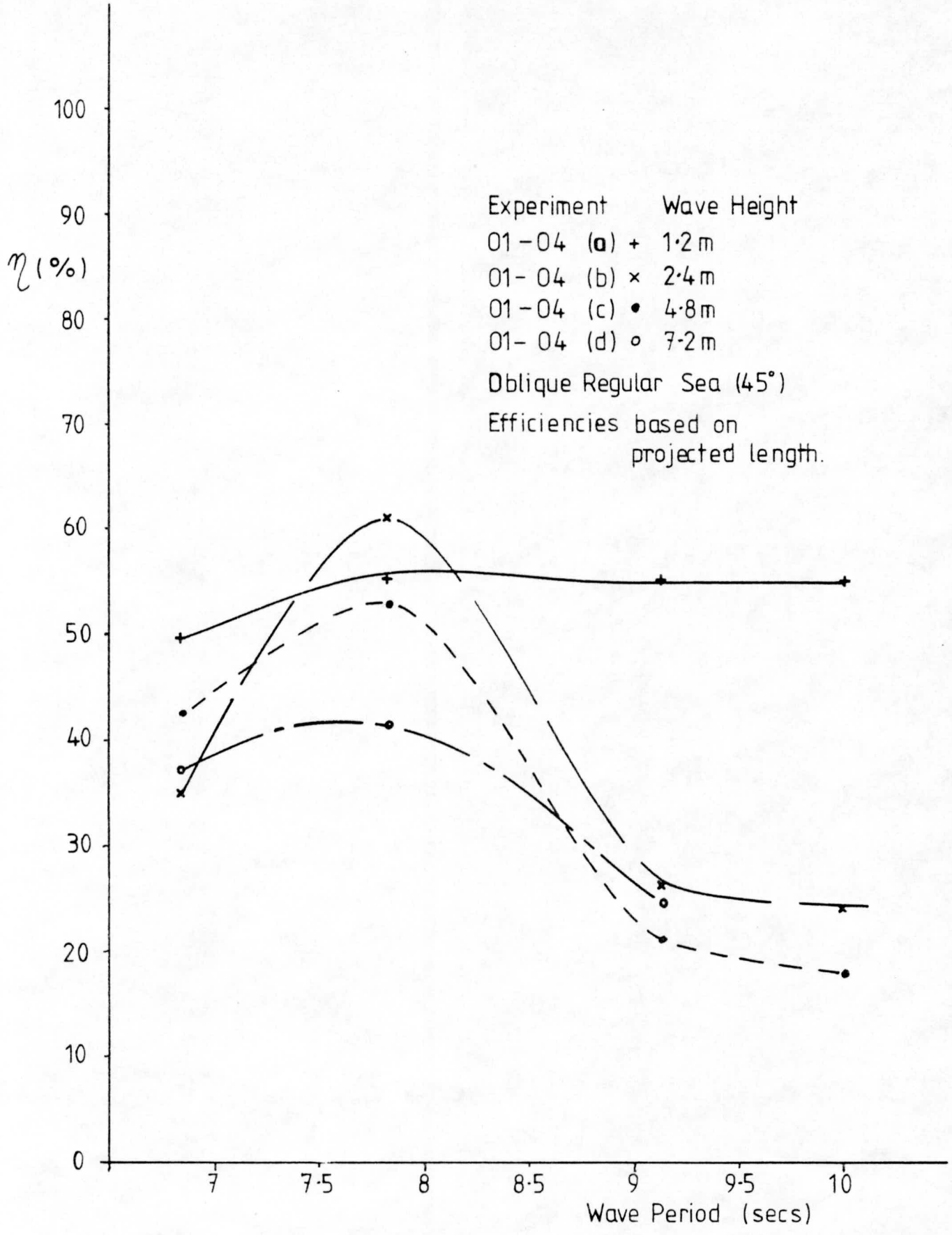

FIG. 2.6. Oblique Sea Efficiencies.

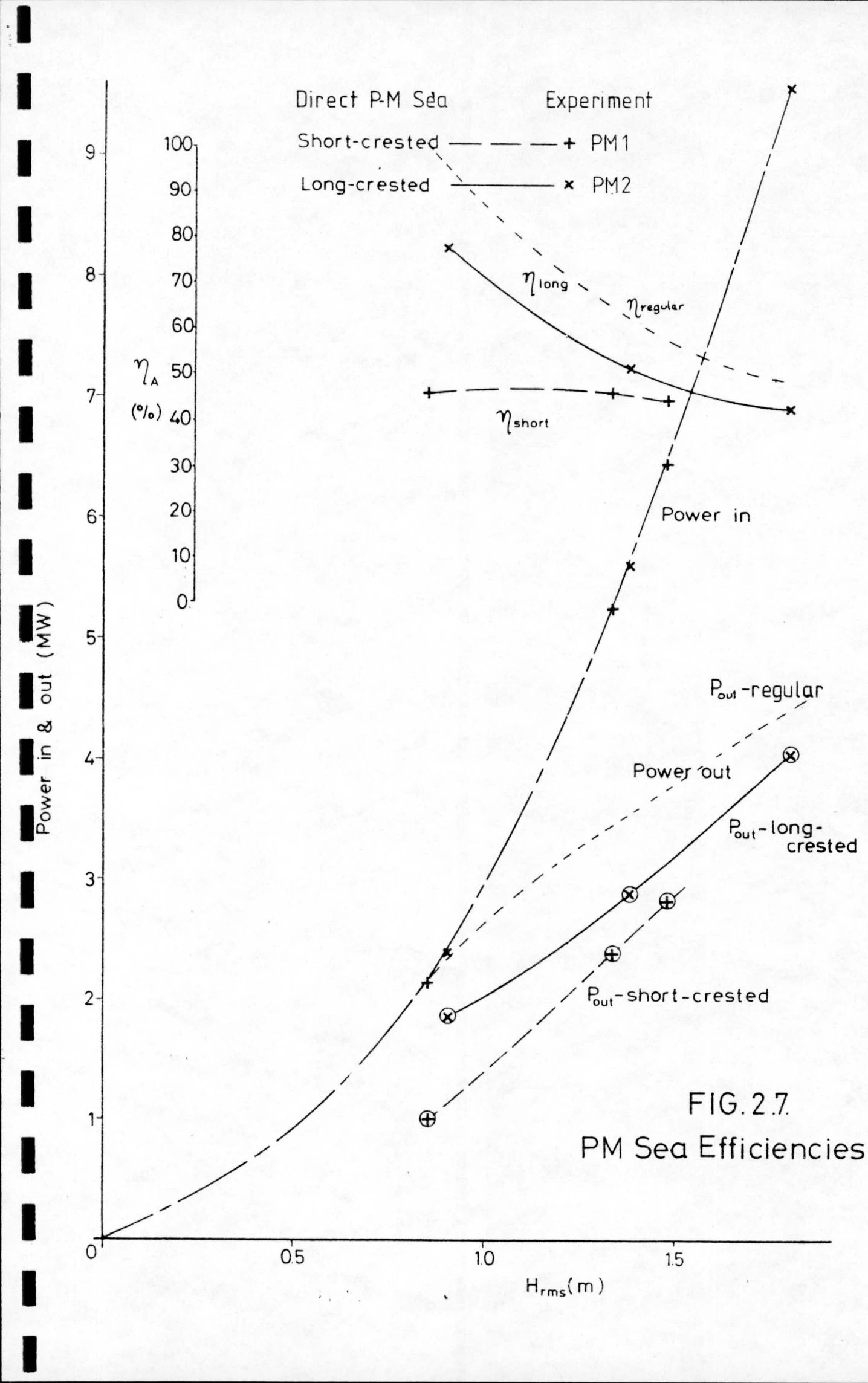

FIG. 2.7.
PM Sea Efficiencies

From Fig. 2.5 it seems reasonable to conclude that the high efficiencies calculated from 2-D theoretical work apply to the 3-D cylinder in waves having incident energy levels of at least 50 kW/m (e.g., up to H_s = 3m, period = 10 seconds, though energy content depends on crest length). Because about 25% of the S. Uist energy spectrum (for 1976/77) lies within this limit, the deviation of experiment from theory shown by Fig. 2.5 for greater wave heights (90% of the S. Uist spectrum lies below the equivalent of H = 4.8m) is perhaps of less immediate concern than how much of the higher energy levels then available should be captured (see also Sections 5 and 7.3).

Fig. 2.6 shows efficiencies based on the projected length of the cylinder in regular waves approaching from 45° to its axis. Peak efficiencies of well over 50% are achieved in small to moderate waves. It is significant that there is much less dependence of efficiency on wave height than for normal waves (Fig. 2.5). For regular waves higher than 5m, more of the incident energy appears to be captured in the oblique configuration, though the data needed to confirm or modify this, and more particularly to assess performance when the incident direction lies between normal and 45° (as it often will be for swell waves - see Section 7.3) has yet to be collected.

Fig. 2.7 shows how, for a P-M sea of constant energy period (T_e = 8 seconds), the efficiency again drops off with increasing wave height. In particular as the incident power rises sharply the power absorbed increases much less quickly. (As before, these results assume that cylinder motion is only restrained by the damping of the power takeoff system : the merits and consequences of incorporating devices to limit this motion above a threshold value are considered in Section 7.3). Also, as expected, the cylinder is more efficient in long-crested than short-crested seas, though less than in regular waves of the same period. From these limited results it is unfortunately not possible to determine how efficiency will change as the energy period of the swell component of incident waves increases. The modelling of representative energy spectra is therefore an urgent task in future laboratory work.

The results presented in Figs. 2.5 - 2.7 imply that, for a nominally 50m long, 12m diameter cylinder, the energy captured in the cylinder could exceed 2 MW when the incident power density is 50 kW/m. With the same energy period this increases to about 4 MW at a sea state yielding 200 kW/m, but to only 2.5 MW if the energy period at this higher density is longer - which it usually will be. Hence the energy captured tends to a self-limiting level. It may therefore be more important to ensure

that the maximum movement of the cylinder does not unduly increase the cost of the power takeoff device rather than the transmitted power levels themselves.

2.2d Mooring Forces

In addition to their function for transmitting the energy absorbed by the cylinder to the power takeoff devices on the sea bed, the rodes also have to secure the cylinder in storm seas. (No detailed considerations of failure probabilities and consequences thereof have yet been made).

Figs. 2.8 and 2.9 show a selection of results for peak-to-peak and r.m.s. rode forces recorded in regular normal waves of varying height and period. The data in Fig. 2.8 for the range of periods 6.8 to 11 seconds have been averaged to give the curve in Fig. 2.10 which also shows other results in similar conditions. (These curves are dependent upon the restoring force provided by the leaf springs used in the 'Edinburgh' rig; Fig. 2.11 shows their non-linear characteristic).

Fig.2.10 also shows the load per corner of the cylinder, including buoyancy, in regular waves up to 9.6m high, for a wave steepness of 1:10. (Section 3.3 describes how this information was extrapolated to 'design' wave conditions, to give a specification for the type and number of rodes needed at each corner of the cylinder). In this respect it was found by calculation that the 'design' wave force had a value less than might be estimated by extending the curves in Fig. 2.10 to the appropriate wave height (i.e., wave period, if the limiting factor is wave steepness). The 'Edinburgh' data only cover regular wave periods up to 12.2 seconds (Fig. 2.8), but they do consistently show that much lower rode forces occur at the same wave height as wave period increases from 11.0 to 12.2 seconds. This is supported by the abrupt drop in efficiency shown in Fig. 2.5 over this range of wave periods (cylinder tuned to 8 secs), which suggests that the drop in efficiency with increasing wave height is associated with a corresponding drop in the rate of increase in rode forces. However, there are insufficient data to explain the shape of the individual curves. Furthermore a recommendation arising from the energy evaluation study reported in Section 7.3, suggesting that the tuned period of the cylinder should be increased to at least 10 seconds, is likely to reduce or reverse these trends in longer waves, though again for lack of data the full position is uncertain.

At an operating wave height of 3m the recorded peak oscillatory load at one corner was about 415 Tf (=250 Tf r.m.s.), giving a peak corner load including buoyancy of 1185 Tf. This is equivalent to a resultant force

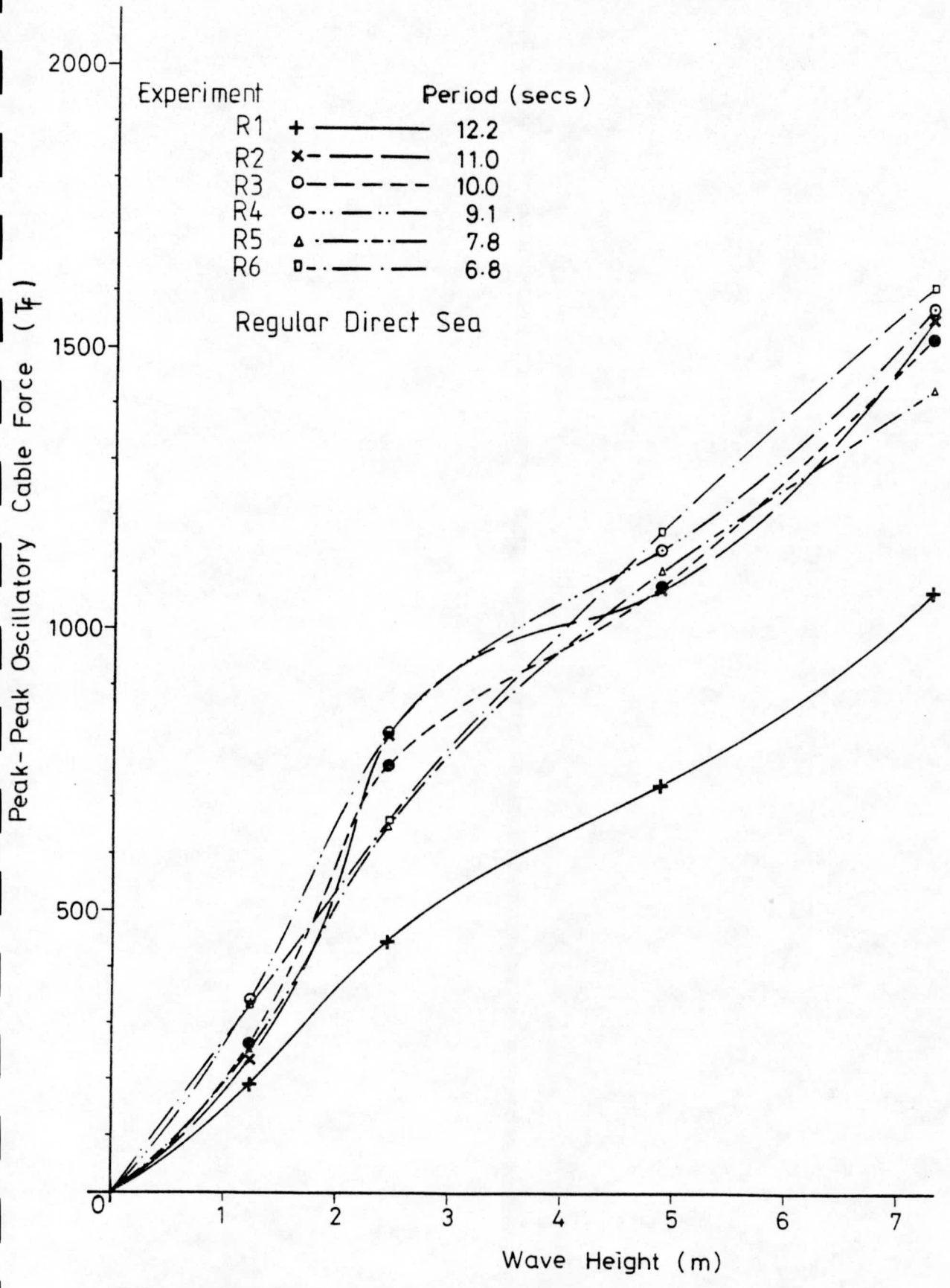

FIG. 2.8. Peak-Peak Loads per Corner

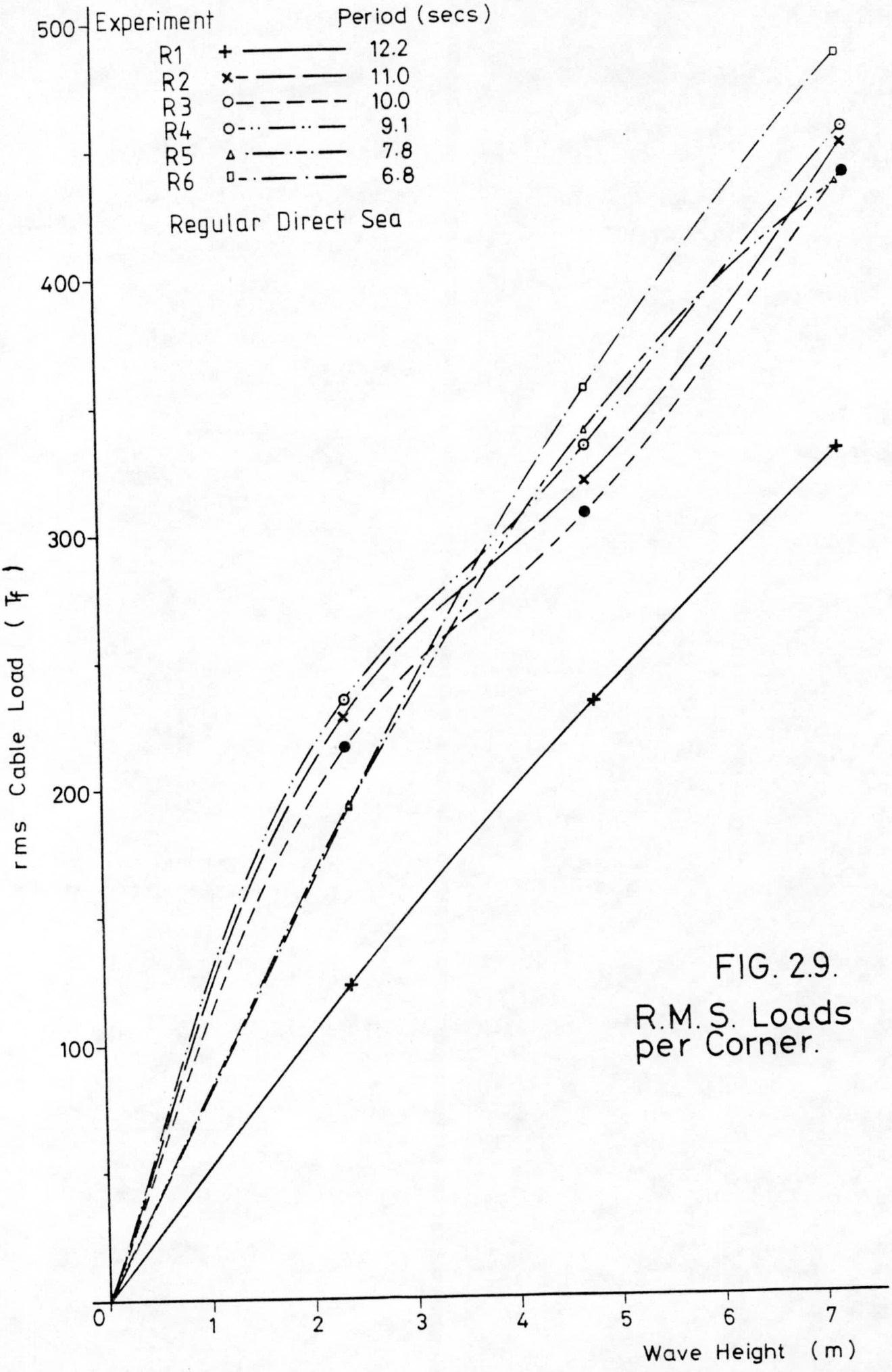

FIG. 2.9.
R.M.S. Loads per Corner.

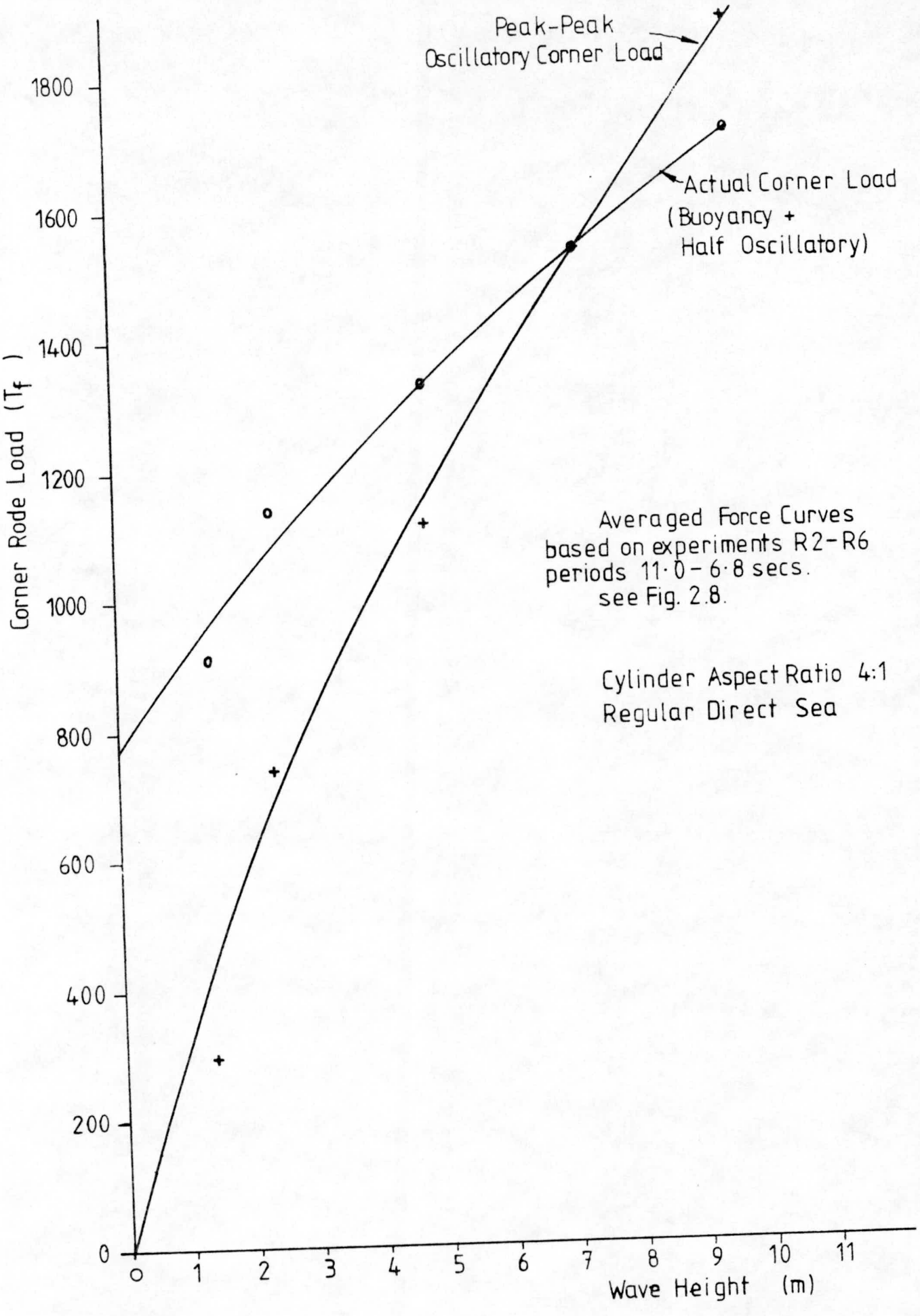

FIG. 2.10. Averaged Loads.

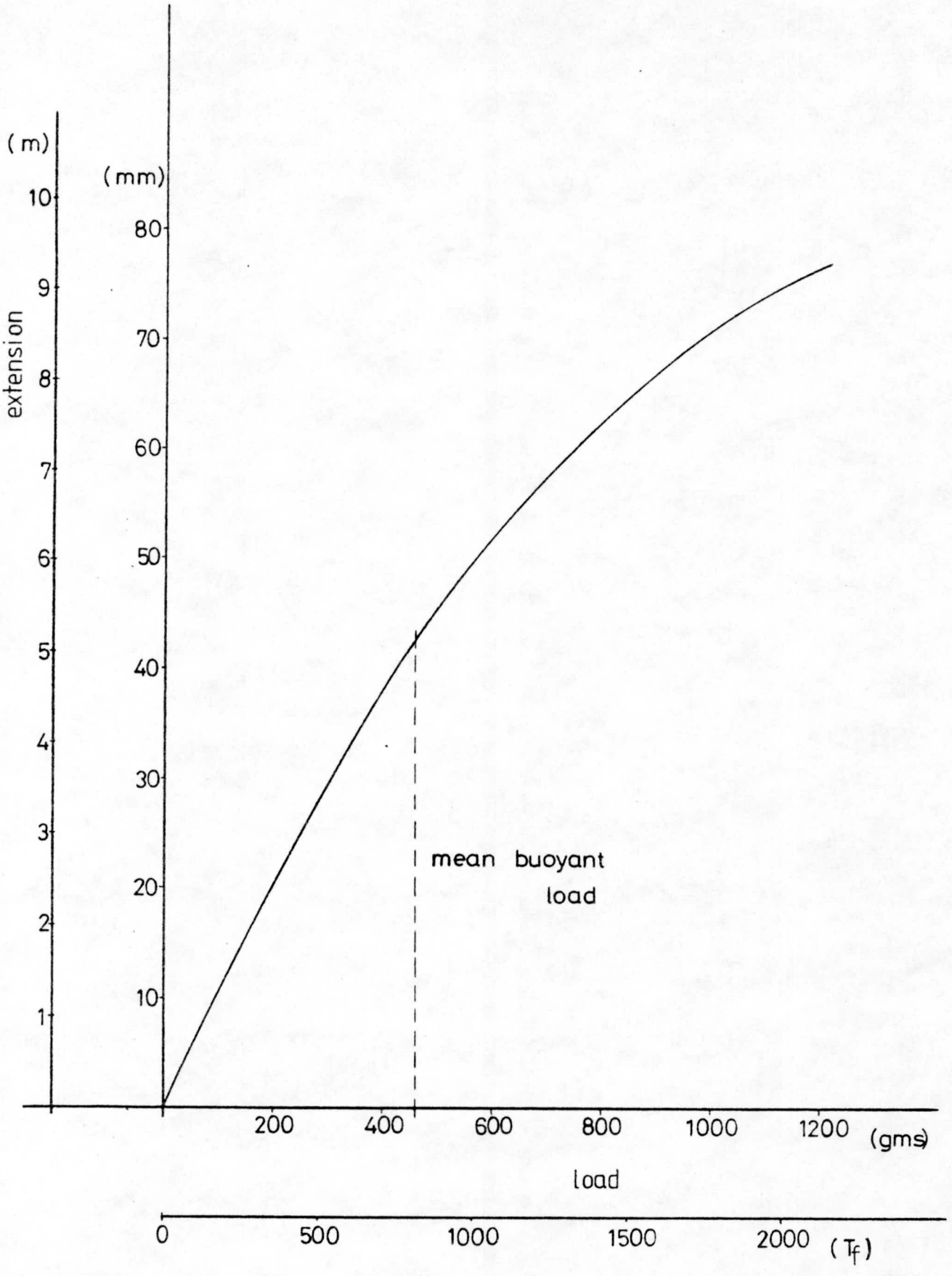

FIG. 2.11. Experimental Spring Characteristic.

over the length of the cylinder of 67 Tf/m. At a wave height of 6m the recorded peak oscillatory load at one corner was about 670 Tf (= 390 Tf r.m.s.), giving a peak corner load of about 1440 Tf, i.e., a maximum resultant force including buoyancy of 81 Tf/m.

The peak-to-peak and r.m.s. loads per corner in six constant energy period P-M seas are shown in Figs. 2.12 and 2.13. Although the r.m.s. load data are probably satisfactory, Fig. 2.12 shows the anomolies that a limited sample of peak force data can introduce unless, in addition to the same H_{rms} value, the waves have the same sequence in each experiment. If this is not the case then different maxima will be recorded. This accounts for the surprising form of the peak-to-peak curves in Fig. 2.12, and it prompts the important question, "What is a representative wave sequence in the storm conditions appropriate to any probability of return?". The effect of build-up to large waves could be explained in simpler testing equipment to give guidance on this matter. However, for the present it leaves some uncertainty about the magnitude of peak loads in P-M seas, though r.m.s. loads are probably quite accurate. It is therefore more appropriate to compare these with the results for regular waves in Fig. 2.9, on the basis that $H = 2\sqrt{2}H_{rms}$. An average line through the data for $6.8 < T < 11.0$ seconds in Fig. 2.9 compares closely with the long-crested curve in Fig. 2.12, whereas the line for $T = 12.2$ seconds in Fig. 2.9 lies below the short-crested line in Fig. 2.13. As before, this may be a consequence of the relationship of tuned to wave energy periods - Fig. 2.13 is for P-M seas with $T_e = 8$ seconds, equal to the tuned period of the cylinder.

2.2e Stability

Although the scaled water depth in the wide tank was more than three times that of the design water depth of 42m, the stability of the cylinder in oblique, side-on, and short-crested seas was impressive. This was without any lateral splay on the rodes, the presence of which would further improve stability. Under the worst conditions, the cylinder swayed from side to side by a total of less than its diameter (12m). Hence allowing for the error in representing depth, the maximum expected excursion would be ±2.5m, which when anchor positioning and safety factors are taken into account suggests that the device separation should be about 10m unless specific restraints against sway are applied.

It should be noted that the significance of this gap to the overal efficiency of energy capture of a linear array of devices decreases a

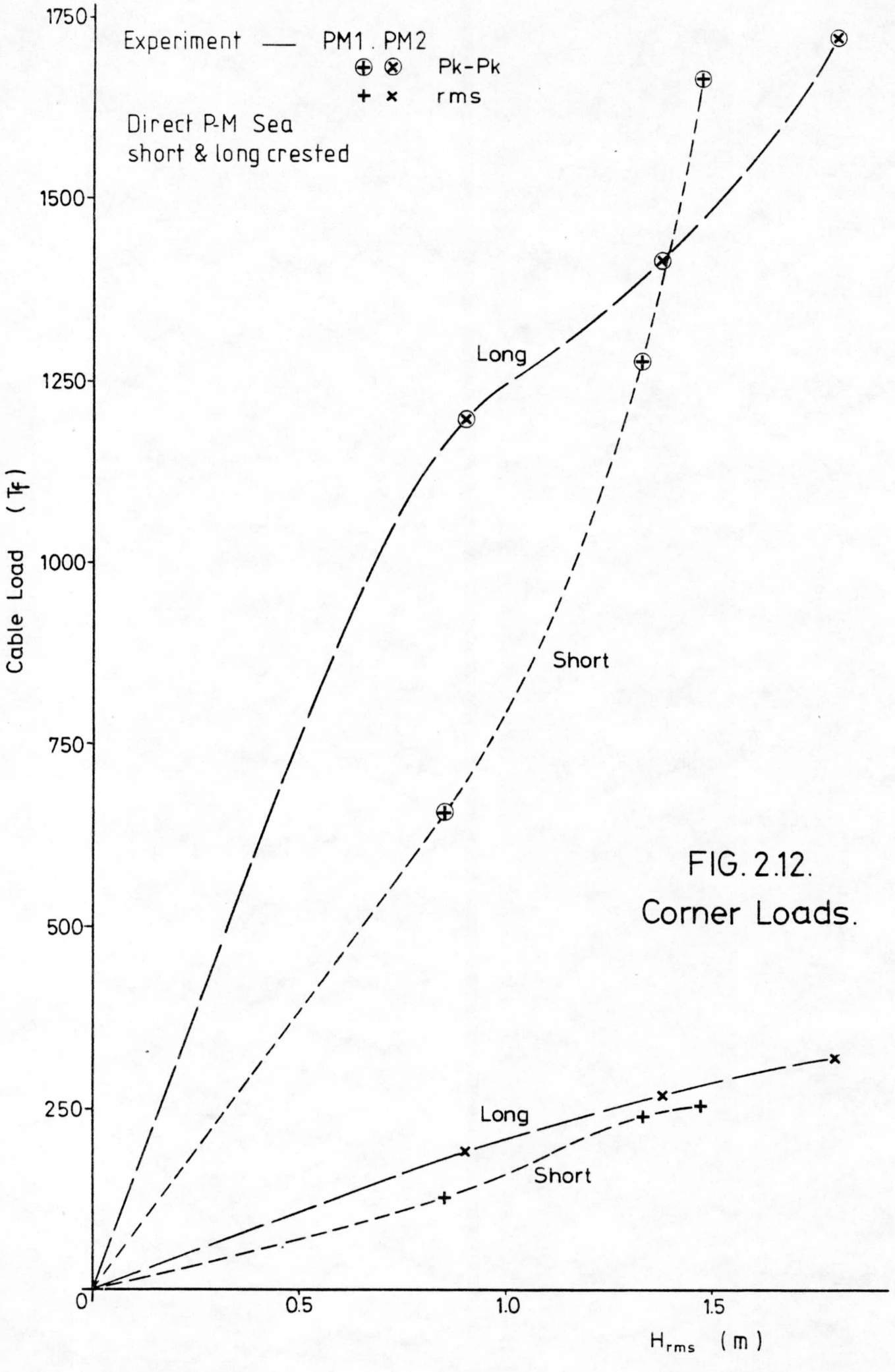

FIG. 2.12.
Corner Loads.

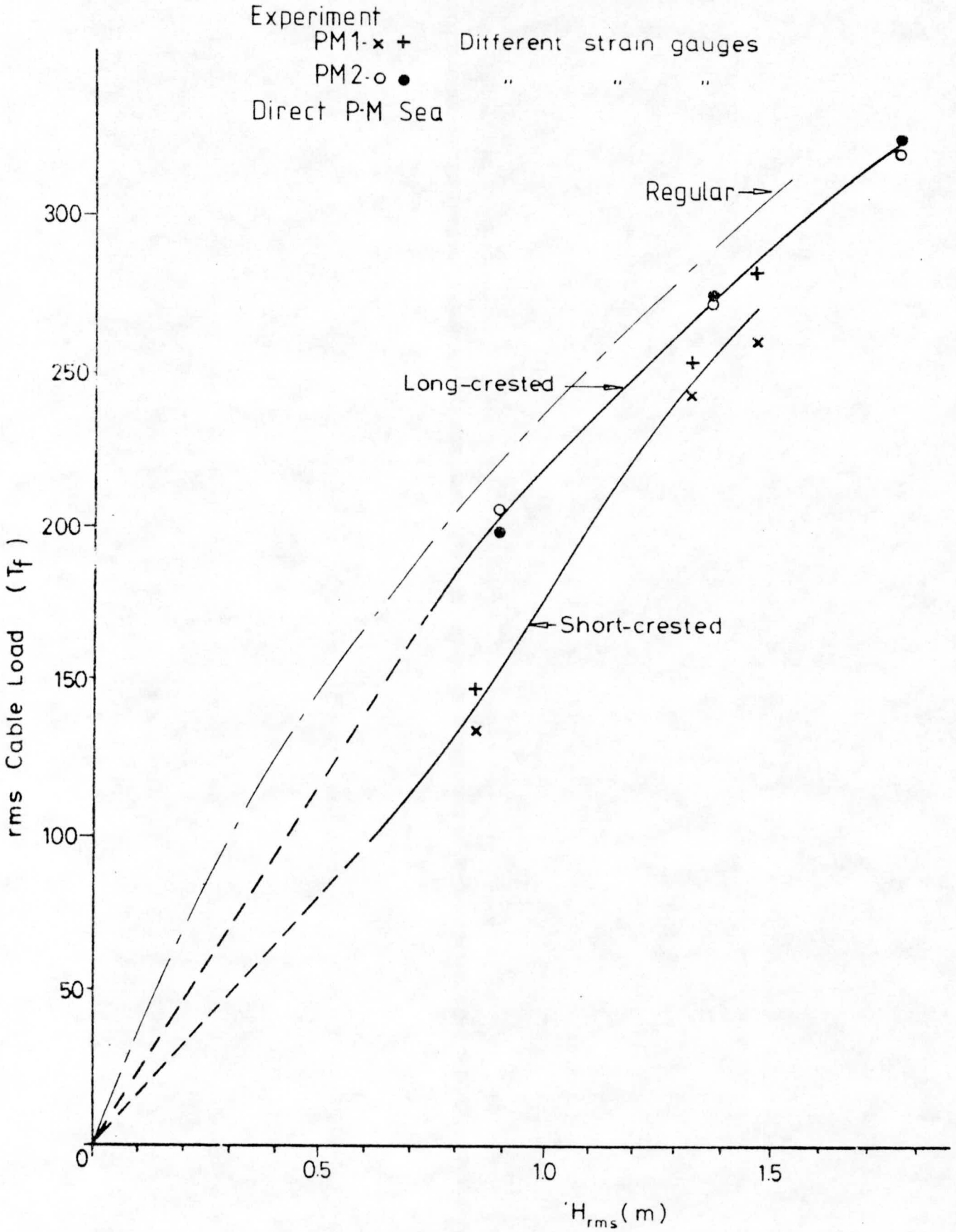

FIG. 2.13. R.M.S. Loads per Corner.

wave inclination to the normal increases. On the simple basis of projected lengths, i.e., neglecting lateral energy capture (Section 2.2c), only 50/60ths of normal incident energy will be intercepted, whereas for regular waves approaching at about 40° to the normal the gaps between the cylinders are not apparent (though some loss between them by diffraction would presumably occur). This suggests that the efficiency curves in Fig. 2.5 are a little high. Their further interpretation, together with the effects of wave inclination to the normal, is made in Section 7.3.

There was no evidence of yaw instability. The only adverse effects were observed on the 6:1 model in oblique regular waves where the leading end of the cylinder remained almost stationary whilst its trailing end executed a near circular motion. The 4:1 cylinder did not seem to display this behaviour.

The cylinder was also tested in a freak breaking wave. This wave, in a P-M sea of energy period 11.6 secs, was positioned to break on the cylinder. Although readings could not be taken during this test, the cylinder reacted abruptly (as may be seen the film), but remained on station and continued to capture energy after the wave had passed.

2.2e Conclusions from Edinburgh Tests

1. The tests in the Edinburgh tank, even for 2 weeks with an untried rig, have established confidence in the cylinder device and given experience with the test rig.
2. The cylinder performed satisfactorily in all sea conditions tested. Its reduced efficiency in larger amplitude, short-crested waves was not a shortcoming since the absolute level of energy capture remained within the upper part of the sensible working range of the power takeoff system.
3. The tuned bandwidth of performance appeared to agree well with 2-D theory and experiment. The tuning of damping (power takeoff), while still needing to be explored in detail, did not appear to be too critical for the present purposes of general assessment.
4. As previously stated in the Interim Report, these results, although lacking in detail, have been taken across a wide spectrum of wave conditions and have clearly shown that the cylinder behaves well in all respects.

Although the S.R.C. funded narrow tank investigations continue at Bristol, further wide tank work is required to answer at least the following questions :

a) How much energy capture from beyond the length of the cylinder can be expected and therefore what is their most economic spacing?

b) What is the best cylinder length bearing in mind the needs for maximum overall capture efficiency and minimum forces in severe seas?

c) What is the overall efficiency of the cylinder when better tuned to the scatter diagram, including more and less mixed seas as appropriate?

d) How is cylinder efficiency modified in high waves by the use of motion-limiting devices?

e) How do adjacent cylinders in an array interact, and how does capture efficiency then vary with wave inclination in typical sea states?

f) Should the cylinders be in a line or staggered?

As before, the optimum research programme will involve answering some of the more important of these questions before others can be investigated efficiently. This suggests that the programme should include a number of short experimental periods with sufficient time between each to consolidate answers from one in preparation for the next.

2.3 Additional Data from 'Bristol' Narrow Tank

Although the nature of real waves and their action on cylinders of finite length introduces such important three-dimensional effects as lateral energy capture to the resulting motion, the basic exchange is two-dimensional. The narrow tank test programme for the submerged cylinder device, funded to Dr. Evans at the University of Bristol by the Science Research Council, has helped to resolve several areas of uncertainty. These include :

1. The motion of the cylinder relative to the incoming wave (Section 2.1). As part of that programme studies have been made of orbit shape, the ratio of orbit diameter to wave height (Fig. 2.2) and the phase lag between water particle orbit and cylinder orbit (Fig. 2.1). From this information a start has been made with the analysis of the energy transfer process from wave to cylinder, from which it is expected that objective decisions will follow regarding optimum values for various parameters involved so that capture efficiencies may be maximised. The same data were an

essential element in the calculation of rode forces (Section 3). The amount of damping applied has been shown to be important, to which the addition of orbit limiting devices (Section 5) must soon be considered. Measurements of the damped phase lags have indicated values of about 270°, confirming that the motion of the cylinder when under load is very much 'inertia dominated'.

2. The effect of cylinder submergence in still water conditions on its overall performance and behaviour. This parameter has been theoretically shown by Dr. Evans to exert quite a significant influence on the peakedness of efficiency curves. Ideally it should be zero. For various reasons this limit was rejected in favour of a submergence of 3m, not least because of tidal effects. The typical 4m spring tide range off the west coast of Scotland, coupled with the need for buoyancy not to be lost, would therefore give a minimum cover of 1m with 3m as the mid-tide value. Although comprehensive efficiency data have only been recorded with 3m submergence, observations of cylinder orbit in regular waves over a range of heights have been made as the submergence is reduced to zero. Although the cylinder orbit becomes a much flatter ellipse and the reflected wave component increases, high efficiencies were maintained. The maximum recorded exposure of the cylinder in waves up to 9m high was one quarter of its diameter, which is roughly the same as for the cylinder with 3m submergence in 9m waves. In future it may therefore be prudent to carry out most of the testing with a submergence of half the range of normal high spring tides at the site(s) under consideration, with limited tests over this range.

SECTION 3

FORCES ON A MOVING CYLINDER

3.1 Introduction

Section 5 of our Interim Report presented the Morison drag and inertia forces on a fixed cylinder for a survival wave 35m high and 16 second period, from which were determined the maximum rode forces. Similar calculations were made for a 16m wave of 11.75s period, and gave peak force values some 10% less.

The graphs also showed that by far the greater wave force was due to inertia effects, which is the product of the coefficient of inertial (mass), the density of water, the volume displaced by the cylinder, and the local wave particle acceleration (which is a vector, having magnitude and direction).

When the cylinder is moving relative to the water (another vector), the same equation applies, but 'local wave particle acceleration' is replaced by 'relative acceleration between cylinder and local wave particle', (again a vector).

The problem is compounded by a phase lag that varies both through a wave cycle and with the degree of damping applied. Furthermore, experiment has shown that neither the cylinder nor the wave orbits are circular in the configurations under consideration.

The present task is to determine rode forces in the above conditions for a cylinder orbiting through prescribed proportions of a specified wave height, these proportions depending upon the damping applied. Because the earlier analyses showed only a small difference in rode forces between 16 and 35m waves, and because more recent information suggests that the 1 in 50 year wave at S. Uist may have a height of about 23m, it was decided to carry out the calculation for the moving cylinder using the 16m wave. Sensible comparisons may then be made.

3.2 Analysis and Results

From photographs (e.g. Fig. 2.1 a-d) from a pulsed storage oscilloscope screen showing surface wave profile and fore and aft rode displacements, for each of 4 wave heights and with minimum and maximum damping, the second derivative of displacement with respect to time (i.e. acceleration) was determined throughout each cycle. The accelerations of 2 rodes on orthogonal axes can be combined with theoretical particle accelerations to produce relative accelerations from which inertia forces, when combined with the buoyancy force, can be resolved back into rode forces.

From the experimental evidence available to date it was assumed that wave particle and cylinder orbits are circular and regular in time. Approximate rode forces were then obtained comparatively quickly. From tests in waves equivalent to 9m high, and assuming that all motions are regular and simple harmonic, the wave investigated analytically is, as before, defined by H = 16m, T = 11.75s d = 42m. The cylinder is tethered at y + d = 33m and can move in restrained orbits. Two loading cases have been studied :

Case 1 Assume the cylinder is under minimum damping conditions, has an orbit diameter of 9.5m and a phase lag of 190° relative to the surface wave crest.

The Morison Drag Force is 474 Tf.

The phased horizontal, vertical and vertical + buoyancy forces are shown on Fig. 3.1.

The vectored resultants are shown on Fig. 3.2.

The phase rode forces are shown on Fig. 3.3 and peak at about 2,020 Tf/side, fore and aft.

Case 2 Assume the cylinder is under maximum damping conditions, has an orbit diameter of 7.0m and has a phase lag of 230° relative to the surface wave crest.

The Morison Drag Force is 1,403 Tf.

The phased horizontal, vertical and vertical + buoyancy forces are shown on Fig. 3.4.

The vectored resultants are shown on Fig. 3.5.

The phased rode forces are shown on Fig. 3.6 and peak at about 2,950 Tf/side, fore and aft.

These rode forces may be compared with the peak 'rigid cylinder' estimate in Fig. 5.10 of our Interim Report (reproduced here as Fig. 3.7). As the cylinder orbit reduces from 9m (minimum damping, 190° phase lag, Fig. 3.3) to 7m (maximum damping, 230° phase lag, Fig. 3.6) to zero (Fig. 3.7), the force per side of the cylinder, including buoyancy, increases from 2020 Tf to 2950 Tf, and finally to 3250 Tf.

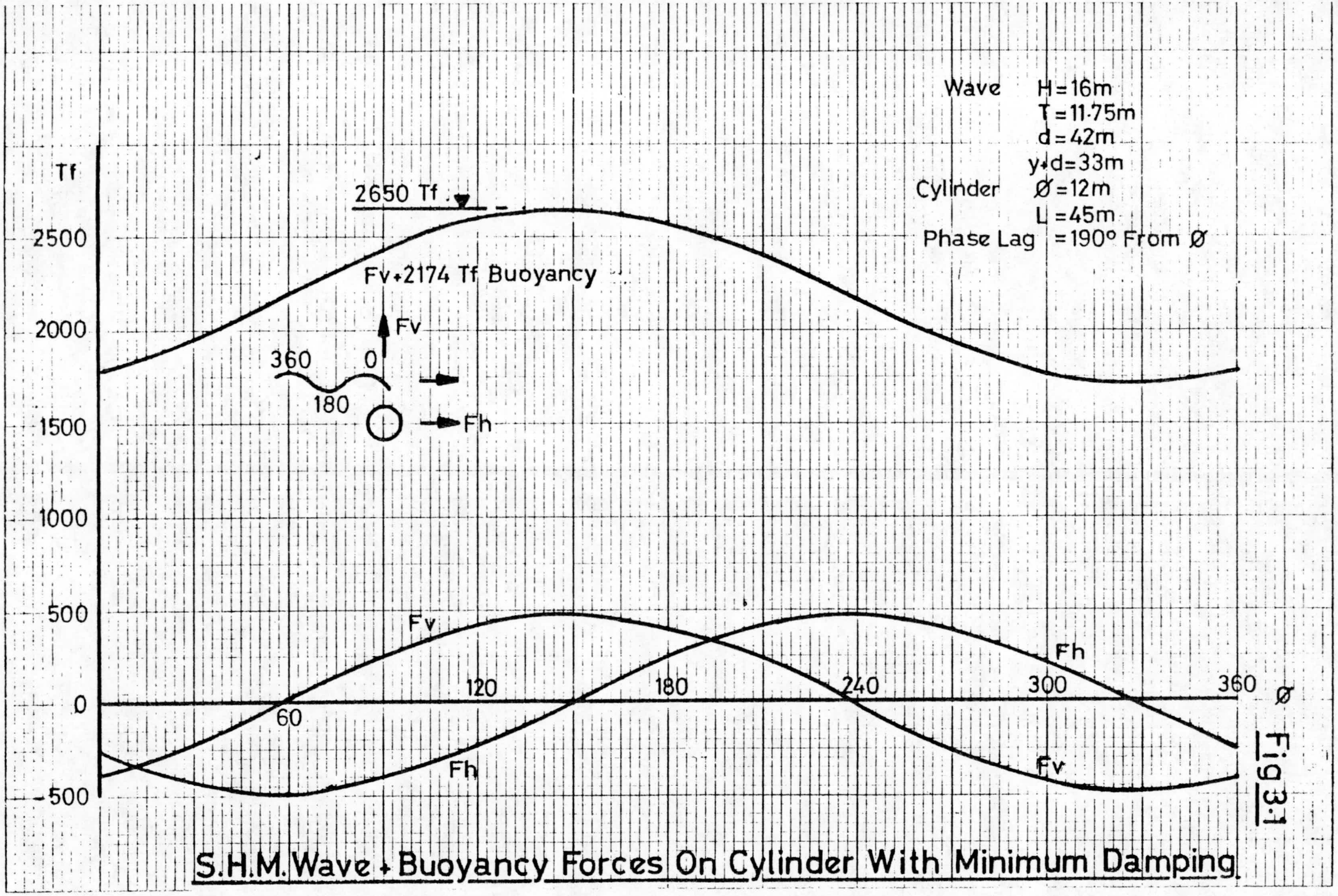

Fig 3.1

S.H.M. Wave + Buoyancy Forces On Cylinder With Minimum Damping

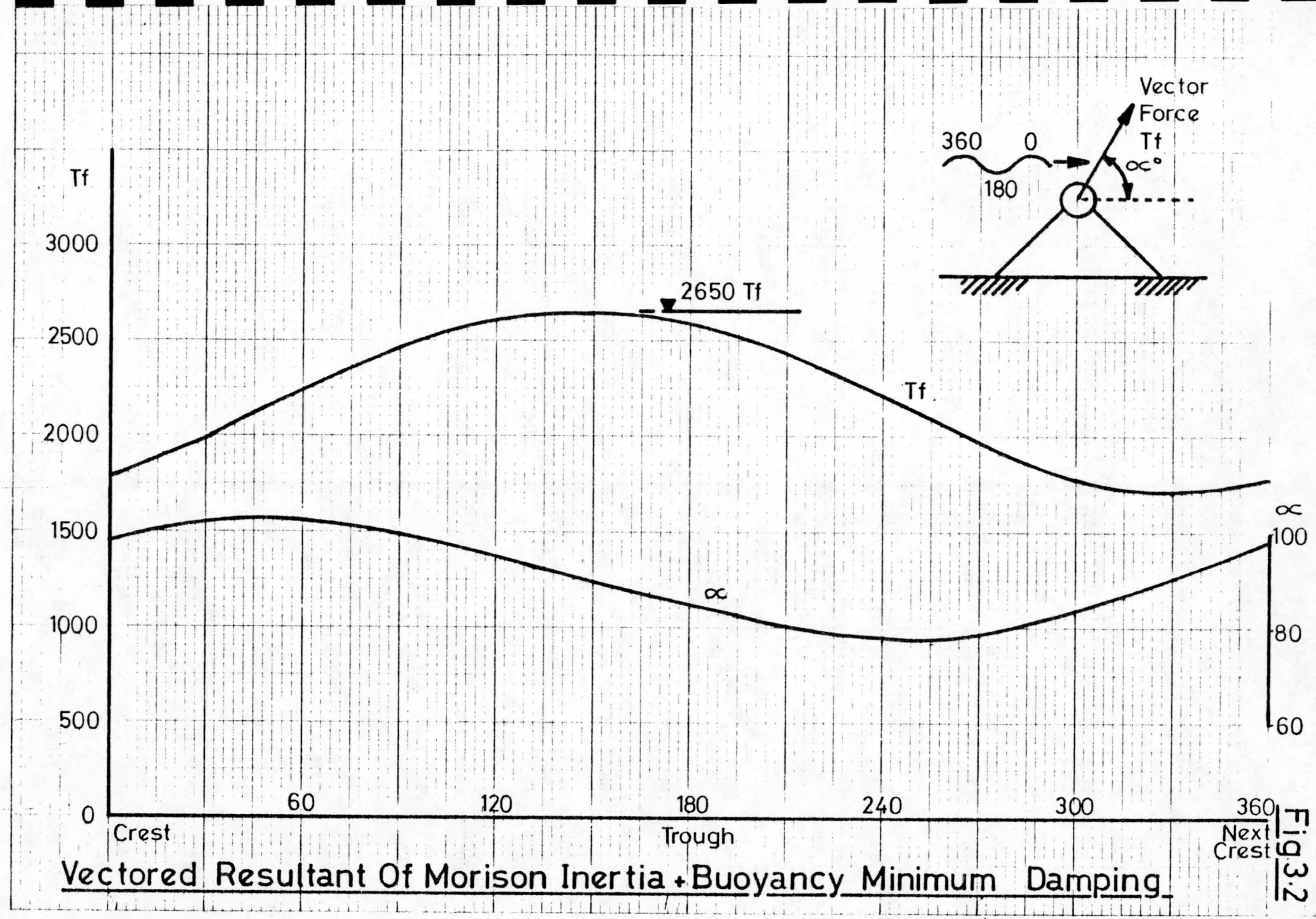

Fig 3.2

Vectored Resultant Of Morison Inertia + Buoyancy Minimum Damping

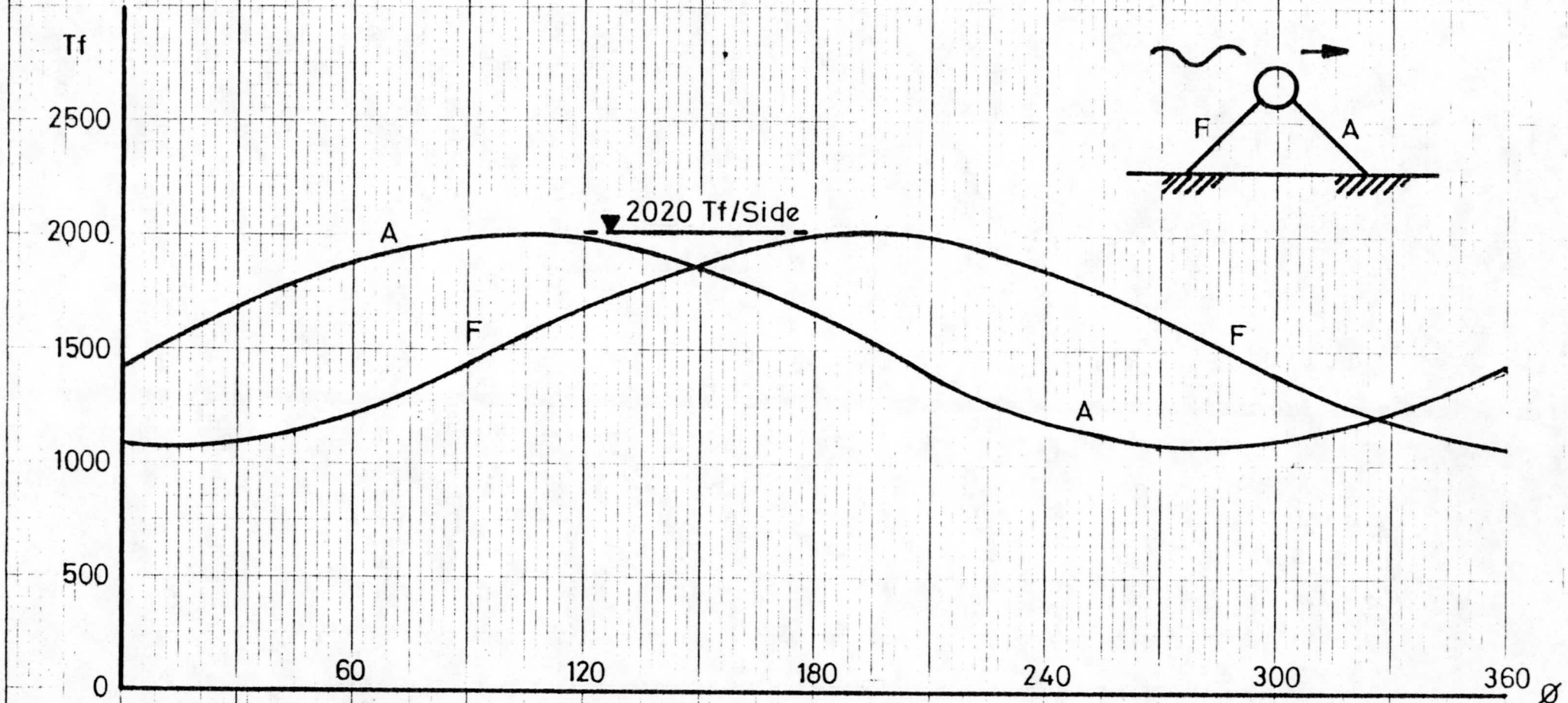

S.H.M. Rode Forces On Cylinder With Minimum Damping.

Fig 3.3

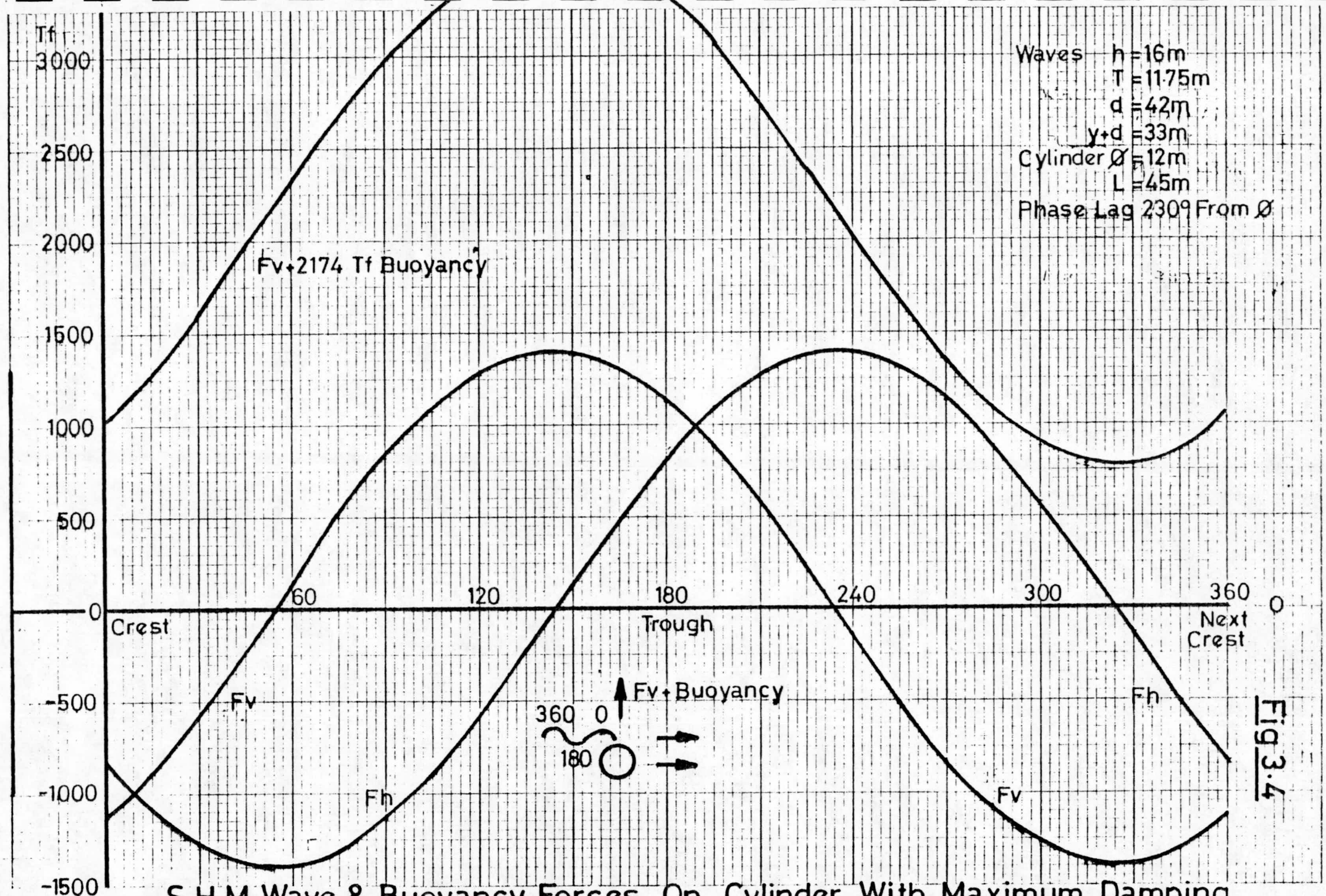

Fig 3.4

S.H.M. Wave & Buoyancy Forces On Cylinder With Maximum Damping

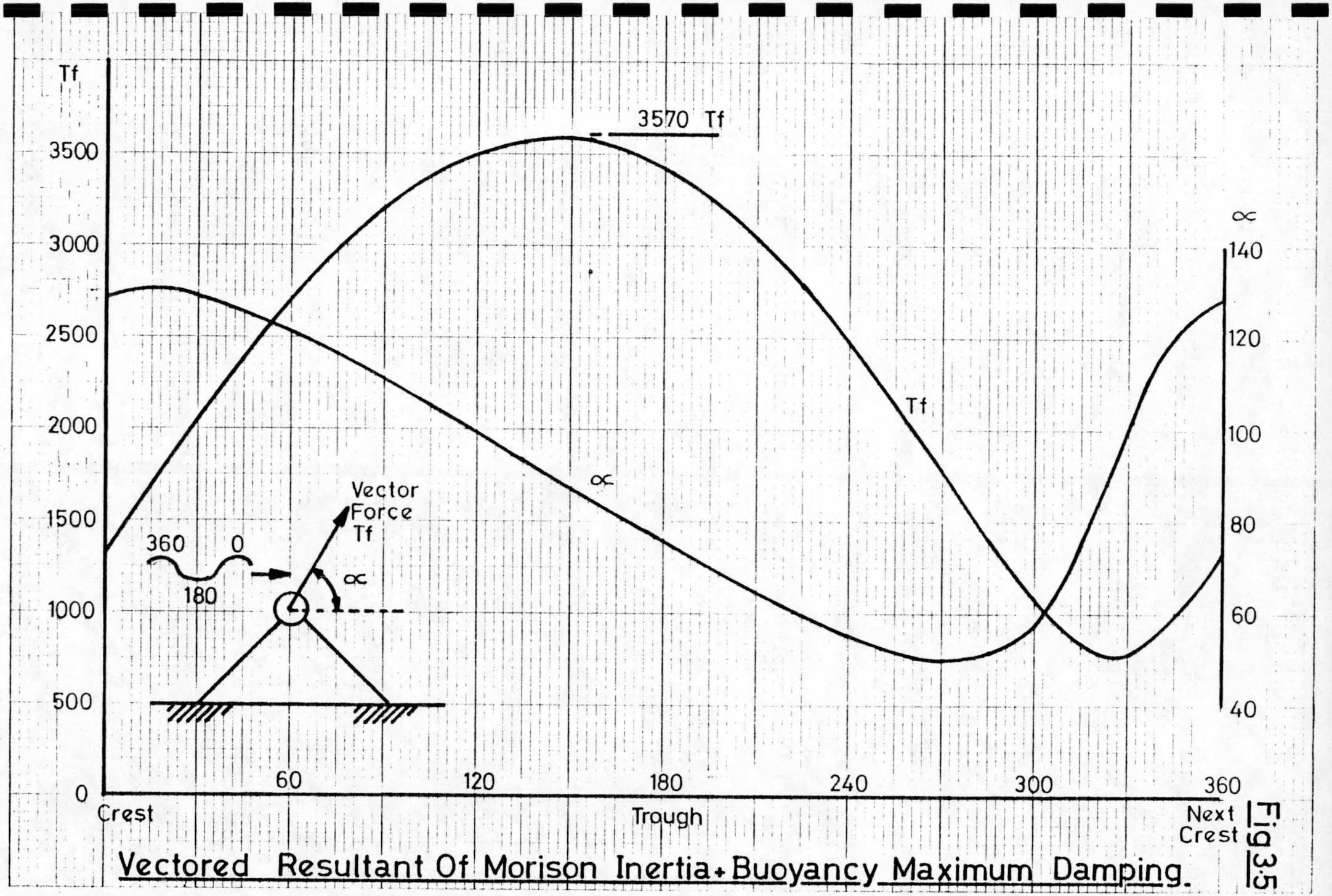

Fig 3.5

Vectored Resultant Of Morison Inertia + Buoyancy Maximum Damping.

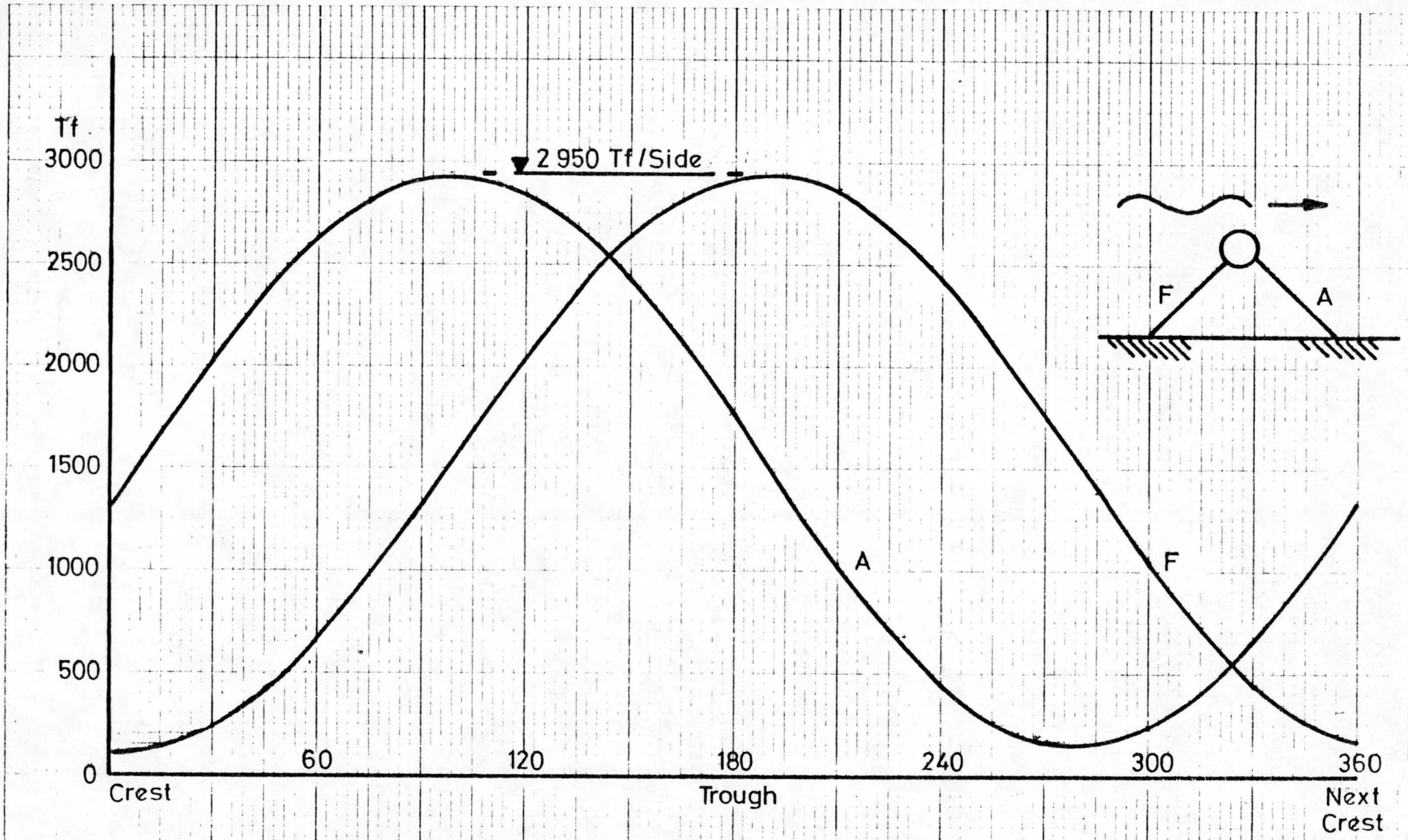

S.H.M. Rode Force On Cylinder With Maximum Damping.

Fig 3.6

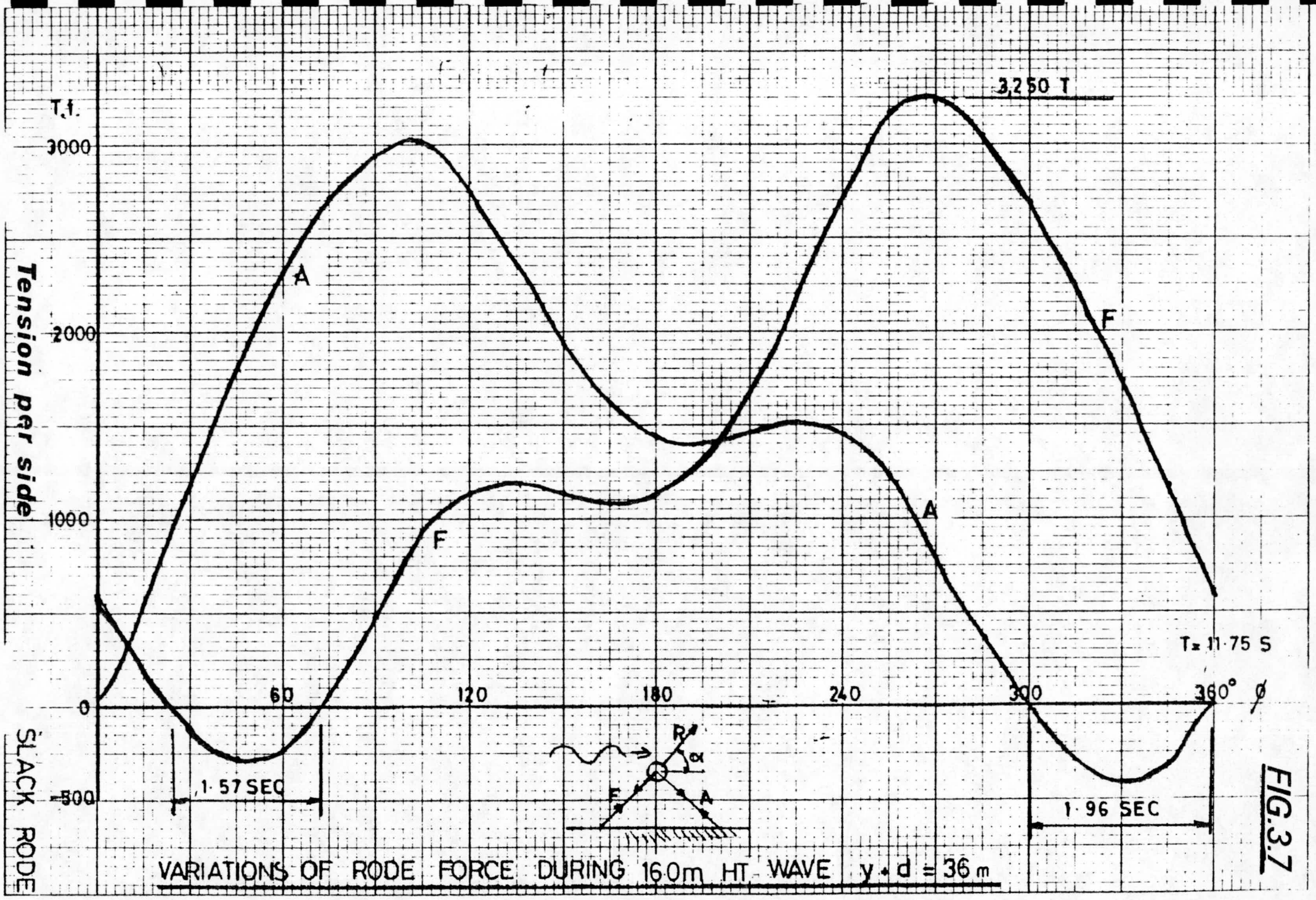

VARIATIONS OF RODE FORCE DURING 16.0m HT. WAVE y + d = 36 m

FIG. 3.7

Clearly the change in phase and the reduction in orbital diameter combine to have a major influence on rode forces. For the reasons discussed in Sections 5 and 7, it is proposed that the orbital diameter of the cylinder is restricted above movements of 3-4m, the preferred amount depending upon the proportion of the available energy resource then sacrificed. Bearing in mind the data in Fig. 2.2, it now seems more likely that a damped cylinder in 16m (regular) waves will have an unrestricted orbit of 4-5m, and that in the short-crested seas if crest lengths are less than 50m, which is typical of higher waves, the motion will be less than this.

For these reasons the proposed 3-4m limit for the power takeoff system has been set. From the force calculations presented above, the rode load may reach about 3000 Tf/side, though the spring constant of the fender used to limit rode movement (Section 5) will determine the rate of deceleration of the cylinder hence the force in the rodes at that time. In view of the non-circularity of the orbits of a cylinder not under this influence in high waves, little reliability can be put on the accuracy of analytic estimates of rode load when the damped cylinder is moving under this influence in these conditions. Clearly it is essential to establish this at the earliest possible time for its affects :

1. The longitudinal bending moments in the cylinder;
2. The necessary number of rodes per cylinder and their distribution along its length (the proposal in Section 3.4 for 3 chains per corner, or 12 per cylinder, is made on the best evidence of loads available to date) - Section 3.3);
3. The design of the fenders and associated framework;
4. The design of the foundations.

Fig 2.1 shows that the cylinder breaks the water surface under certain wave and submergence (depth to crown in still water) conditions. The film confirms that this tends to occur after the trough of the wave has passed, when the water level is rising. The difference in level then quickly set up across the cylinder produces a nappe of water over it, giving a local patch of 'white water'. Because of the curved form of the cylinder it progressively loses buoyancy, and this helps to limit the vertical component of its motion. As a consequence, in high waves the cylinder orbit is elongated horizontally. The further design of the mooring arrangements may need to give particular attention to the influence exerted by this component of motion on the fender-induced forces.

3.3 Comparison of Experiment (Section 2.2d) and Calculation

The relevant values of maximum rode (i.e. corner) loads on the cylinder in regular waves are:

1. Experimental Data (Edinburgh) - Fig.2.10

H(m)	L(m)	Steepness	Max.Corner Load (Tf)
3	128	1/42	1150
9	128	1/14	1670
16	128	1/8	2000-2200 approx. (by extrapolation)

2. Calculation (3rd Order Stokes and Morison)

(a) Fixed Cylinder (Interim Report, Section 5)

H(m)	L(m)	Steepness	Max.Corner Load (Tf)
3	150	1/50	1025
16	204	1/13	1625
35	394	1/11	1772

(b) Moving Cylinder (Present Report, Section 3.2)

Minimum Damping (i.e. relatively free)

16	204	1/13	1010

Maximum Damping (i.e. power takeoff operating)

16	204	1/13	1475

The cylinder device operates in the inertia dominated regime. The above figures confirm that the forces then imposed are determined more by wave steepness than by absolute wave height.

Two variables which greatly affect the calculated loads are phase lag and relative cylinder orbital diameter.

The conditions given in 2(b) above may be interpreted to the experimentally observed conditions of a phase lag of 270° (instead of 230°) and an orbit diameter of 3.75m (instead of 7m) in 16m waves (Fig.2.2). This leads to a maximum corner load of 1726 Tf.

By comparison, the experimental data in Fig.2.10 give, for a steepness of 1/13 and height 9.85m, a corner load value of 1727 Tf. However, we do not know the exact damping constant in use during these tests, hence the figures cannot be compared exactly though the agreement is close.

The very limited data collected in large amplitude mixed seas produced a maximum corner load of about 2600 Tf in a peak wave 22m high. However, we do not know either the steepness or short-crestedness of this wave, so cannot judge how realistic it might be. It is obviously important that this be resolved, though it may be difficult to prescribe a design wave sequence and its lateral structure in terms of probability of recurrence. It may be better to carry out a range of tests to determine the significance of wave height, sequence and short-crestedness.

It is interesting to note that, at 1726 Tf, the loads for the corrected moving cylinder case are marginally higher than for the fixed cylinder case (1625 Tf). The effect of limiting the stroke (orbit) of the cylinder in very high waves will be to make it effectively fixed for a proportion of these cycles according to the limiting value chose (Fig. 2.2). The limits will, of course, be applied towards the ends of the stroke, that is when the (inertia) wave force on the cylinder is decaying and reversing. A much elongated orbital motion in the horizontal direction such as occurs with small submergence in high waves, may produce severe arresting loads in these conditions. It will be difficult to estimate these accurately from calculation methods alone.

3.4 Design of Rodes

In order to carry the peak corner load of 2600 Tf measured in the Edinburgh tank for a 22m wave, the rodes have been redesigned from the proposal for 5 chains per side in our Interim Report to 6 chains per side, arranged 3 per corner.

The chains are still of stud link chain cable, in supergrade steel, 130mm diameter, with a proof load of 1249 Tf and an average breaking load of 1590 Tf. Load is shared evenly by a 4-point balancing beam (Fig. 6.4).

Under this loading condition the average load in each of 3 chains is 867 Tf, or 69.4% of proof load. This should be acceptable as a peak load, occurring approximately once in 50 years (Section).

Although we question the specification of such a steep wave for design purposes, the theoretical load of about 1700 Tf per corner estimated in Section 3.3 produces an average load in each chain of 567 Tf, or 45.4% of proof load. This suggests that the 6-chain proposal offers the necessarily long fatigue life.

SECTION 4

CYLINDER CONSTRUCTION

The following details should be read in conjunction with Section 8 of our Interim Report.

(A) The preferred method of construction consists of Precast Segments of the cylinder, each 3m in length, with a central stiffening rib or, in two cases, with bulkheads. They would be closed with end caps and stressed together with epoxy mortar joints between segments. Fig.4.1 and 4.2.

Construction Sequence - Parallel Cylinder Ring Sections

1. Reinforcement cage with stressing ducts is prefabricated round post type jig allowing Electric overhead travelling (EOT) crane to lift completed cage off jig (Fig. 4.1).

2. EOT crane transports cage and lowers it onto permanent lower mould consisting of tapered, epoxy resin coated concrete plug.

3. EOT crane positions outer circular shutter in three sections, clipped together with over-centre toggle clamps.

4. Upper steel mould plug is then transported by EOT crane and lowered into upper section of reinforcement cage. This stands on its own spider of legs outside the segmental outer shutter and the legs are clamped to the ground to resist upthrust.

5. A counterweighted concrete delivery pipe of 6m radius on a central pivot is then lifted onto the centre of the upper shutter spider (Fig. 4.2).

6. Concrete delivery pipe is connected to the base of the pivoted boom and concrete is pumped into the mould. The upper mould and external circular steel shutters are permanently fitted with external vibrators to ensure compaction and removal of air bubbles.

7. The pivoted boom assembly is lifted off when concreting is complete and the free surface of the concrete is trowelled off smooth and flush.

BRISTOL S.C.W.I.D.
PROPOSED LAYOUT FOR
FACILITY TO PRODUCE
2No S.C.W.I.D.S PER WEEK

FIG. 4·1

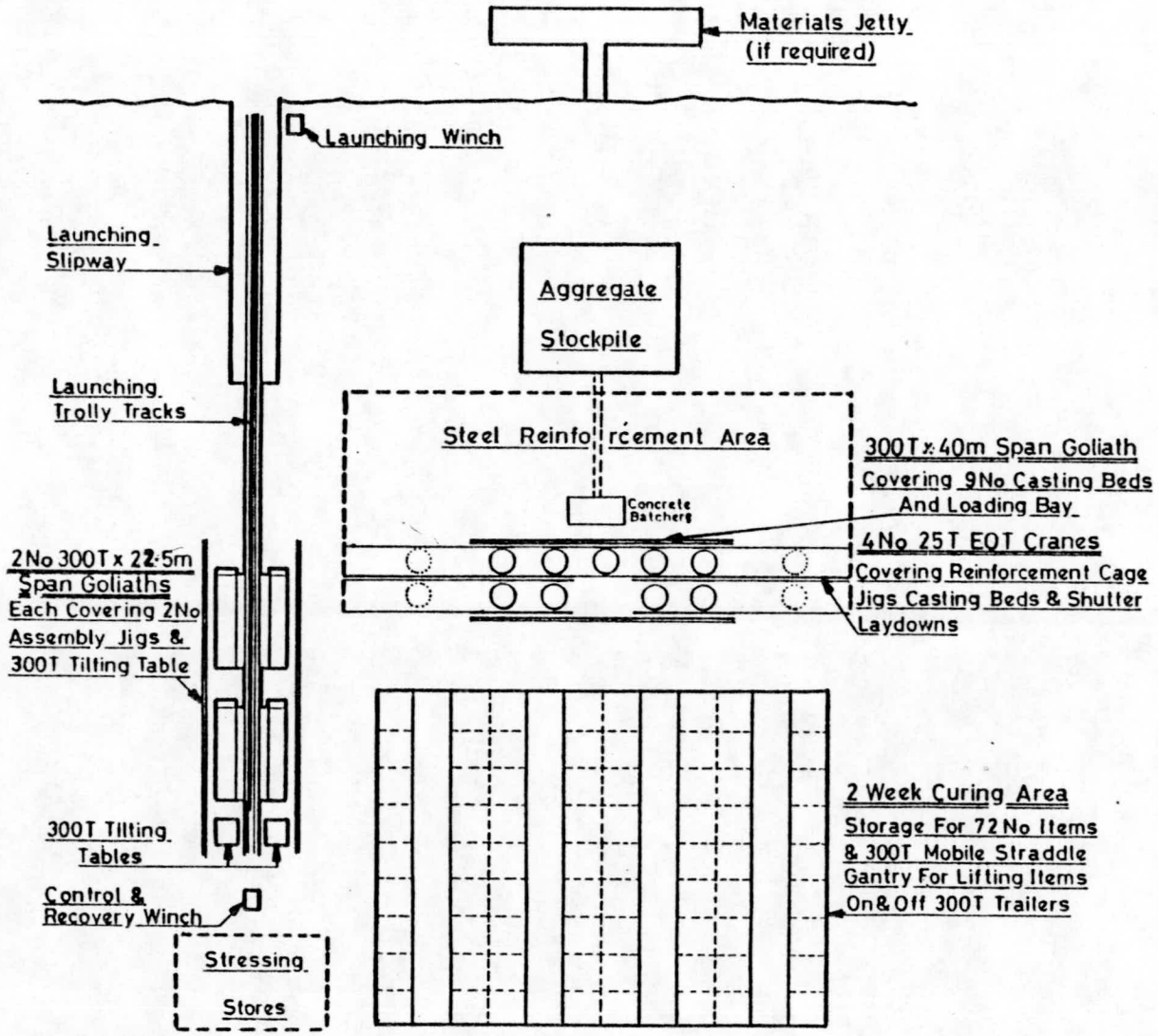

Works Area Required
Excluding Offices etc.
500m x 350m
17·5 Hectares

This Drawing To Be Read In Conjunction With Detail Sketches And Construction & Erection Notes

NOTES

1. REINFORCEMENT CAGES COMPLETE WITH DUCTS OR ANCHORAGES ARE PREFABRICATED AND TRANSPORTED TO MOULDS BY E.O.T. CRANE.
2. RINGS AND END CAPS, AFTER CASTING, ARE LIFTED FROM MOULDS BY 300T GOLIATH. MOVED TO LOADING BAY AND PLACED ON TRAILERS.
3. UNITS TRANSPORTED FROM LOADING BAY TO CURING AREA BY TRAILER.
4. UNITS LIFTED FROM TRAILER IN CURING AREA BY STRADDLE GANTRY.
5. UNITS REMAIN IN CURING AREA FOR 2 WEEKS.
6. UNITS RELOADED ON TRAILER AND MOVED TO TILTING TABLE.
7. TRAILER AND UNIT LOCKED TO TABLE AND TILTED TO VERTICAL POSITION.
8. UNIT LIFTED IN VERTICAL POSITION AND MOVED TO ASSEMBLY JIG.
9. UNITS JOINTED ON ASSEMBLY JIG TO FORM COMPLETE CYLINDER.
10. CYLINDERS STRESSED, GROUTED AND ANCHORAGES PROTECTED ON ASSEMBLY JIG.
11. MOORING POINTS ARE CONCURRENTLY STRESSED TO END CAPS.
12. COMPLETED CYLINDER IS THEN ROLLED TO LAUNCHING TROLLEYS BY WINCH ROPE.
13. CYLINDER TRANSPORTED ON LAUNCHING TROLLEYS INTO BASIN WHERE IT FLOATS OFF TROLLEYS. TROLLEYS AND CYLINDER CONTROLLED BY WINCH ROPES.
14. LAUNCHING TROLLEYS ARE THEN RETURNED TO RECEIVE NEXT CYLINDER.

SKETCH OF CASTING MOULD PRINCIPLE FOR CYLINDER RINGS

BULKHEAD RINGS SIMILAR BUT WITH FLAT TOP TO LOWER MOULD AND CONTINUOUS PLATING TO BOTTOM OF UPPER MOULD FITTED WITH AIR RELEASE HATCHES.

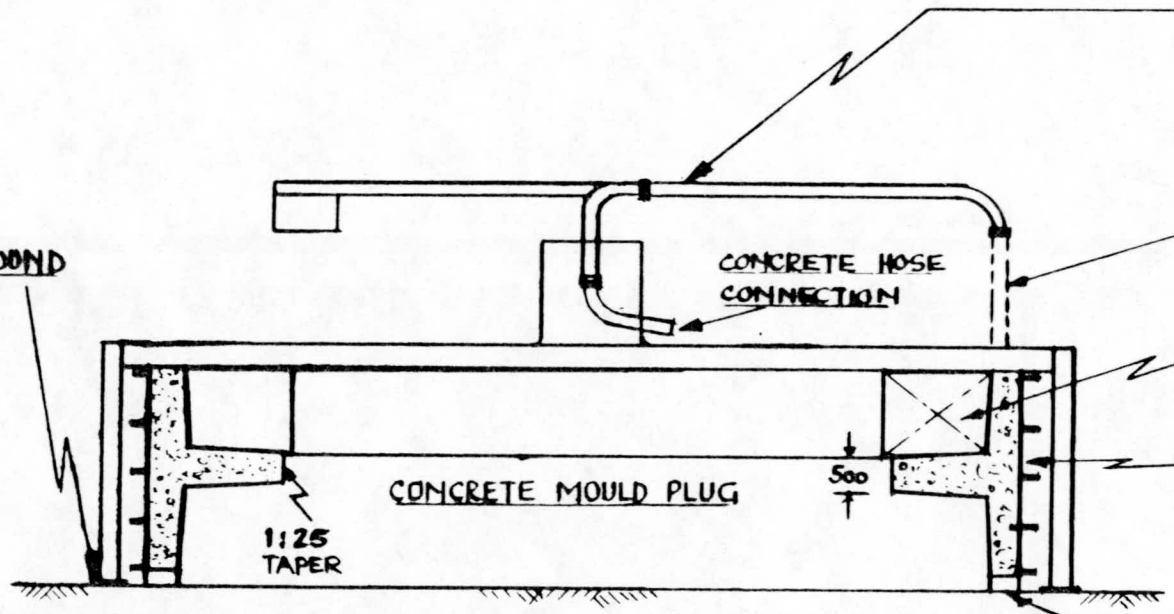

EXT. DIAM. ------ 12M
INT. DIAM. OF RIB - 9·4M

WALL THICKNESS 375mm @ EDGES
HEIGHT OF RING ---- 3M.

SCALE 1:100. 12th OCT 79

FIGURE 4·2

8. When the initial set has occurred, the upper mould legs are unclamped and the mould lifted off by EOT crane.

9. The circular external shutter is then unclamped and the sections removed by the EOT crane.

10. After a curing period, currently thought to be between 12 and 18 hours, the annular steel platform around the bottom mould, on which the ring is standing, is jacked up to release the ring from the bottom mould plug.

11. After release, a lifting spider is connected to the annular platform and the ring lifted off the mould by Goliath Crane and moved to the loading bay.

12. The lower mould plug is then cleaned, a fresh annular platform fitted around it and the cycle recommenced.

13. At the loading bay, the Goliath Crane lowers the ring onto a 300T Trailer which transports it to the Curing area.

Construction Sequence - End Caps

1. Reinforcement cage is prefabricated, complete with stressing anchorage trumpets, transported by EOT crane, and lowered into steel mould.

2. Mooring point fixings are then fitted and the shutter completed ready for concrete.

3. Concrete is pumped and placed in a normal manner using poker vibrators.

4. After initial set has occurred, the peripheral shutter and the special sections around the mooring points are struck.

5. After an initial curing period, probably 24 hours, the end cap is lifted out of the mould by a lifting spider connected to a ring of lifting points cast into the top of the concrete, which is the inner face of the cap. The cap is then stored for further curing.

Erection Seqence - P.C. Units into complete Cylinder

1. One end cap is lifted at the curing store by Straddle Gantry (Fig. 4.3), placed onto a 300T Trailer which is towed to the Assembly area and run onto a tilting table where it is turned onto its correct vertical alignment. The end Cap is then lifted off the table and moved to the assembly jig by a Goliath Crane (Fig. 4.4 and 4.7).

2. The end cap is supported in the vertical position and temporary stressing cables and jacks positioned at some of the trumpets.

3. The first end ring is similarly raised to the vertical, brought to the assembly jig and placed a short distance from the end cap.

4. The temporary stressing cables are threaded through the appropriate ducts in the ring and locked to thrust pads at the free face (Fig. 4.5).

5. Epoxy mortar designed with the necessary retarded curing time is spread, by trowel or gun, on the mating surface of the end cap and the ring skidded along the jig by the temporary stressing cables until the faces meet. Sufficient pressure is then applied by the cables to ensure that an even joint of mortar is formed between the ring and end cap.

6. Pressure is maintained until the epoxy mortar is set. The jacks are then released and the thrust pads removed from the free face of the ring.

7. Subsequent rings are jointed in a similar manner and finally the other end cap is placed and jointed.

8. The temporary stressing cables are then removed, the permanent stressing cables threaded, stressed, grouted and anchorages protected.

9. The axial stressing platforms are then removed and the mooring points stressed to the end caps.

10. The assembly jig is then tilted by hydraulic jacks so that the completed cylinder rolls onto launching trolleys which then transport it down a ramp into the water, where it floats off the trolleys and they are returned up the ramp for re-use (Figs. 4.6 and 4.7).

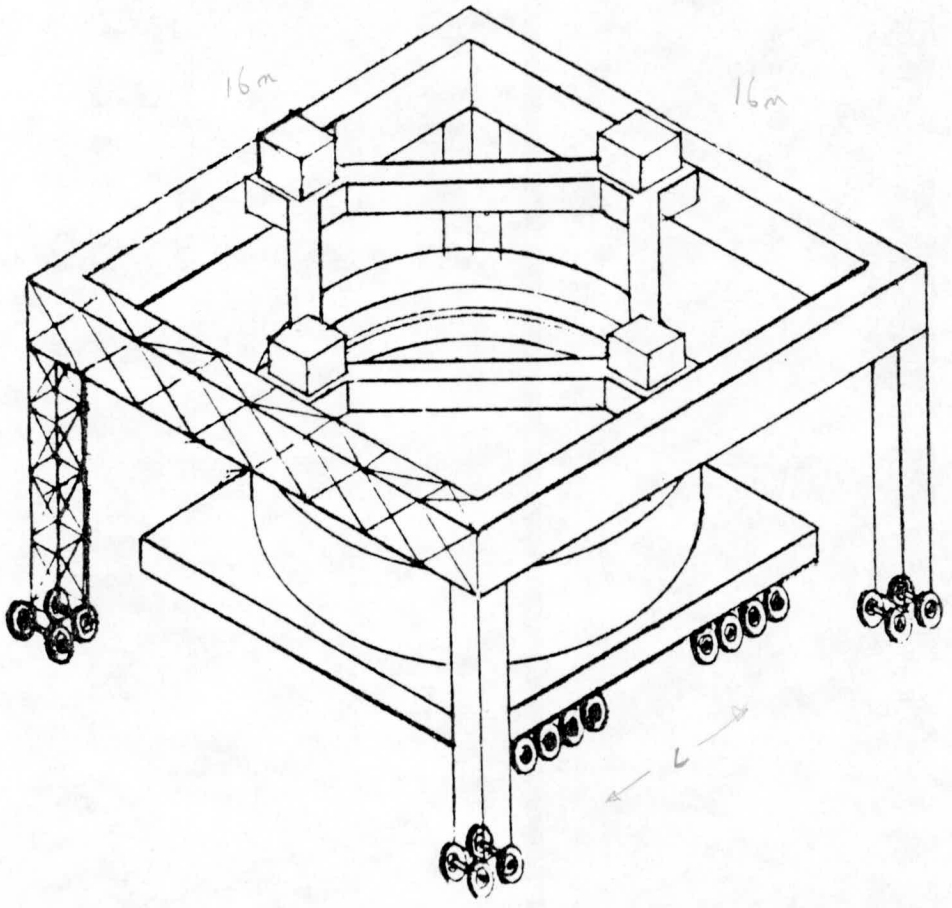

SKETCH SHEWING PRINCIPLE OF MOBILE STRADDLE GANTRY.

LATTICE CONSTRUCTION SHEWN IN PART ONLY.
LEG BRACES OMITTED FOR CLARITY.
WHEELS RETRACTED OR SPUD FEET EXTENDED WHILST LOAD IS ON GANTRY.
HOISTING BY SYNCHRONISED WINCHES IN POSITIONS SHEWN.

SCALE - 1 : 200 BHRP 26 OCT 79

Read $L = L \times \frac{1}{0.866} \times 200$

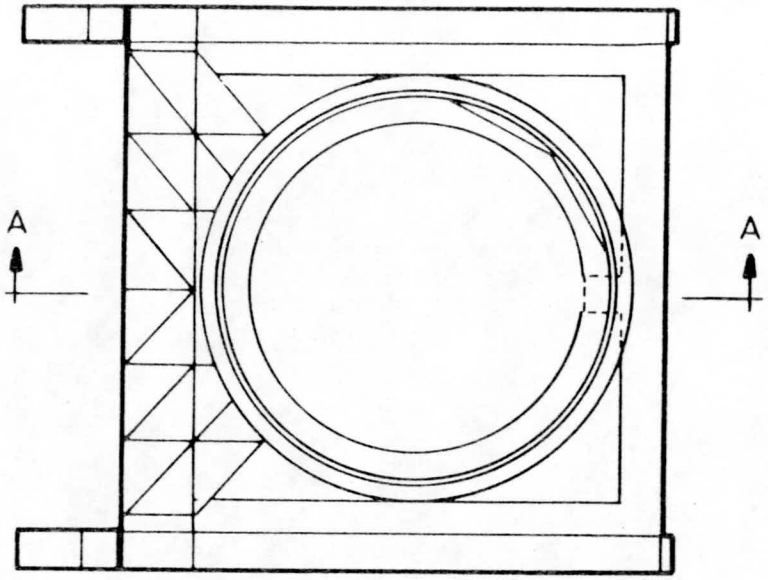

Plan of Tilting Table With Pit Under

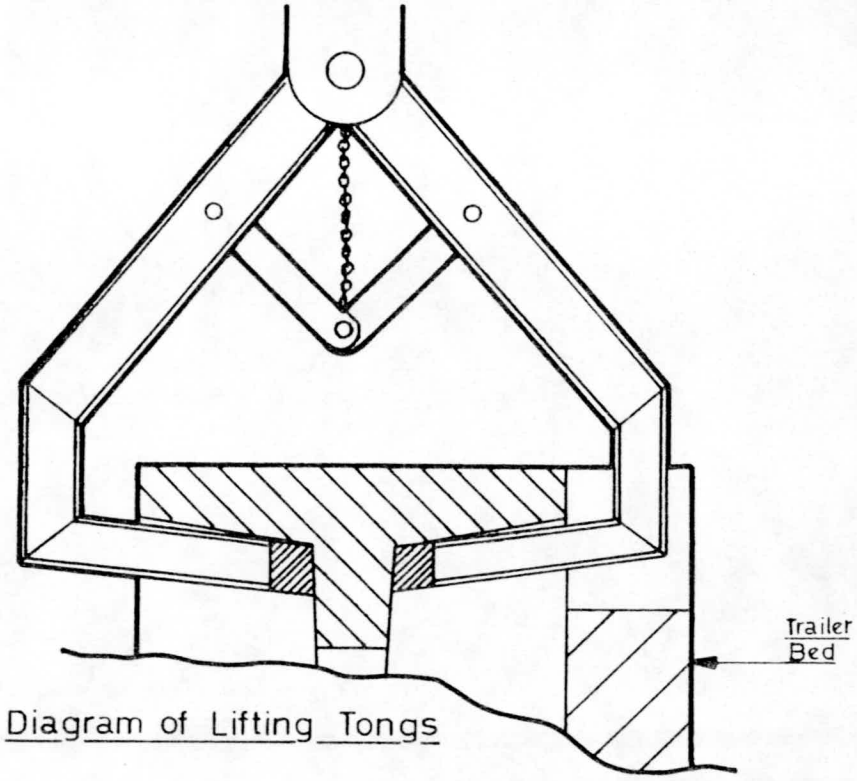

Diagram of Lifting Tongs

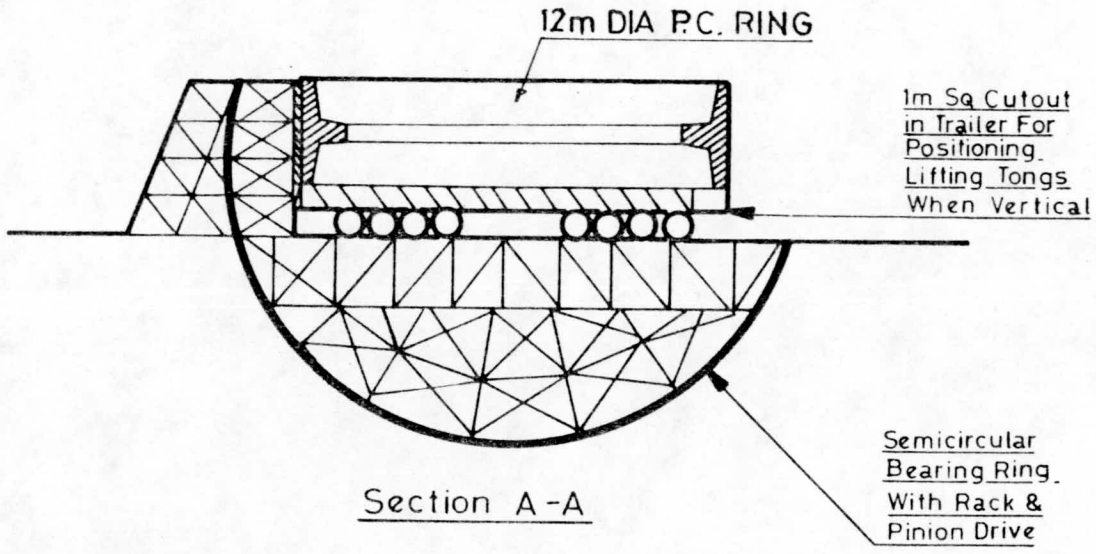

Section A-A

Sketch Showing Ring on 64 Wheeled 300T Trailer Loaded on Table With Ring Bearing Against Arch Support Ready For Tilting to Vertical Position Under Goliath.

FIGURE 4.4

SKETCH SHOWING SEGMENT ABOUT TO BE JOINTED WITH TEMPORARY CABLES, JACKS & THRUST PAD.

SCALE:-1:200 12th OCT'79

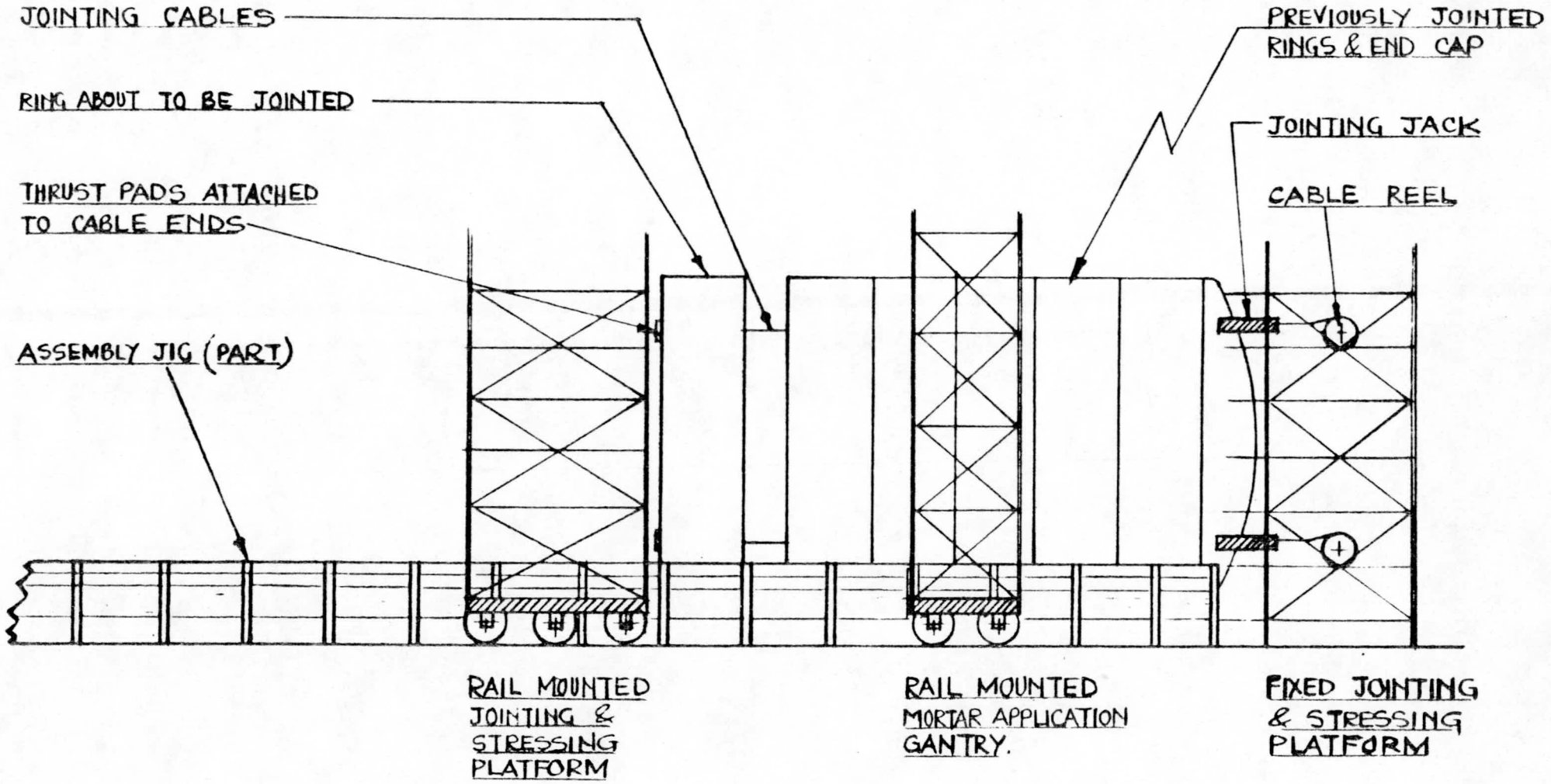

FIGURE 4·5

SKETCH SHOWING PRINCIPLE OF TRANSFER FROM ASSEMBLY JIG TO LAUNCHING TROLLEYS

SCALE 1:100 12th OCT '79

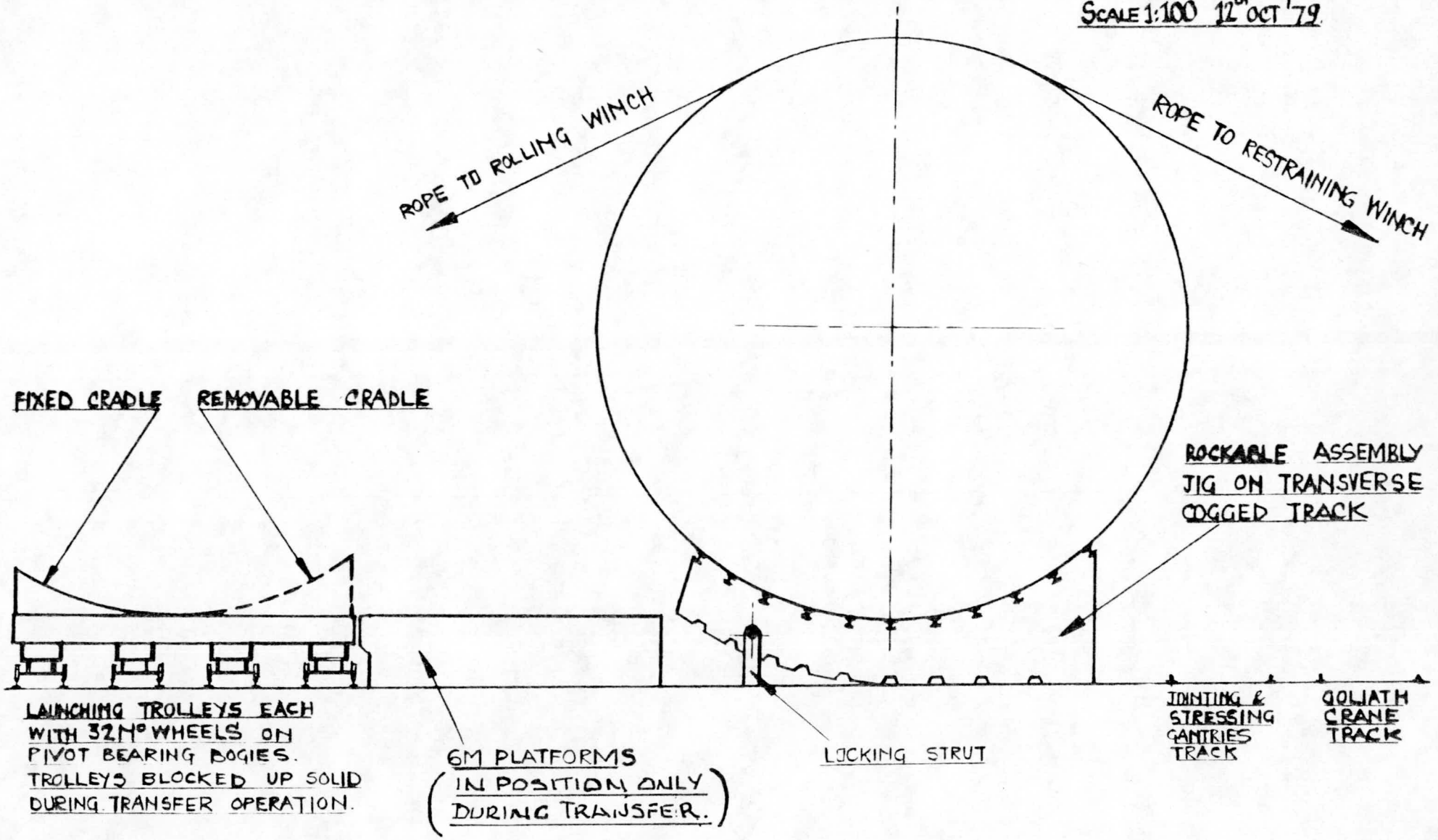

FIGURE 4.6

SKETCH SHOWING COMPLETED CYLINDER ABOUT TO BE LAUNCHED & GOLIATH BRINGING IN FIRST RING OF NEXT CYLINDER

SCALE:- 1:1250 16th OCT '79

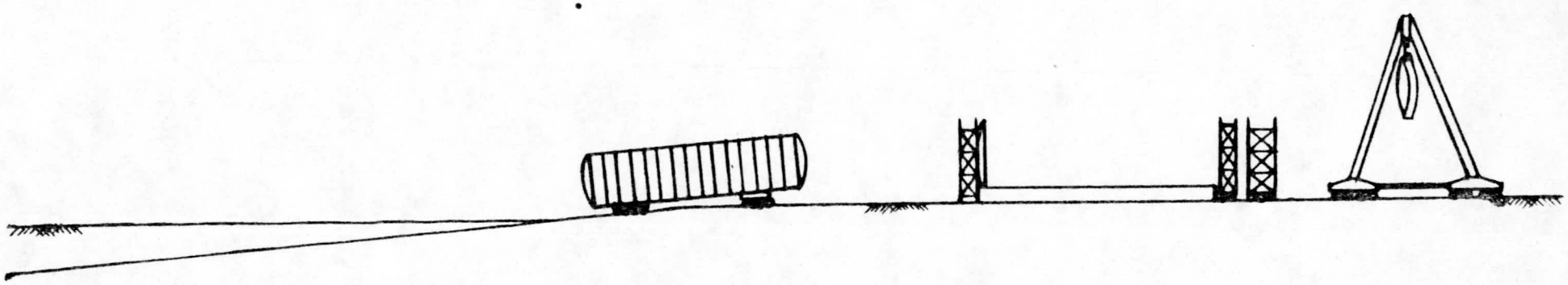

FIGURE 4-7

Assembly Jig - Brief Description (Figs. 4.5 and 4.6)

The assembly jig consists of a steel structure approximately 8m wide x 50m long, capable of rocking sideways through 45° whilst under firm control. The upper surface consists of rails set to a curve of 6m radius crosswise and horizontal longitudinally.

At one end is a fixed structure supporting platforms for stressing and jointing. At the other is a similar structure which can move along the length of the jig for restraint of the sections during jointing and for eventual permanent stressing and sealing of stressing anchorages.

Alongside the jig is a rail track for the launching trolleys, which describes a vertical curve down a ramp under water to a depth of approximately 8m (Figs. 4.1 and 4.7).

Reference should be made to the attached programme which illustrates the time necessary to obtain the heavy equipment, set up the construction facility and commence installation of the cylinder units.

(B) An alternative method of construction consists of one Precast End Cap, a Slipformed cylinder wall and one In-situ End Cap. Stiffening ribs are formed in steel at 3m centres with two watertight bulkheads, also in steel. The ribs and bulkheads are positioned after the slip of the cylinder and jointed to the cylinder wall by packing with epoxy mortar (Fig. 4.9).

Construction Sequence - Slipformed Cylinders with Steel Ribs

1. End Caps are precast with dead end anchorages for Macalloy stressing bars, cured, mooring points fitted and transported to a loading basin by 325 Tf Goliath crane.

2. Three End Caps are placed onto a floating pontoon with prepared sockets (Fig. 4.9).

3. The Pontoon is towed to and moored alongside a Construction Jetty in a minimum water depth of 40m (Fig. 4.10).

4. A combined slipform shutter for the three cylinders is set up on the End Caps with a concrete distribution boom mounted on the shutter construction (Fig. 4.11).

SUBMERGED CYLINDER DEVICE

PRECAST CONSTRUCTION

FIG 4·8

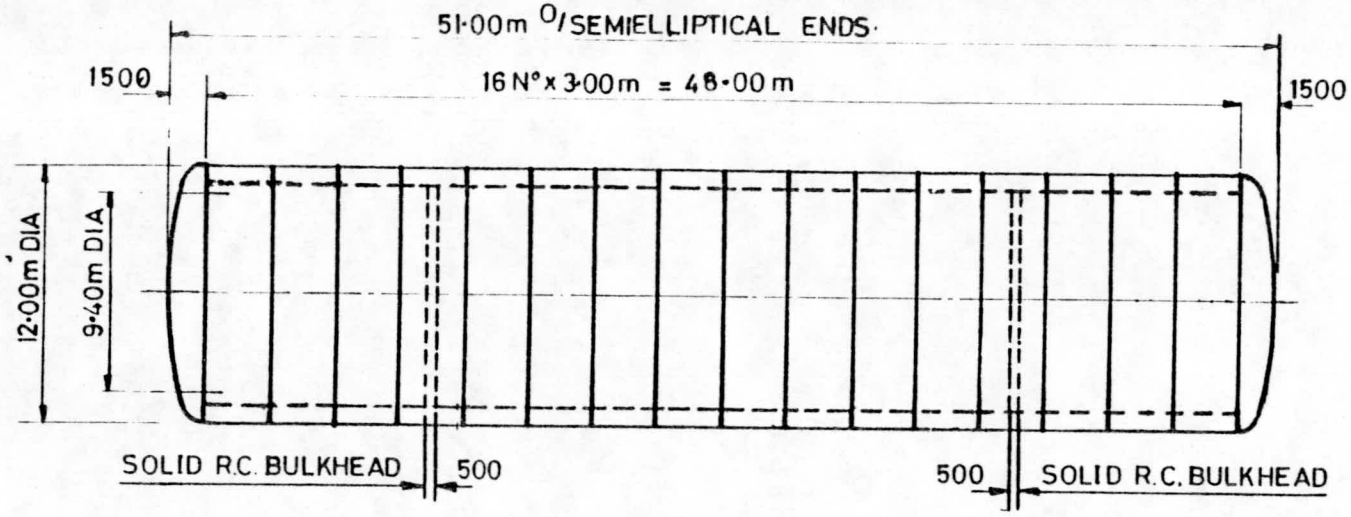

ELEVATION

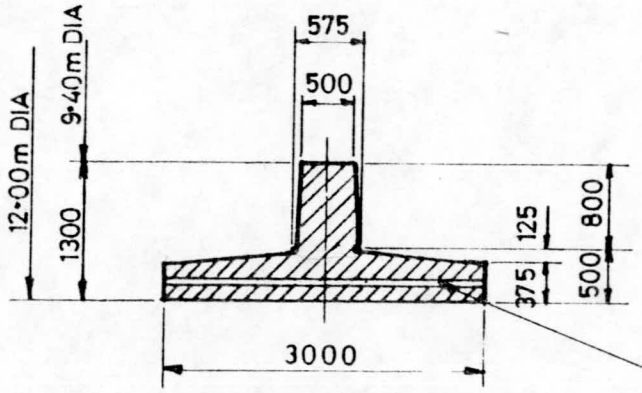

RING SECTION FOR HORIZONTAL POST TENSIONING ASSEMBLY

75mm DIA DUCTS EACH FOR 7N° 18ϕ DYFORM STRANDS

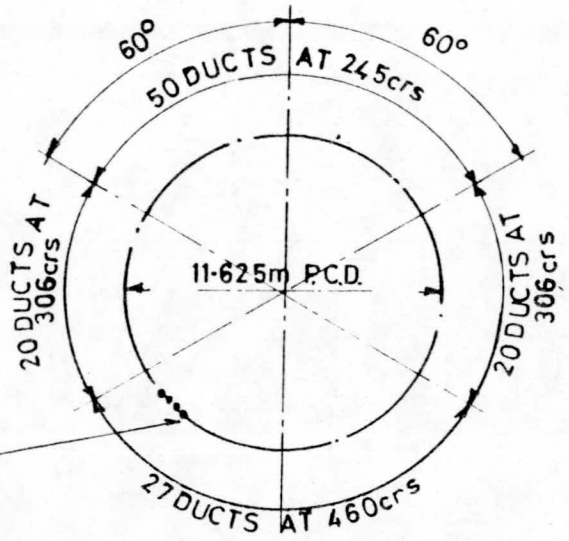

DUCT SETTING OUT

N° OFF DUCTS = 50 + 20 + 20 + 27 = 117 TOTAL

N° OFF STRANDS = 7 x 117 = 819 TOTAL AT 18mm ϕ

SUBMERGED CYLINDER DEVICE

SLIPFORM CONSTRUCTION

FIG. 4·9

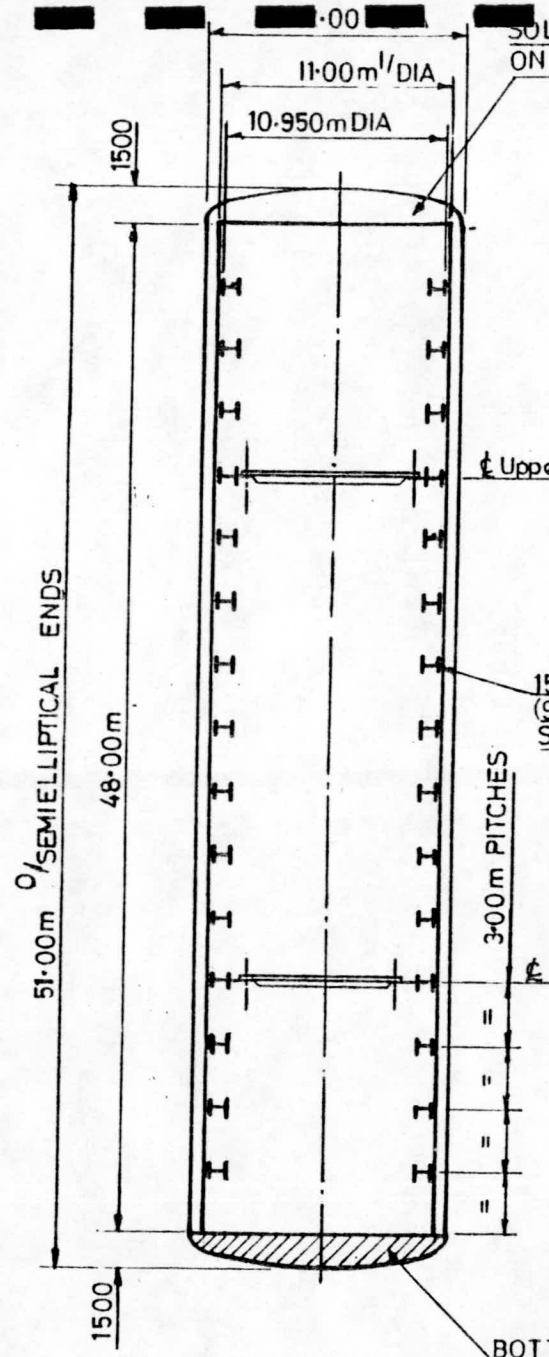

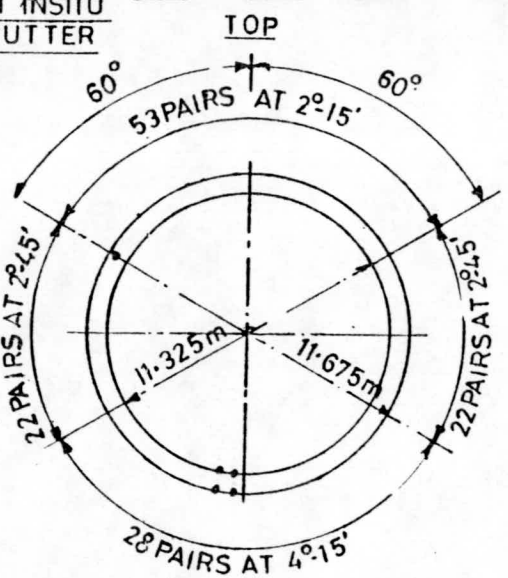

TENDON SETTING OUT

TUBE IS POST TENSIONED AS SLIP PROCEEDS, USING 40ϕ MACALLOY BARS IN DUCTS. — IN 2N°ANNULAR RINGS AT 11·675m & 11·325m P.C.D.

N°OFF TENDONS = 2(53+22+22+28) = 250

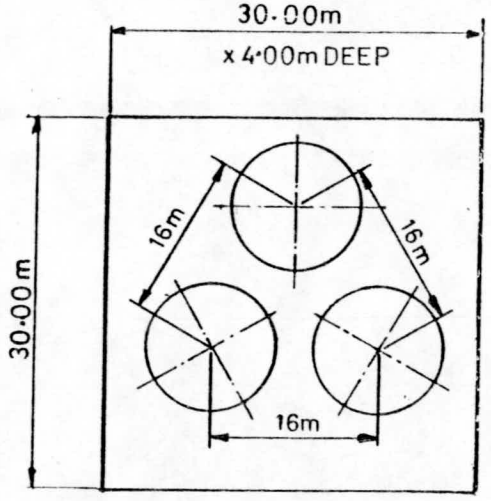

VERTICAL SLIPFORMING ON STEEL PONTOON. 3N° UNITS BRACED TOGETHER.

PONTOON DESIGNED FOR 14·00m MAX. IMMERSION

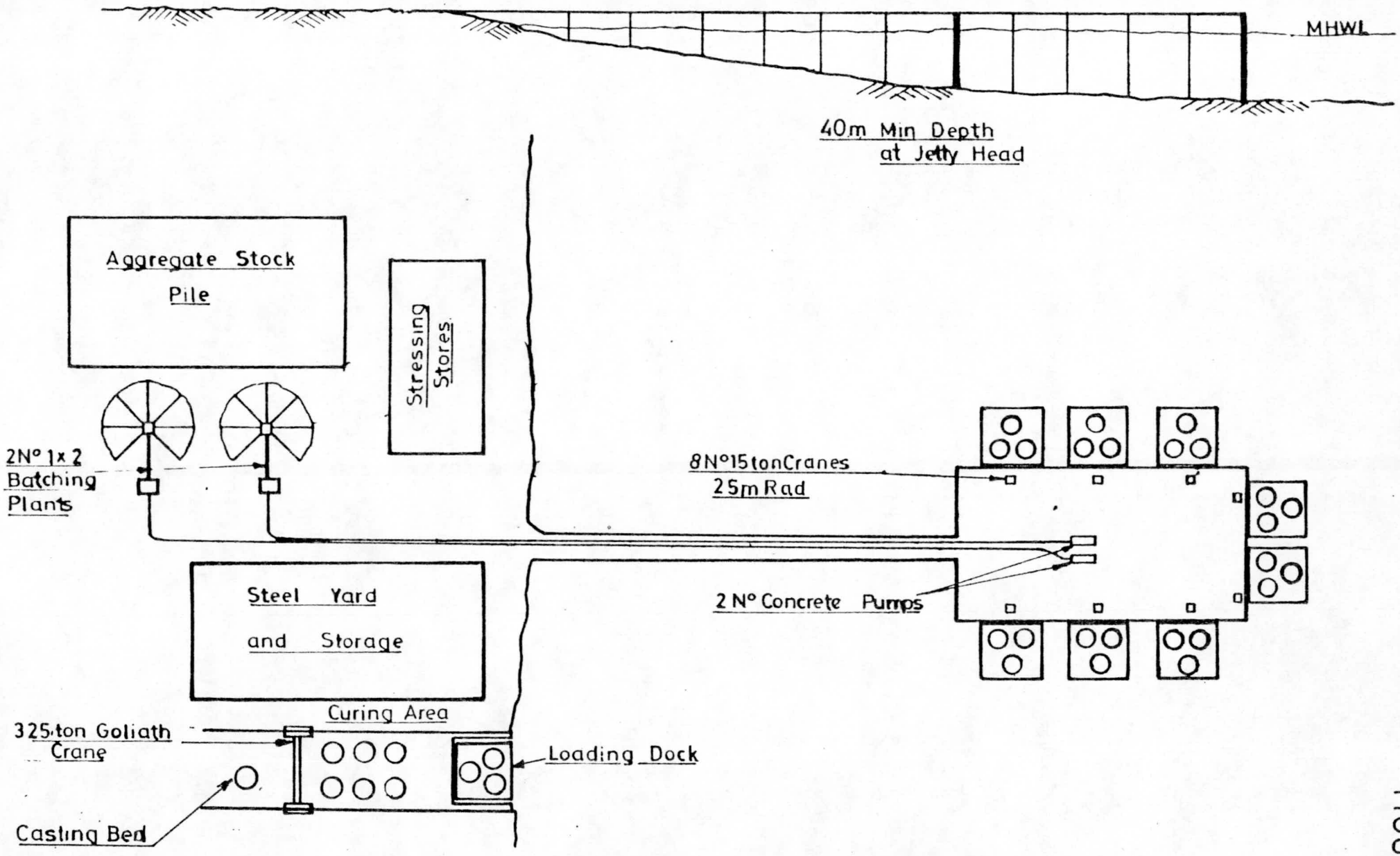

SLIPFORM CONSTRUCTION

LAYOUT OF FACILITY FOR PRODUCTION OF 2N° S.C.W.I.D.S. PER WEEK

FIGURE 4·10

Fig 4·11

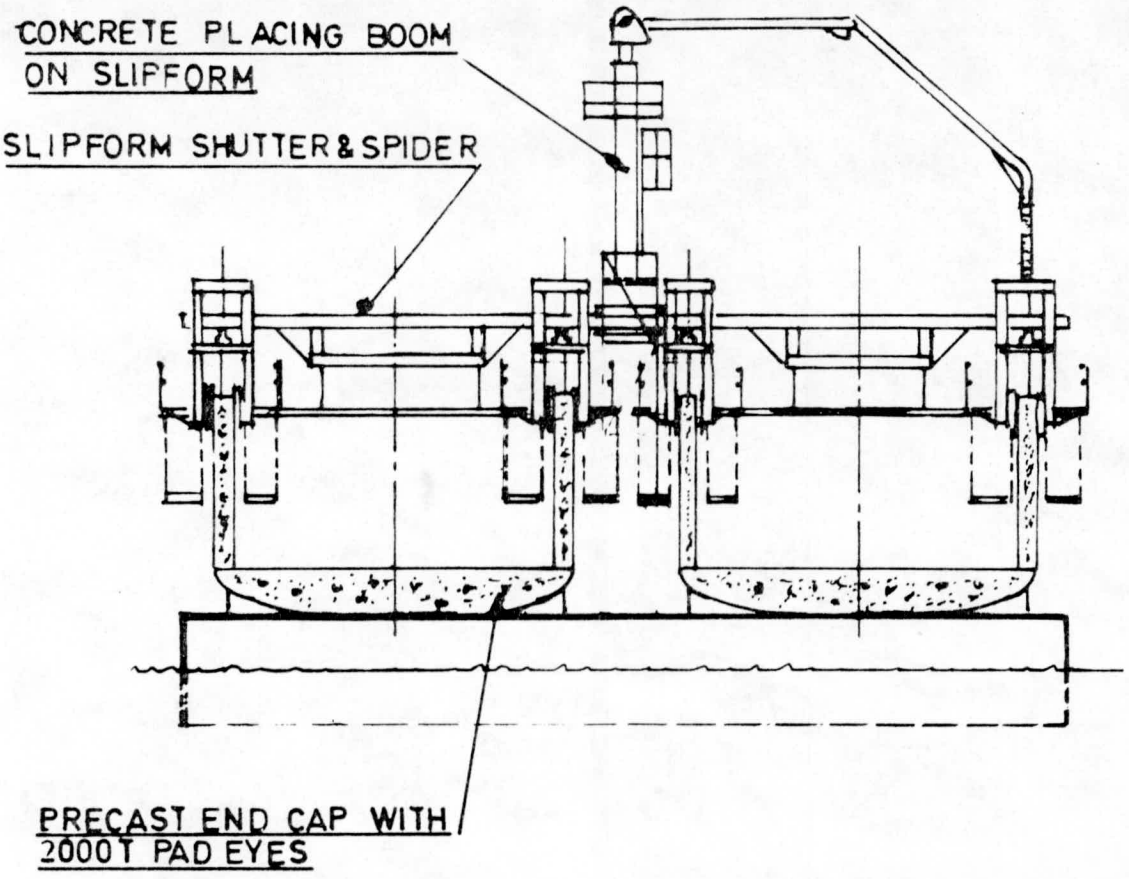

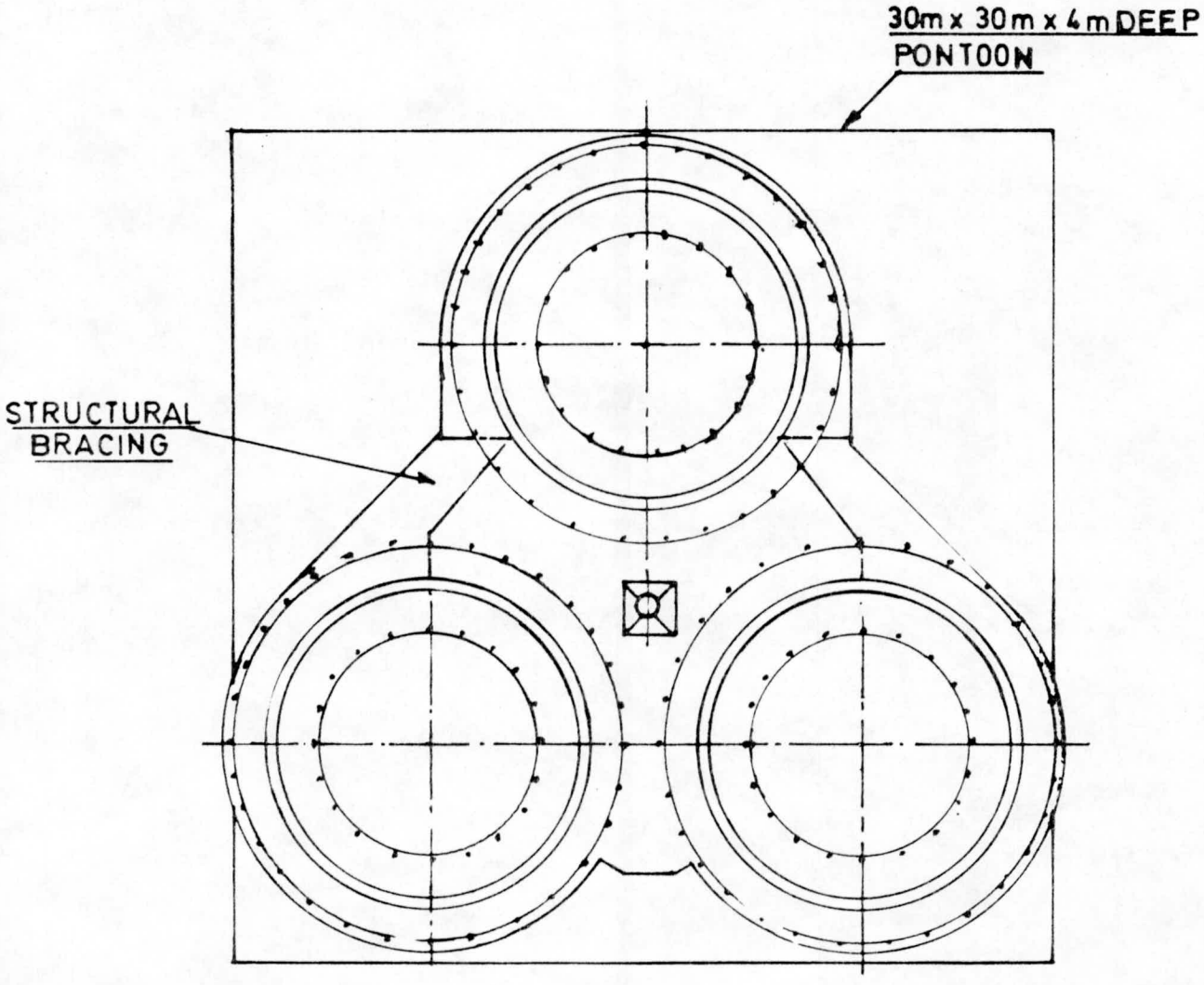

3 UNIT VERTICAL SLIPFORMING ON STEEL PONTOON

5. The three cylinders are slipformed in one continuous 8 day operation. The cylinders are bracketed and strapped together as the slip proceeds.

6. When the slipformed cylinder walls have reached a height of 14m above the P.C. End Cap, the Pontoon is ballasted down and removed for reloading with three more End Caps. At this stage, the three partly formed cylinders will float with approximately 4m freeboard.

7. At completion of the slip, the slipform shutter will be removed, cleaned and re-erected on the next pontoon and end caps.

8. During the slip of the cylinder walls, plates will have been cast into the inner surface at 3m height intervals, 3 plates at each level.

9. A scaffold tower with cantilevered extensions will then be commenced inside the cylinder and brackets will be welded to the cast-in plates at the lowest position.

10. The first steel stiffening rib will then be lowered into the cylinder until it rests on these brackets. The gap between the outside of the rib and the inside of the cylinder will then be caulked at the bottom and filled with epoxy mortar.

11. The scaffold tower will be extended to the level of the next rib and the same process repeated. All ribs will be fixed in this manner and the scaffolding lifted out of the cylinder.

12. The fourth ribs from each end of the cylinder will be specials, having an internal flange onto which can be bolted, with a gasket to ensure watertightness, a steel disc to form the watertight bulkheads. These discs will then be lowered into position and bolted to their respective flanges. The lower disc will be smaller than the upper in order to allow it to pass through the upper flange.

13. A lost shutter is placed on the top of the cylinder and the top end cap is cast in-situ.

14. When the top end caps are sufficiently cured, the Macalloy rods, which have been extended up the cylinder as the slip progresses, will be stressed and grouted, utilising grout tubes cast in with the ducts.

15. The anchorages will then be sealed and protected whilst the mooring point padeyes are bolted onto the end caps.

16. All construction equipment, with the exception of the brackets and straps linking the three cylinders, will then be removed.

17. The three linked cylinders will then be towed to deeper water where they will be ballasted down until they are individually stable and the brackets and straps removed.

18. They will then be separated and the ballast water pumped out so that they float horizontally, ready for tow to site.

SECTION 5

POWER TAKEOFF SYSTEM

5.1 Introduction

The power takeoff system consists of units mounted on the sea bed (see photograph of model and Fig. 5.1). These :

1. provide the restraining force to counteract the cylinder buoyancy in a resonant system.
2. pump sea water to a water turbine (as mentioned in Section 1 the decision in favour of hydraulic rather than electrical coupling between cylinders, leading to a 'central' turbine, was taken at the start of this Study. We appreciate that this choice could be reversed by the outcome of on-going generic studies, in which case the details that follow here would have to be changed to suit).

The design point for each unit was taken to be 600 kW output with a stroke of 2.4m with a ten second period. The maximum power per unit is then 900 kW with a stroke of 3.6m. The possible case for higher ratios of power/stroke, as implied in Section 2.1, could be accommodated by adjusting the details give below.

The design philosophy is to employ existing technology and use standard components wherever possible. Robustness and simplicity are essential where installation and maintenance are expensive and hazardous.

5.2 Design Limitations

In order to produce a design for the units, certain limits are placed on the main variables. In the extreme wave height conditions the cylinder orbit might be in excess of 9m. The present design limits the stroke to 4m to keep ram velocity, hydraulic accumulator capacity and maximum spring force within realistic limits.

The water pump pressure differential should be as high as possible in order to reduce the water flow rate and piston area. On the other hand high pressures lead to increased leakage losses and dictate the use of Pelton Wheel Turbines rather than Francis turbines. The present design is based on 5.25 MPa (approx.750 lb/in^2) which leaves the turbine choice open.

Fig 5.1

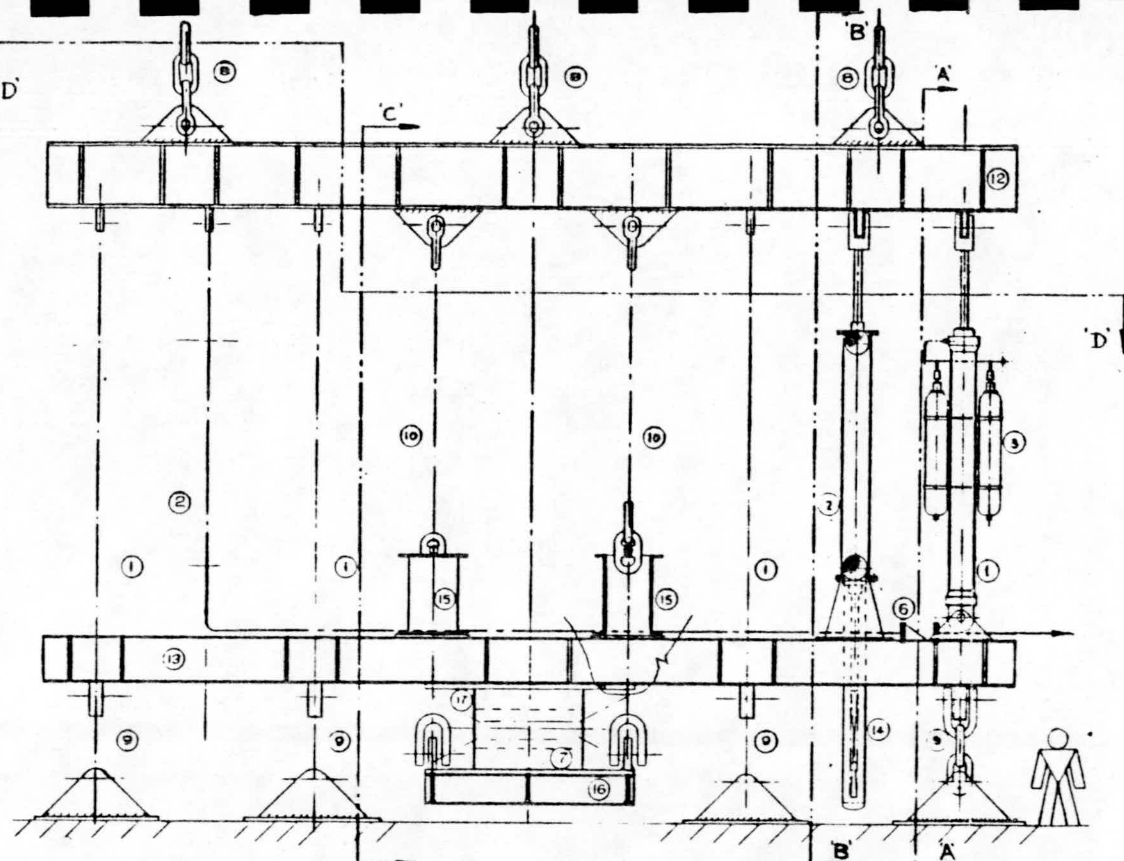

ELEVATION

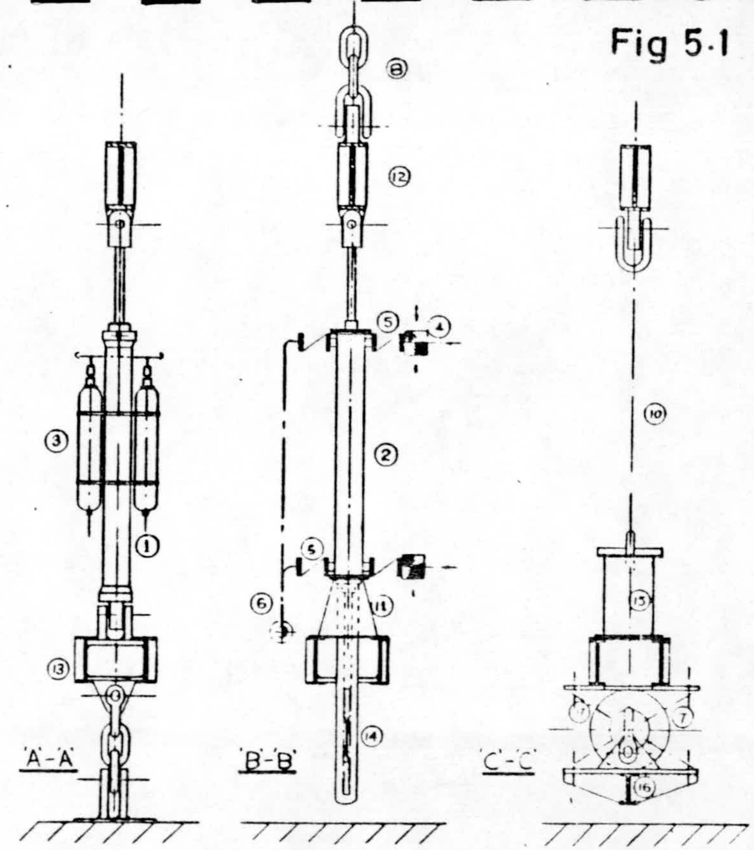

END ELEVATIONS SEE NOTE 4

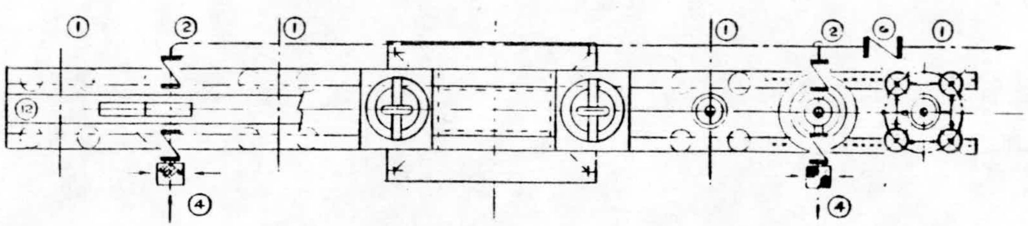

PLAN 'D'-'D'

ITEM Nº	Nº OFF	DESCRIPTION
1	4	HYDRAULIC RAM - STROKE - 4M BORE - 400MM
2	2	DOUBLE ACTING PUMP - STROKE 4M
3	6	ACCUMULATOR
4	4	BASKET TYPE SEAWATER INLET STRAINER
5	8	8" NON RETURN VALVE
6	1	10" NON RETURN VALVE
7	1	DUNLOP HOLLOW CYLINDRICAL RUBBER FENDER
8	3	RETAINING CHAINS (150 mm)
9	4	SEABED ANCHORING ASSEMBLY
10	2	FENDER LOADING CHAINS (30 mm)
11	2	PUMP SUPPORT SKIRT
12	1	UPPER MAIN BEAM (270 x 560)
13	2	LOWER EQUIPMENT SUPPORT BEAM (770 x 420)
14	2	PUMP SHAFT GAITER
15	2	FENDER CHAIN GUIDES
16	1	FENDER LOADING PLATFORM
17	4	FENDER LOCATING CHAINS

NOTES

1. POWER TAKE-OFF UNIT SHOWN AT APPROX MID POSITION IE 2M STROKE
2. UNIT TOTAL STROKE 4M
3. FENDER LOADING CHAINS WILL BE IN TENSION DURING TOP 1M OF STROKE
4. END ELEVATIONS SHOWN WITH AXIS VERTICAL FOR CONVENIENCE. IN OPERATION AXIS IS AT 45° TO VERTICAL.

DATE	ISS	DESCRIPTION	DRN	CHD	APP
[illegible]	4	REVISED [illegible] STUDY	[illegible]		
[illegible]	3	FIRST DESIGN STUDY	PJW		
[illegible]	2	REVISED PRELIMINARY	PJW		
[illegible]	1	[illegible]	[illegible]		[illegible]

HUMPHREYS & GLASGOW, LTD. LONDON SW1

PLANT
CLIENT WAVE ENERGY STUDY
LOCATION

SCALE 1:50 | DRAWN [illegible] | CHECKED | APPROVED
A1 SHEET | ORIGINAL FRAME SIZE 584 x 841 MM

TITLE LAYOUT OF 'POWER TAKE-OFF UNIT'

DRG No C0231-L50-001

SCALE ~ 133 1:1 / mm plot

The maximum working pressure for the hydraulic system is 300 bar, limited by the rating of available accumulators. A higher pressure, (say 400 bar which is possible for the rams), should be considered for future designs to minimise capacity, if higher pressure accumulators can be found.

5.3 Basic Design

The philosophy and limitations already described lead to a design of power takeoff unit which is a linear array of four hydraulic rams, each with four accumulators, two water pumps and a stroke limiting device. These items are arranged in parallel between two beams, one attached to the cylinder rodes and the other attached to the sea bed. The action of the hydraulic rams is always to pull the beams together. The linear arrangement allows the unit to sway by a few degrees with the rode motion and makes possible the use of a number of anchoring attachments. Alternatively, the units could be secured in a horizontal position and connected to the inclined rodes by pivoted rocker arms. The items are spaced out to allow for individual inspection and replacement.

5.4 Beams

The top beam is designed for the attachment of three chains with a maximum storm loading of 700 Tf per chain (2100 Tf per corner). The lugs for shackles are spaced to minimise the bending moment on the beam. The beam could be an I-section 1200mm x 500mm fabricated from 50mm plate for the web and 75mm plate for the flanges. Stiffening webs on both sides are employed at the attachment locations.

The bottom beam could consist of two universal beams 914mm x 418mm, side by side with a space between. Plates are welded between the beams at intervals. The skirts of the pump bodies are mounted on top of the beams. The anchoring is to lugs welded to the transverse plates. The hydraulic ram ends are pinned through two lugs, one on top of each beam. The dummy piston rod on the pumps and the chains for the stroke limiting device pass between the beams.

5.5 Pumps

The two pumps are double acting with piston rods connected to the top beam. A dummy piston rod is used at the bottom to provide guidance and prevent buckling on the down stroke. The cylinder bore is 420mm with 150mm diameter piston rods. The cylinder ends contain rod guides and simple seals.

The flow control is by means of externally mounted check valves. On the inlet valves strainer baskets are fitted. The outlet valves are manifolded through a secondary check valve for the whole unit. This allows for the removal or servicing of one pump without the requirement for isolating valves. The active piston rod is connected by a pin joint to the top beam. The bottom of the cylinder is supported on a conical skirt mounted on the bottom beams.

The pump pressure differential is 5.25 MPa giving a rod load of 63 Tf. The pressure regulation will be at the turbine, but blow-off valves should be provided for each complete cylinder system (i.e. four power takeoff units).

The dummy piston rod is encased in a rigid closed cylinder projecting between the bottom beams.

5.6 Hydraulic Springs

Each hydraulic ram has a piston diameter of 400mm and a rod diameter of 150mm giving a force of 325 tonnes at the maximum working pressure of 300 bar. Each ram is single acting and directly connected to four nitrogen filled bag type accumulators of 200 litres capacity. The nitrogen and oil fills are arranged to give a ram force of 1200 tonnes at full stroke and 770 tonnes (buoyancy load) at mid stroke.

The rod is protected by a rubber gaiter which may require to be pressurised with air. The accumulators are mounted round the ram and supported by it. The accumulators are coupled via a short ring main to the ram using the shortest possible pipe lengths.

The unpressurised end of the ram would be evacuated. Should this prove impracticable after endurance tests, an alternative arrangement would use essentially unpressurised hydraulic fluid connected to a bladder subjected to constant external pressure.

5.7 Stroke Limiter

The device for limiting the stroke to 4m employs chains and a section of hollow cylindrical rubber fender under the bottom beams. Beyond 3m stroke the chains connecting the top beam to a platform beneath the bottom beams become taut. A further 700mm of stroke give a fender force of 240 Tf. The spring rate of the fender then increases and by 4m stroke the fender force is 1000 Tf. For short strokes the slack chain is held above the bottom beams by bars passing through the links resting on the bottom beams.

The maximum force is adjustable at the final design stage by varying the length of fender employed. The present design has a single 2m length of fender mounted in the centre of the unit.

5.8 Operating Conditions

It is recommended (Section 8) that a large scale model of a refined version of a power takeoff unit, probably much as described above, should be tested in the sea. This is needed to demonstrate the lifetime of its components, hence its maintenance costs. The growth rates of marine roughness on the pistons in conditions representing, say, their average movements during each month of the year (Appendix and Fig.A.4) is one of many important factors to resolve at an early stage.

5.9 Bus Pipes

The details given below are for hydraulic mains connecting the outputs of a large number of wave energy devices to a single turbine. The specification for the pipes was based on pump outputs up-rated from that given in Section 5.2 because of the advantages that such a change was subsequently found to give to overall system performance.

One pair of double acting pumps force sea water at a pressure of 5.25 MPa (= 750lb/sq.in = 527m head) into a 250mm bore flexible (reinforced plastic) pipe, including a non-return valve.

The flanged outer end of this feeder line is bolted to a 1.0m bus pipe, of assumed bore area 0.671m^2 inside the lining.

The maximum outputs of eight wave energy devices produce a total flow of 3.75m^3/s, hence a final velocity of flow in the bus pipe of 5.57 m/s. Total friction and entry losses on feeders and a bus pipe 3,000m long are 53m or 10%.

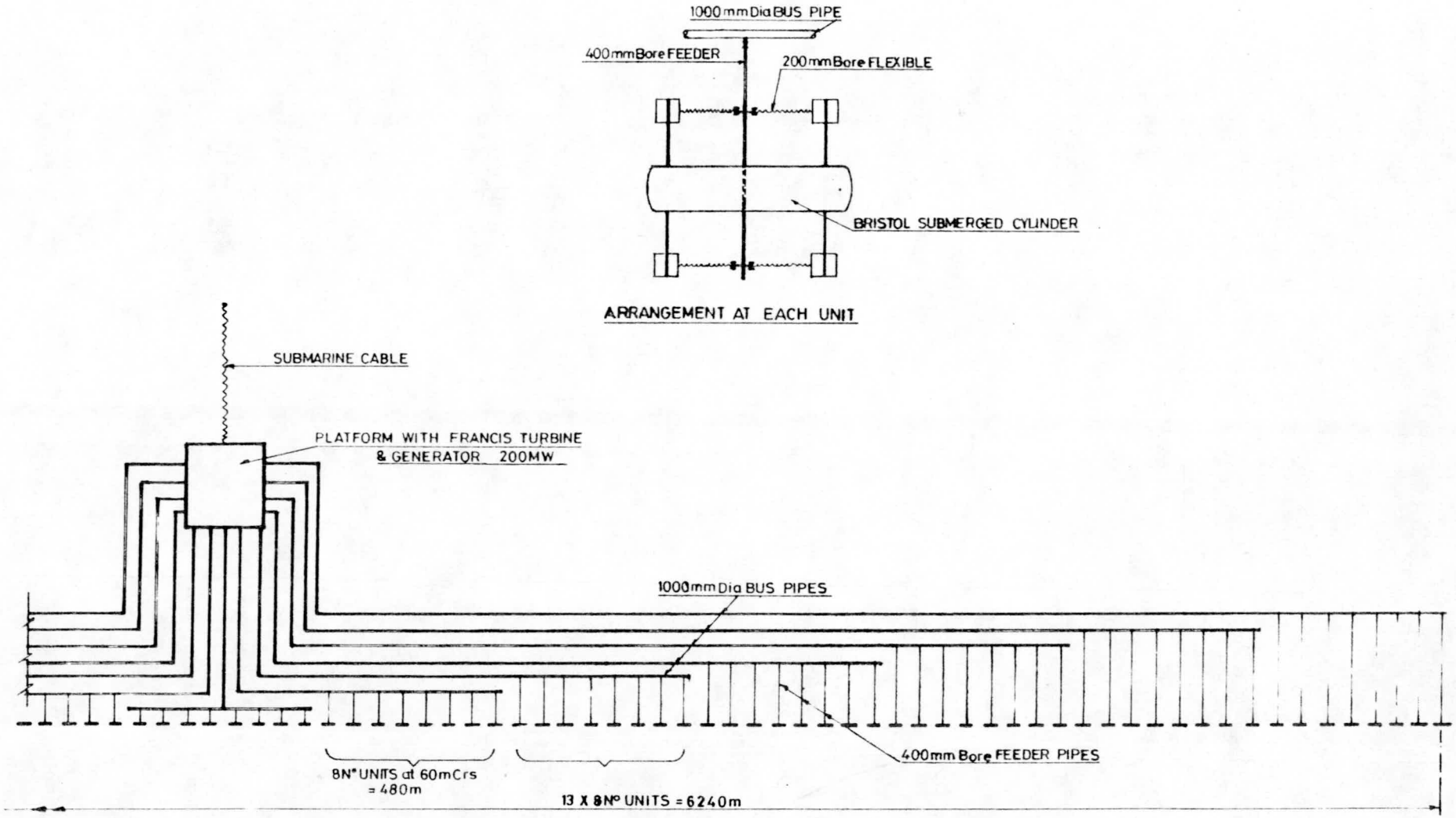

DIAGRAMMATIC LAYOUT OF SCWID UNITS, BUS PIPES & FEEDER PIPES, TO TURBINE & GENERATOR PLATFORM

FIGURE 5.2

Thirteen such bus pipes, but of generally shorter lengths, collect a nominal 208MW of captured energy, and deliver it, less an average of 7% friction and entry losses, to a Francis turbine driving a generator, both mounted above water level on a gravity-type platform.

The pipes are designed as thin walled, to BS.806, to an allowable tensile stress of 21,000 lb/sq.in. The hydraulic design assumed a roughness (k) of 0.06m. It is, of course, important that this roughness does not increase appreciably with time.

The bus pipe can span some 75m unsupported, but the end reactions may produce buckle propagation, hence long spans should be avoided. All pipes can be held in position by saddle weights to resist current and wave forces. Trawling would have to be forbidden.

Laying of pipes of this size at sea is common practice. The maximum feasible size at present is thought to be 1.5m but we are not proposing to use them in this scheme which has been based on well established technology.

5.10 Turbo-generator

Preliminary details of the principal dimensions and probable costs of turbines suited to the duty required have been received from two major manufacturers of this type of plant. A Francis-type unit of 200MW is likely to run at 428rpm (14 pairs of poles) and could be mounted above sea level on a platform (Section 5.11) with its axis either vertical or horizontal. Alternately, two units each of 100MW could be used. There would not appear to be a significant cost penalty in doing this, whereas conversion efficiencies from the variable flows delivered by the devices from, say, month-to-month (see Appendix) would be higher. The same trend towards more smaller turbines, but each coupled to fewer devices, would reduce the high cost of pipework, and may offer significant cost savings (Section 7.2).

5.11 Design of Gravity Platform

The turbines, generators and ancillary electrical gear are carried on gravity platforms of reinforced concrete construction. The design of these platforms would be in accordance with North Sea practice. The platform for 75m depth of water as designed last year, when amended for say 40m depth, could be sailed with all equipment completed, from a West Coast of Scotland yard, and remain stable on passage and during installation on the prepared sea bed by controlled flooding.

SECTION 6

ANCHORAGES

The seabed in the area West of South Uist is reported as of rock, uneven with a standard structural deviation for level of 4m, and with thin sedimentary deposits in depressions.

Under such conditions where drag anchors cannot be used, the choice of anchor is limited to either gravity or to tension piles.

Gravity Anchors

Gravity anchors depend on friction to prevent sliding and weight to develop friction and prevent uplift. The anchors should be light enough to float and if of roofed cellular form, strong enough to be ballasted down. They should preferably be without internal support from compressed air but have sufficient remaining volumes to take the water required to give the anchor its submerged weight. If the cellular anchor is not roofed, then uncontrolled flooding occurs during immersion, and heavy crane ships are needed to control the descent. Rapid ballasting with solid material must then follow. Both operations are weather sensitive.

We chose the roofed version, as being more tolerant to bad weather on tow and during placement; two versions have been prepared in reinforced concrete (Fig.6.1) and in grade 50 steel (Fig.6.2).

When installed, the water ballasted anchor has to resist wave and buoyancy forces on the cylinder as well as submerged wave forces on itself. These forces, horizontal and vertical, vary through a wave cycle.

Assuming the anchor caisson is landed on banks of tipped stone or middle chalk, the coefficient of static friction is only 0.25. A factor of safety of 1.6 is required against sliding. The required minimum caisson weight of 10,500 Tf per device is derived from Fig. 6.3, which also shows the cyclic forces for a 16 m wave of 11.75 seconds period.

SUBMERGED CYLINDER DEVICE
R.C. GRAVITY ANCHOR

FIG. 6·1

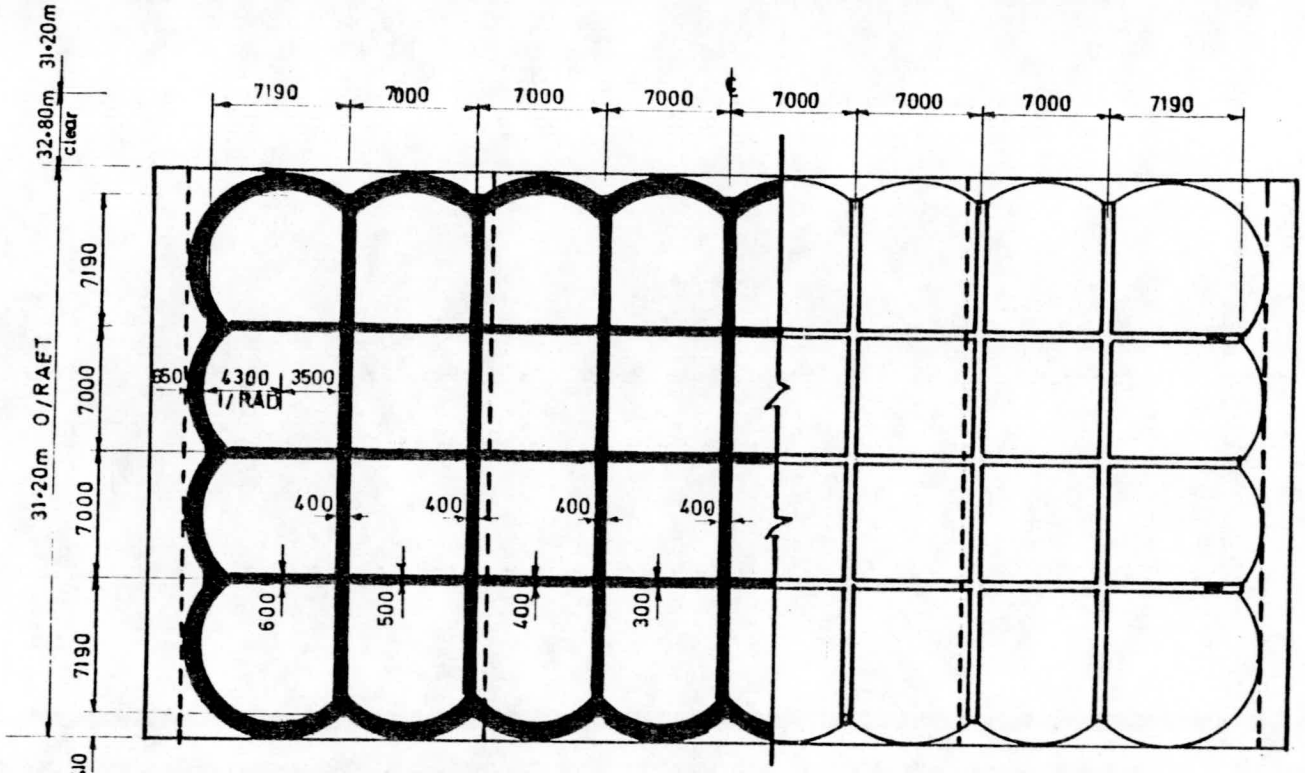

HALF PLAN ON WALLS

HALF PLAN ON ROOF

Concrete To Be Grade 50 N/mm²

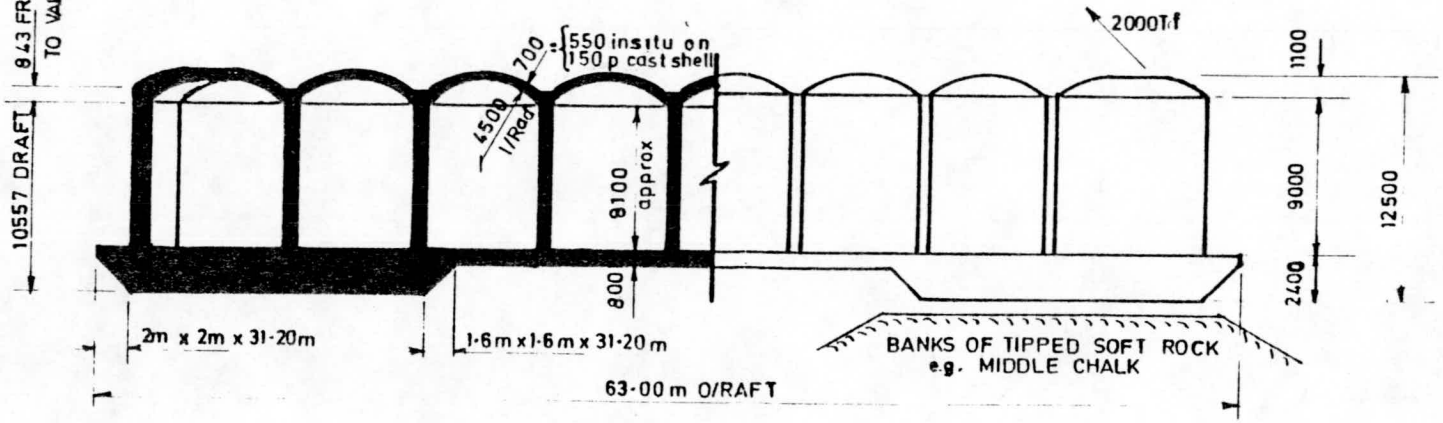

HALF ELEVATIONS

The preparation of the seabed is the same for either design of caisson. On a map of the seabed, contoured at say 0.5m intervals, the optimum location and orientation of each device is plotted, followed by plotting and quantifying the two mounds of tipped stone under each anchor. The seabed is signposted with transponders during the original survey, and these may be used again when tipping.

A pontoon, with its four energy conversion mechanisms and mooring chains and stub pipe water line, is towed into position slightly westwards of its final position and held by four tugs riding at anchor. An umbilical containing six each flood and vent lines is connected to a command ship. Partial flooding of the west end compartments takes that end under and flooding is continued until that end touches the bottom. Tugs correct its position and orientation as necessary, then flooding of all compartments is continued to completion.

A caisson ballasted to about 40° dip has a slow heave or roll response, and placing by ballasting ought to be possible in waves up to 2m high, which may be beyond the sea-state at which accurate positioning can be measured or controlled.

A caisson can be raised by blowing out ballast water with compressed air but it is safer and more controllable if built-in pumps are used. These would require a diver or mini-sub to connect umbilical power and control cables from a surface command ship.

Tension Piles

Spudable pontoons exist that can raise themselves out of water 60m deep and vertical holes of 2.5m diameter have been drilled under water into hard rock.

The requirement for a rode of 2,000 Tf capacity safe working load per corner of each device at 45° dip means that each cylinder requires four tension piles capable of resisting some 1,500 Tf vertically and horizontally.

Without knowing that the rock is unfissured and uncracked granite, it is prudent to limit the horizontal imposed loading on the rock to some 435 Tf/m^2 (40 tons/sq.ft). The pile is then of 2.5m dia. to keep bending and shear stresses down to manageable proportions. Also, if the rock is too broken to take tension, the necessary bond length is some 14m at 45° spread (Fig.6.4).

Proof of the existence of unbroken unmetamorphosed granite would lead to some reduction in pile diameter and length. The ability to drill into rock at an angle other than vertical would also lead to a reduction in pile diameter (Fig.6.5).

The construction procedure is as follows :-

Tugs tow the floating pontoon into position and hold it while the spuds are lowered to the seabed. The pontoon then climbs up the spuds using a 'caterpillar' jacking action. (Spuding and despuding on rock requires fairly calm seas - say wave height 1.0m maximum). All reachable holes are now drilled, working over the side. All holes are sleeved through sedimentary deposits and up to a common level per cylinder, then flushed out. An assembly of tension and shear reinforcement, and full depth grout pipe, all connected to a casting incorporating a padeye for a 2,000 Tf SWL shackle (pin dia. = 0.35m plus), is lowered into and orientated in the hole, which is then grouted up to overflowing from the pontoon.

It then only remains to connect the power take off device by a single shackle to the completed and matured tension pile.

Caution - it is possible that the bulk of a gravity anchor may adversely modify the surface and submerged wave motions over it. If the gravity anchor is more attractive than tension piles, this feature should be tank tested during Stage 3: it may require moving the devices to a correspondingly greater depth. Conversely it is possible that changes in shape of the gravity anchor ends could modify the wave to increase cylinder movement.

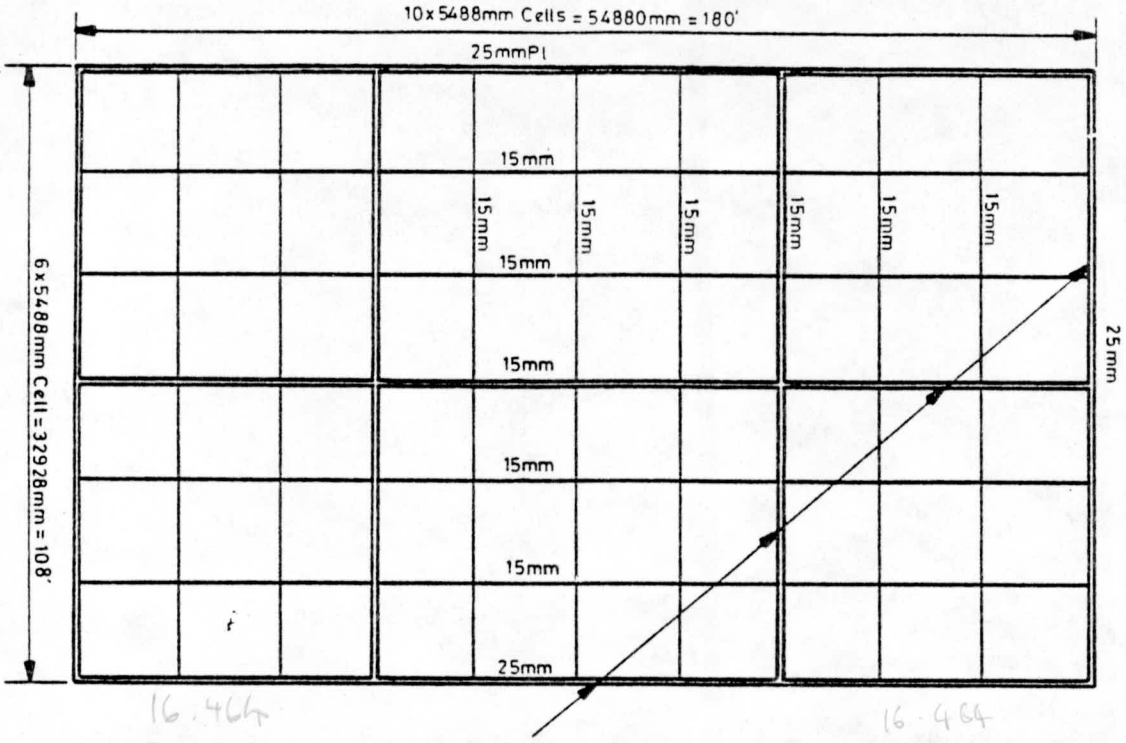

Water Tight Bulkheads To Provide 6 Separate Compartments. Each Compartment To Be Piped For Flooding & Venting By Umbilical. Cells In Each Compartment To Be Interconnected For Flooding & Venting.

PLAN

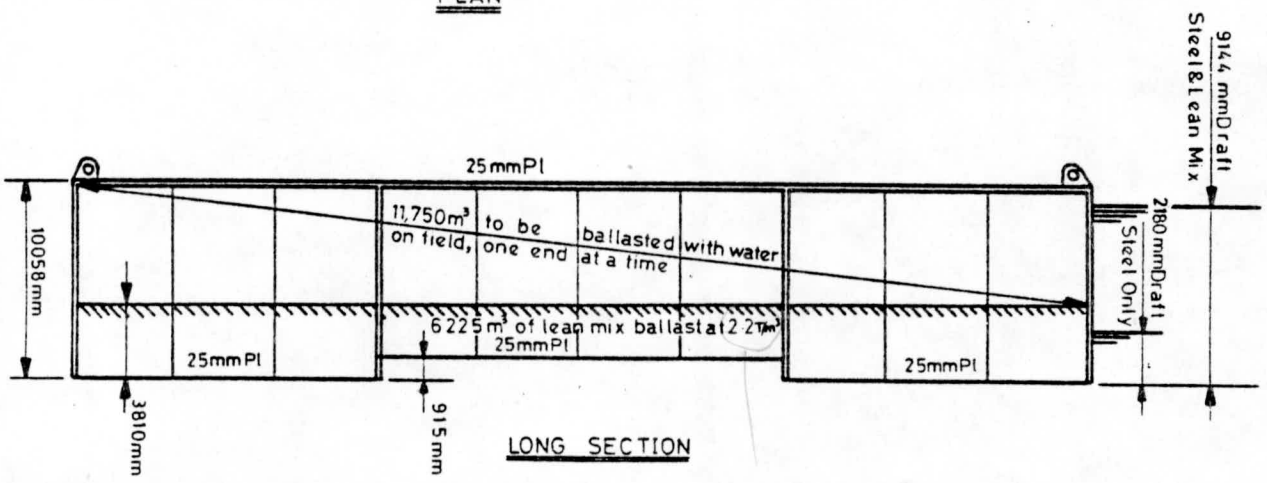

LONG SECTION

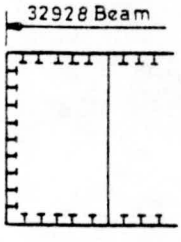

SCRAP CROSS SECTION

Showing Longitudinal Stiffeners of x Tees (Ex305x914x253kg/muc) At 914mm CRS Through Out On Perimeter Faces
Average Fillet Weld Size 13mm

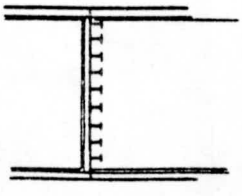

SCRAP VIEW OF TRANSVERSE INT' BULKHEAD

Showing 305x305x97 kg/m U.C. Props (2 Ways) To Long' Stiffeners
10 B/HD Thus

SUBMERGED CYLINDER DEVICE
STEEL GRAVITY ANCHOR

FIG. 6·2

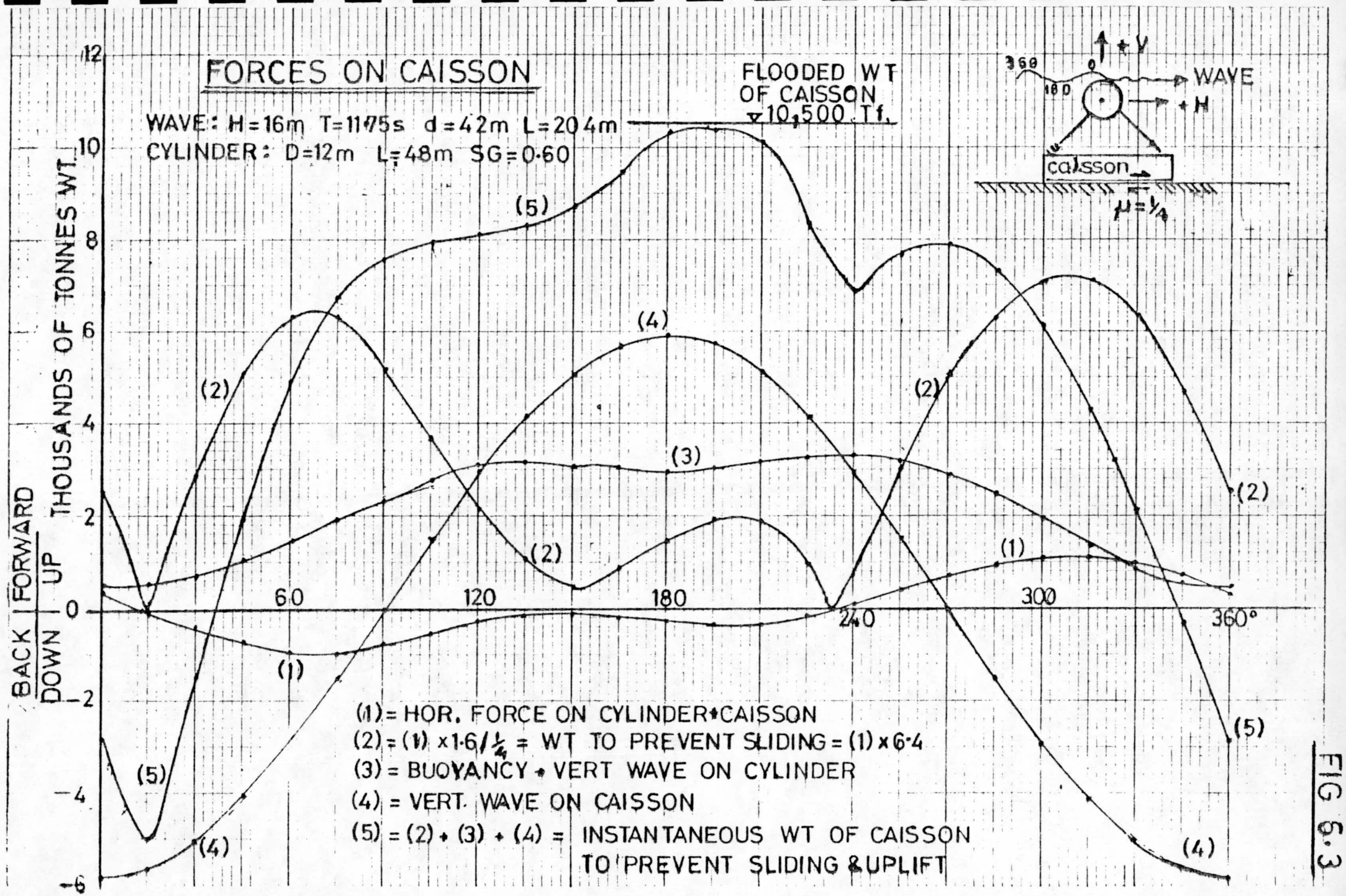
FORCES ON CAISSON
WAVE: H=16m T=11·75s d=42m L=204m
CYLINDER: D=12m L=48m SG=0·60
FLOODED WT OF CAISSON ▽10,500 Tf.
+V
360
0
180
WAVE
+H
caisson
μ=¼
BACK | FORWARD
DOWN | UP
THOUSANDS OF TONNES WT.
12
10
8
6
4
2
0
−2
−4
−6
60
120
180
240
300
360°
(1)
(2)
(3)
(4)
(5)
(1) = HOR. FORCE ON CYLINDER+CAISSON
(2) = (1) x 1·6/¼ = WT TO PREVENT SLIDING = (1) x 6·4
(3) = BUOYANCY + VERT WAVE ON CYLINDER
(4) = VERT. WAVE ON CAISSON
(5) = (2) + (3) + (4) = INSTANTANEOUS WT OF CAISSON TO PREVENT SLIDING & UPLIFT

FIG 6.3

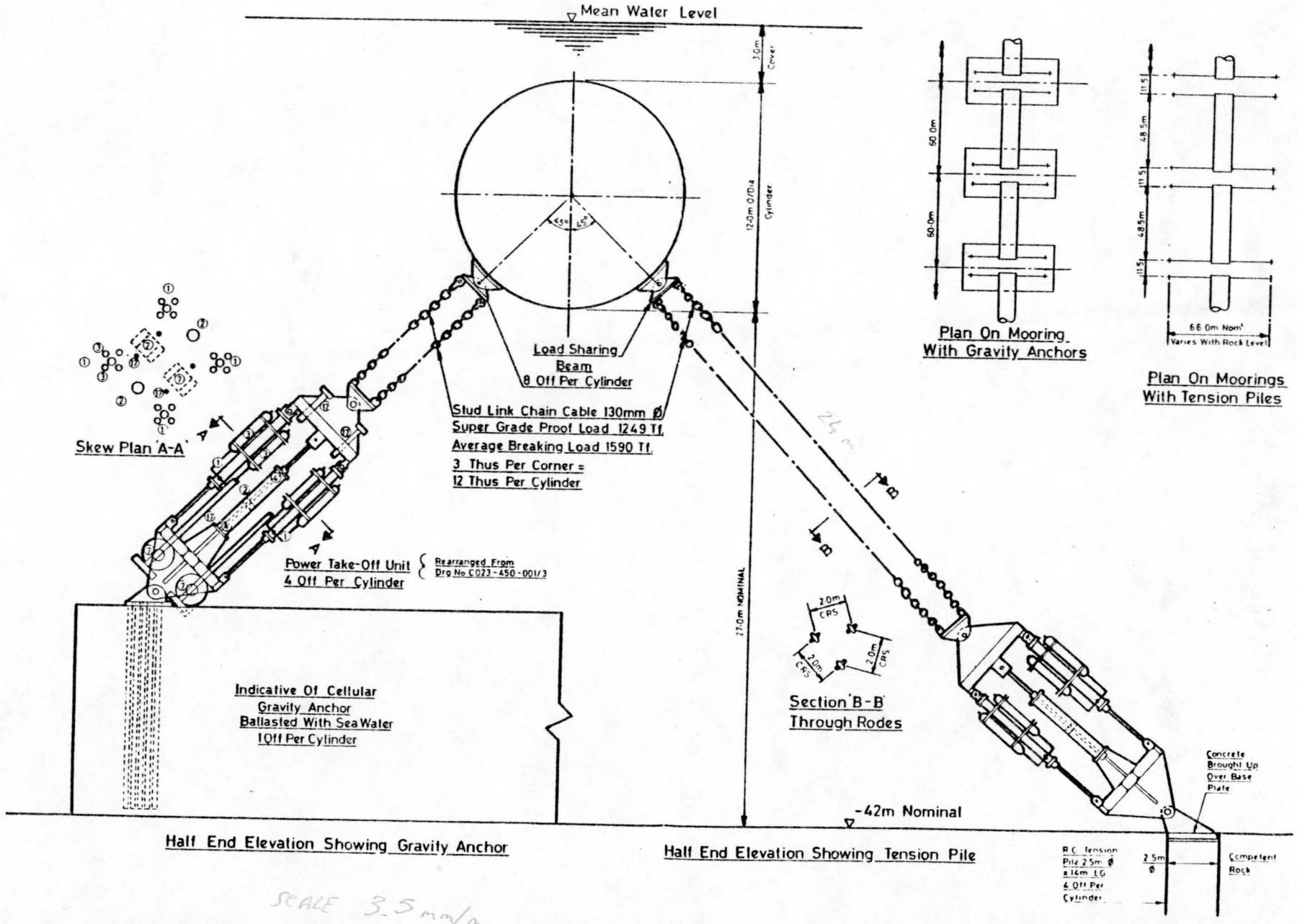
Mean Water Level
3.0m Cover
12.0m O/Dia Cylinder
27.0m NOMINAL
-42m Nominal
45°
45°
Load Sharing Beam
8 Off Per Cylinder
Stud Link Chain Cable 130mm Ø
Super Grade Proof Load 1249 Tf.
Average Breaking Load 1590 Tf.
3 Thus Per Corner =
12 Thus Per Cylinder
Skew Plan 'A-A'
Power Take-Off Unit
4 Off Per Cylinder
Rearranged From
Drg No C023-450-001/3
Indicative Of Cellular
Gravity Anchor
Ballasted With Sea Water
1 Off Per Cylinder
Half End Elevation Showing Gravity Anchor
Section 'B-B'
Through Rodes
2.0m CRS
Concrete Brought Up Over Base Plate
Half End Elevation Showing Tension Pile
R.C. Tension Pile 2.5m Ø x 14m LG 4 Off Per Cylinder
2.5m Ø
Competent Rock
50.0m
50.0m
Plan On Mooring With Gravity Anchors
48.5m
48.5m
66.0m Nom.
Varies With Rock Level
Plan On Moorings With Tension Piles
SCALE 3.5mm/m

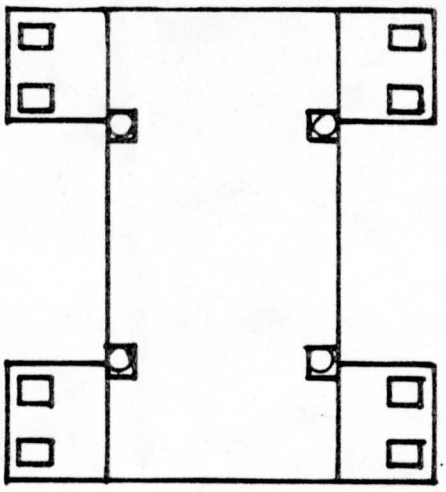

PLAN

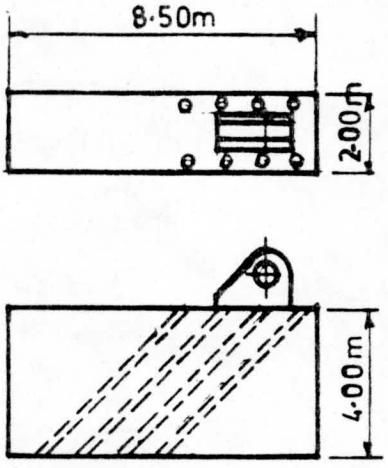

ANCHOR BLOCK
1:200

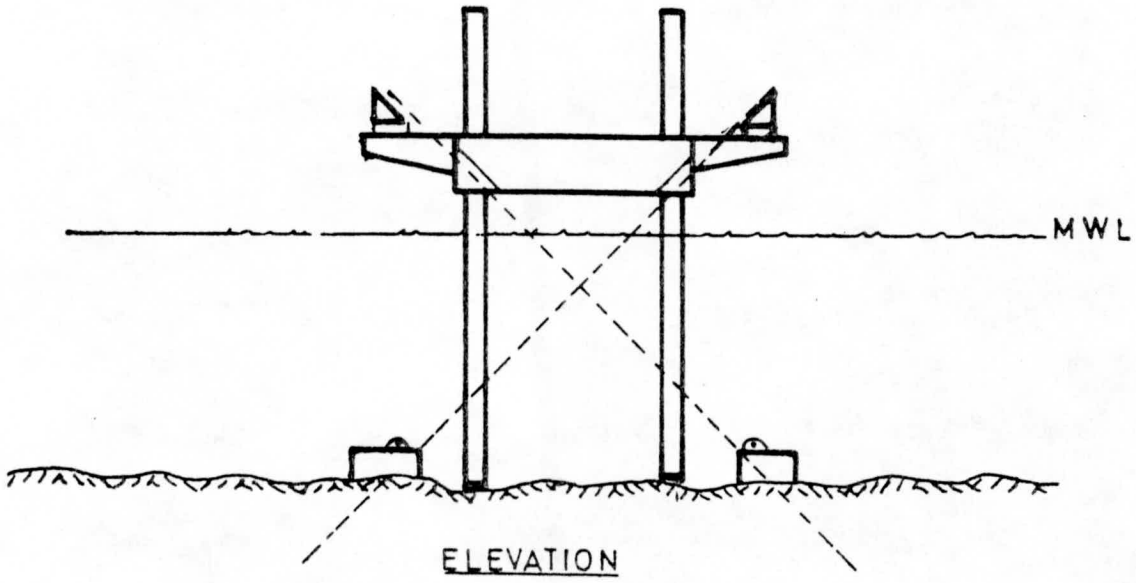

ELEVATION
1:1250

1 PC ANCHOR BLOCKS LOWERED INTO POSITION. PADEYE & DRILL HOLES CAST IN.
2 DRILL HOLE TUBES LOWERED & LOCKED TO P.C. ANCHOR BLOCKS.
3 8N° 230mm HOLES PER BLOCK. DRILLED 16N° SIMULTANEOUSLY.
4 EACH HOLE FITTED WITH 3N° 40mm MACALLOY BARS GROUTED TO BLOCK.
5 OUTPUT PER BARGE EXPECTED TO BE 2N°ANCHOR SETS PER WEEK,
6 ASSUMING A 6MONTH WEATHER WINDOW 2N° BARGES REQUIRED.

LAYOUT OF 80m x 40m SPUD BARGE TO INSTALL RAKING GROUND ANCHORS.

SECTION 7

BUDGET COST ESTIMATES AND ANNUAL ENERGY OUTPUT

7.1 Introduction

A range of cost estimates through to and including the turbo-generator have been prepared. These are presented in Section 7.2. The available performance data is assembled in Section 7.3 to suggest the annual energy output of the generator for each cylinder device connected to it. From these two estimates, various methods of quoting unit costs are evaluated (Section 7.4).

The worth of electricity generated from this source is explored in the Appendix.

7.2 Budget Cost Estimates

The unit cost figures contained in Table 7.1 have been based upon the preliminary examination of five types of sea bed anchorage and two methods of cylinder construction. A comparison is made of the likely costs of each. The unit cost is that per cylinder device, taking into account the proportion of the associated costs that it should bear.

The alternative systems are :-

(a) Anchor Units (Section 6)

- (i) Reinforced concrete gravity anchor (Fig. 6.1);
- (ii) Reinforced concrete tray and rock kentledge;
- (iii) Steel box and concrete ballast gravity anchor (Fig.6.2);
- (iv) Large diameter piled anchor (Fig. 6.4);
- (v) Ground anchors (Fig. 6.5).

(b) Cylinder Construction (Section 4)

- (i) Precast sections (Figs. 4.1 to 4.8);
- (ii) Insitu slip formed shells (Fig.4.9)

Current rates for labour and materials have been used.

The budget cost exercise has assumed a 10 year construction period for a 2000 MW Station (1000 cylinders) and a maintenance period over a lifetime of 20 years. As will be seen from Table 7.1, allowance has been made for the replacement of anchor chains and power takeoff units twice during this period, and for maintenance at varying rates for other components.

TABLE 7.1

Unit Costs per 2MW Cylinder

x £1000

Anchorage Type	Concrete Gravity		Concrete/ Rock Gravity		Steel/ Concrete Gravity		Piled		Ground Anchors	
Cylinder Construction	Precast	Insitu	Precast	Insitu	Precast	Insitu	Precast	Insitu	Precast	Insitu
1. Anchor	1342	1342	1100 —	1100	1643	1643	850	850	1397	1397
2. Anchor Chains	80	80	80 8	80	80	80	148	148	148	148
3. Cylinder	375	552	375 5	552	375	552	375	552	375	552
4. Tow and position cylinder	120	120	120 1	120	120	120	120	120	120	120
5. Pipework	1085	1085	1085 15	1085	1085	1085	1085	1085	1085	1085
6. Power take off units	1400	1400	1400 140	1400	1400	1400	1400	1400	1400	1400
7. Converter towers	235	235	235 1	235	235	235	235	235	235	235
8. Turbine generators	105	105	105 1	105	105	105	105	105	105	105
	4742	4919	4500	4677	5043	5220	4318	4496	4865	5042
Contingency 1 - 10% 2 - 10% 3 - 15% 4 - 10% 5 - 10% 6 - 25%	663	694	644	691	698	724	626	653	681	708
	5410	5613	5144	5368	5741	5944	4944	5149	5546	5750
Maintenance over 20 years 1 - 0% 2 - 200% 3/ 4 - 25% 5 - 30% ÷ 20 6 - 200% 7 - 10% + £10,000 8 - 20%	183	185	183	185	183	185	190	192	190	192

TABLE 7.1

The rates used in the cost estimates are deemed to be sufficient to cover sundry components and labour. They may be summarised as follows :

Concrete (reinforced or prestressed) generally taken at £50/m^3

Shuttering rates vary between £6.00 and £50/m^2

Steel reinforcement taken at £350/T

Prestressing steel taken at £1,400/T

Structural steel taken at £350 to £450/T with special cases higher.

All the above rates are for supply and place or fix as appropriate.

Sea bed pipeline costs are very approximate and as advised by BP to Wavepower Ltd.

Major items of marine plant have been priced at current rates either experienced in the North Sea or obtained in the course of carrying out this and other current studies. Smaller craft are covered in a general preliminary percentage. All major marine operations such as piling or installing cylinders have been assumed to suffer 50% downtime due to weather; either standing time has been priced or alternatively provision made for mooring in safe harbours during the winter months.

A general allowance of 15% has been made on most operations to cover the cost of back-up labour and plant and general preliminaries including management. It is recognised that this percentage will in fact vary widely and a more detailed pricing exercise would take this into account. It is believed that this across-the-board addition should be sufficiently accurate for present purposes.

It will be seen that contingencies have been allowed at varying rates in Table 7.1. The variation represents the degree of definition in design or pricing of the elements but in no way reflects on the feasibility of the proposals.

It is recognised that contingency factors and maintenance allowances could be subject to considerable difference of opinion and hence it has been thought desirable to set out clearly the allowances made.

Though it will be seen from Table 7.1 that the cheapest solution is the combination of concrete box/rock fill anchor with a precast cylinder construction, it is recommended that for the time being the cost studies should be based on the use of the large diameter piled anchorage as proposed by Raymond International. There are two factors with the rock filled concrete tray requiring further study in the next stage of work :-

(a) the vulnerability to bad weather during tow and installation, and;

(b) the effect of so large an anchor block in 40m depth of water on the waves. This problem is common to all the gravity anchors considered.

The recommended budget estimates for one cylinder, out of 2000MW power station, complete with moorings, power takeoff and proportion of seabed pipework, converter tower and turbo-generator are :-

Capital cost estimate including installation and 5% design fees - £5,250,000

Maintenance allowance estimate - £ 200,000 per year

These cost estimates include no allowance for financing costs other than an allowance for building finance on the construction facilities.

No further work has been done in this study on the converter towers and figures have been taken from last year's work with adjustment for reduction in water depth. It is also proposed to take transmission costs from the converter towers to the grid at 1p per kWh as advised by TAG6; this has been included in the figures used in Section 7.4.

The designs were formulated at a late stage of the relatively short study period and this has left little time for a cost estimate study. It is recommended that attention should be paid to this in the next phase of the study in conjunction with optimisation of design.

7.3 Annual Energy Output Estimates

The calculations reported in this Section are based on the 1976/77 wave scatter diagram for the offshore buoy at S. Uist (Fig. 7.5) and the 3-D experimental data given for regular waves (Fig. 2.5) and directional waves (Fig 2.7).

As reported in Section 2.2, the directional data are for one energy period only (8 seconds), hence they are of very little value for the interpretation of the regular data to real wave conditions. In any case, the full form of natural waves is uncertain as far as directional spread is concerned. Hence there must be considerable room to doubt the accuracy of the results given here. An estimate of accuracy is given at the end of this Section.

Fig. 7.6 has been prepared from Fig. 2.5 on the following assumptions :-

FIG. 7.5

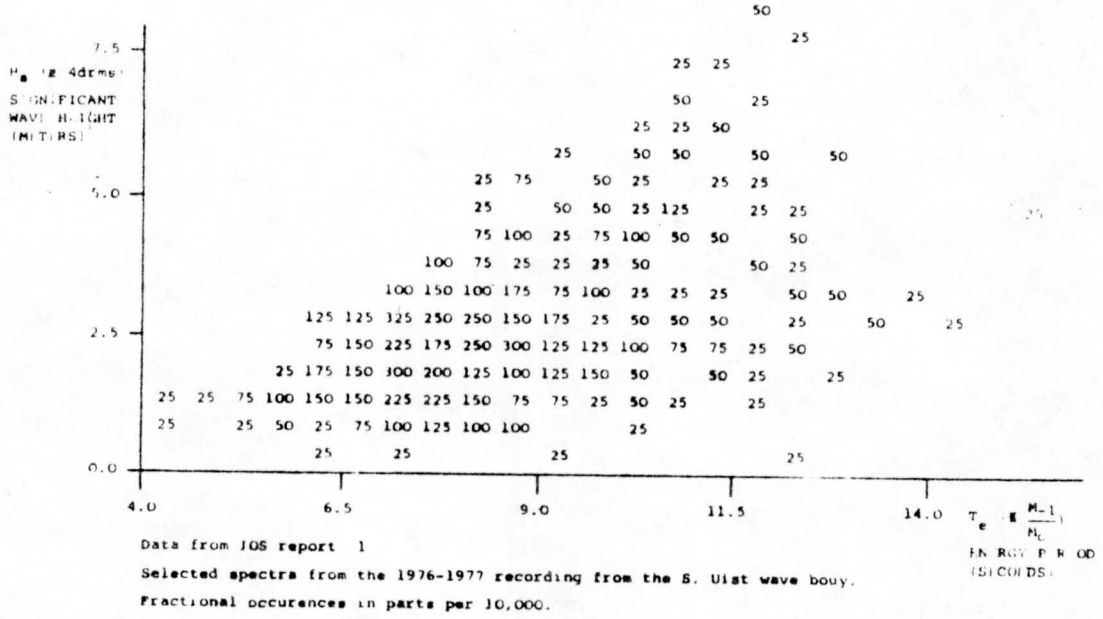

Data from JOS report 1

Selected spectra from the 1976-1977 recording from the S. Uist wave bouy.

Fractional occurences in parts per 10,000.

REFERENCE CLIMATE SCATTER DIAGRAM

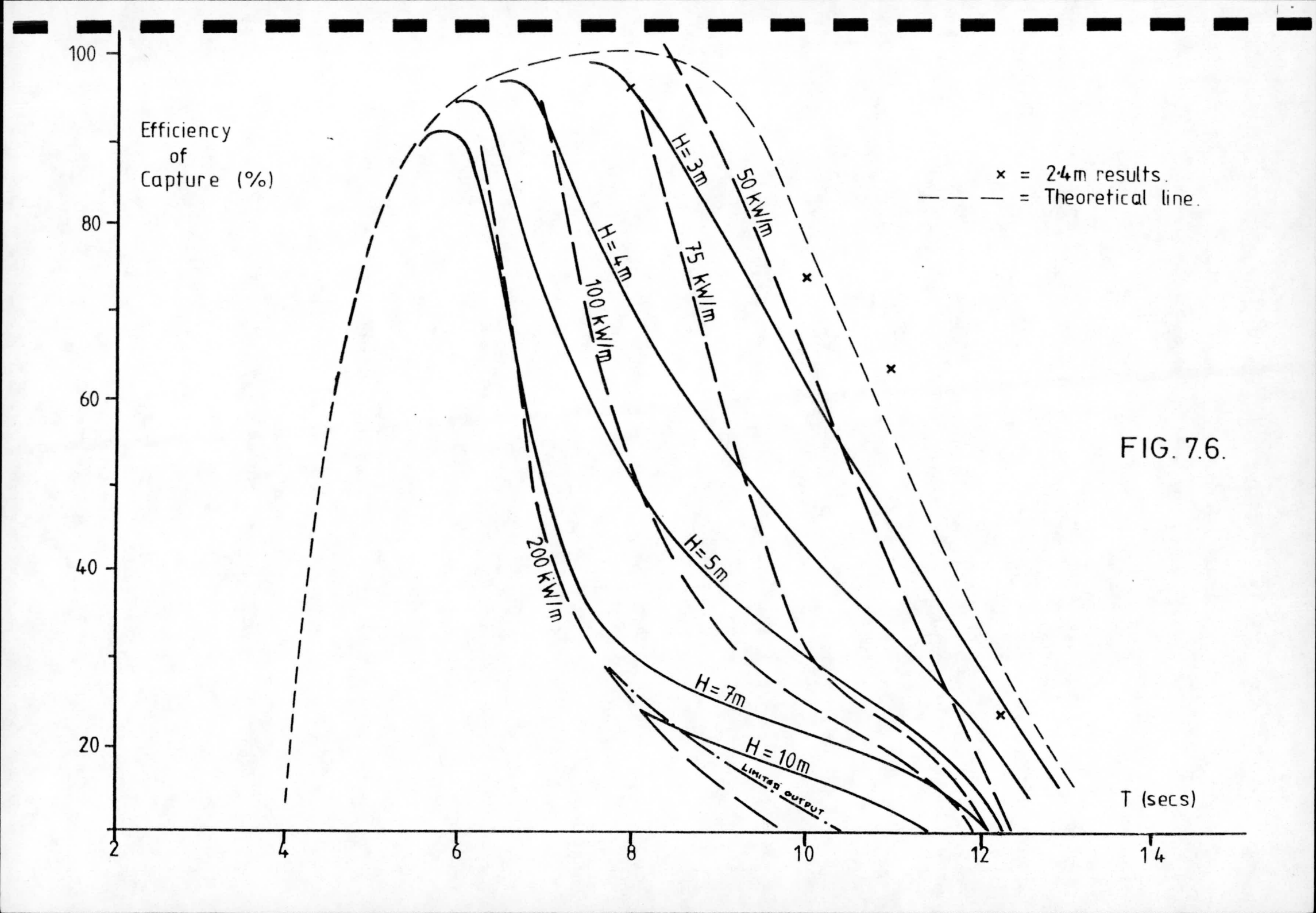
Efficiency of Capture (%)
100
80
60
40
20
2
4
6
8
10
12
14
T (secs)
× = 2·4m results.
— — — = Theoretical line.
H=3m
50 kW/m
75 kW/m
H=4m
100 kW/m
H=5m
200 kW/m
H=7m
H=10m
LIMITED OUTPUT

FIG. 7.6.

1. The small-amplitude (dashed) theoretical line in Fig. 7.6 applies to a cylinder diameter of 12m tuned to 8 seconds, when the submergence is 3m. This outer envelope (Fig. 2.5) is closely fitted by the experimental data recorded in the Edinburgh wide tank for a 4:1 aspect ratio cylinder, submergence 3m, diameter 12m in normal regular waves 2.4m high (H_S up to 3.4m depending on directional spread), over the range of periods 7-12 seconds. It is assumed that the same curve also applies to all waves of smaller amplitude approaching normal to the cylinder, giving a capture efficiency of 100%. It is assumed that the 3m and 4m contours should be interpreted to the data recorded for regular waves of 2.4m and 4.8m, though in practice such a discontinuity at 2.4m is improbable. The amount of energy captured in the important range of, say, $3.4 < H_S < 4.5$m (Fig. 7.5) may therefore be understated - (Fig. 7.7).

2. The curves make no attempt to allow for lateral energy capture from beyond the axial length of the cylinder. Although there is strong theoretical evidence for this, the experimental justification is limited to visual impressions plus a single efficiency measurement of 125% in 2.4m waves at 7 seconds. Also there is the fact that, as shown in Fig. 7.6, the 2.4m curve appears to correspond closely to the two-dimensional small amplitude theoretical line, whereas at least marginally lower efficiencies might then be expected. (Note that the length of a 7s wave is about 80m, i.e. the steepness when H = 2.5m is 1:32, or 3%). Hence the curves for wave heights of less than 2.4m may be pessimistic : efficiencies may exceed 100% because of the ability of the device to capture energy from beyond its length. If this is more prevalent at wave periods below, say, 8s, the total energy gain is unlikely to exceed 10% and the recommendation in Para 4 below to consider tuning the cylinder to greater wave periods may possibly reduce this. In fact, however, theory suggests that lateral capture will be greater in longer waves.

3. Below T = 7s, the only evidence available, in addition to theory, is the 'heavy cylinder' experimental data recorded by Dr. Evans in a flume at Edinburgh University. These data have helped resolve the shape of the latest Edinburgh plots in this short wavelength range, though below T = 5s the incident energy levels are a very small proportion of the total (Fig. 7.8).

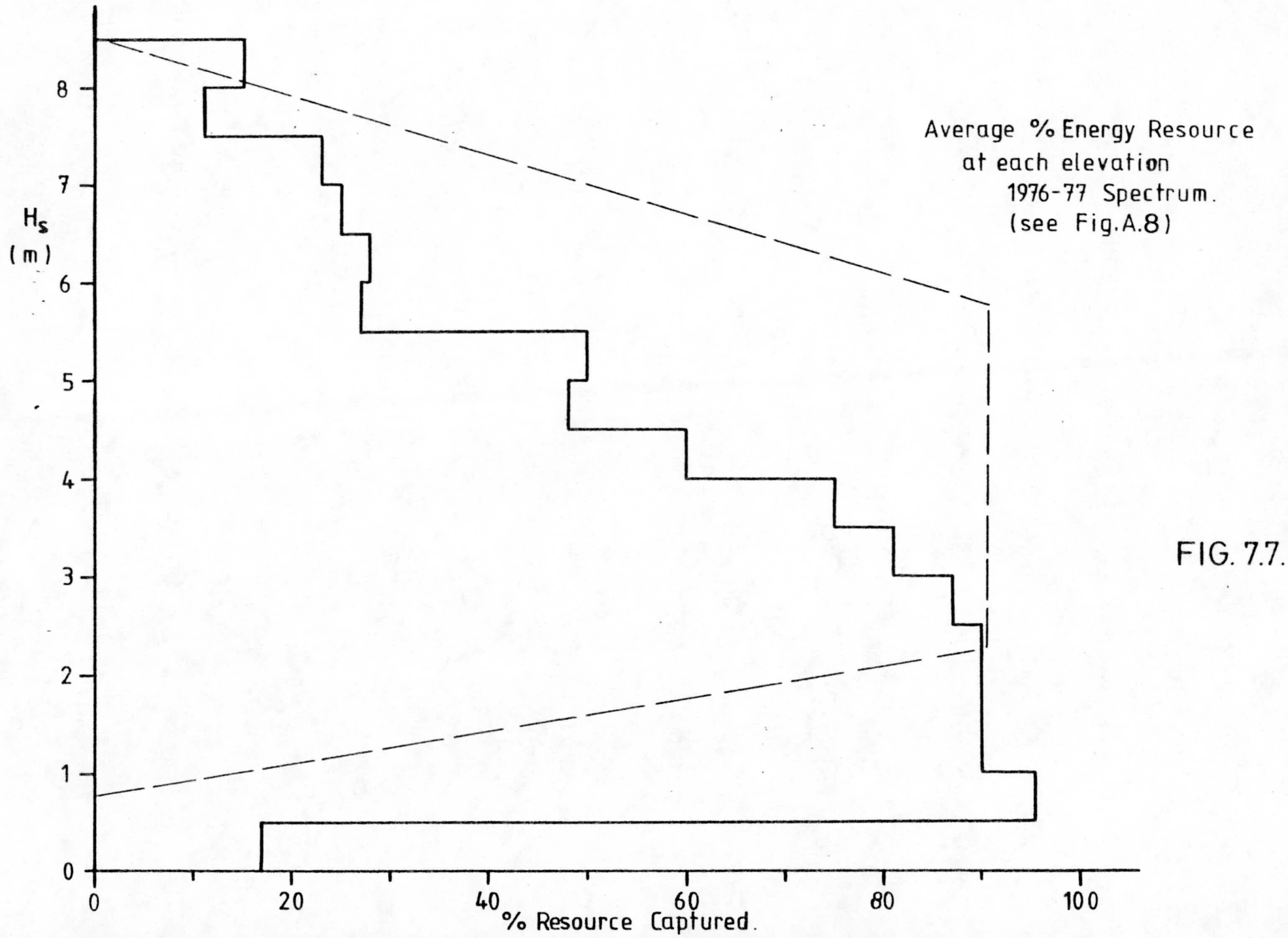
Average % Energy Resource
at each elevation
1976-77 Spectrum.
(see Fig.A.8)
H_s
(m)
8
7
6
5
4
3
2
1
0
0
20
40
60
80
100
% Resource Captured.

FIG. 7.7.

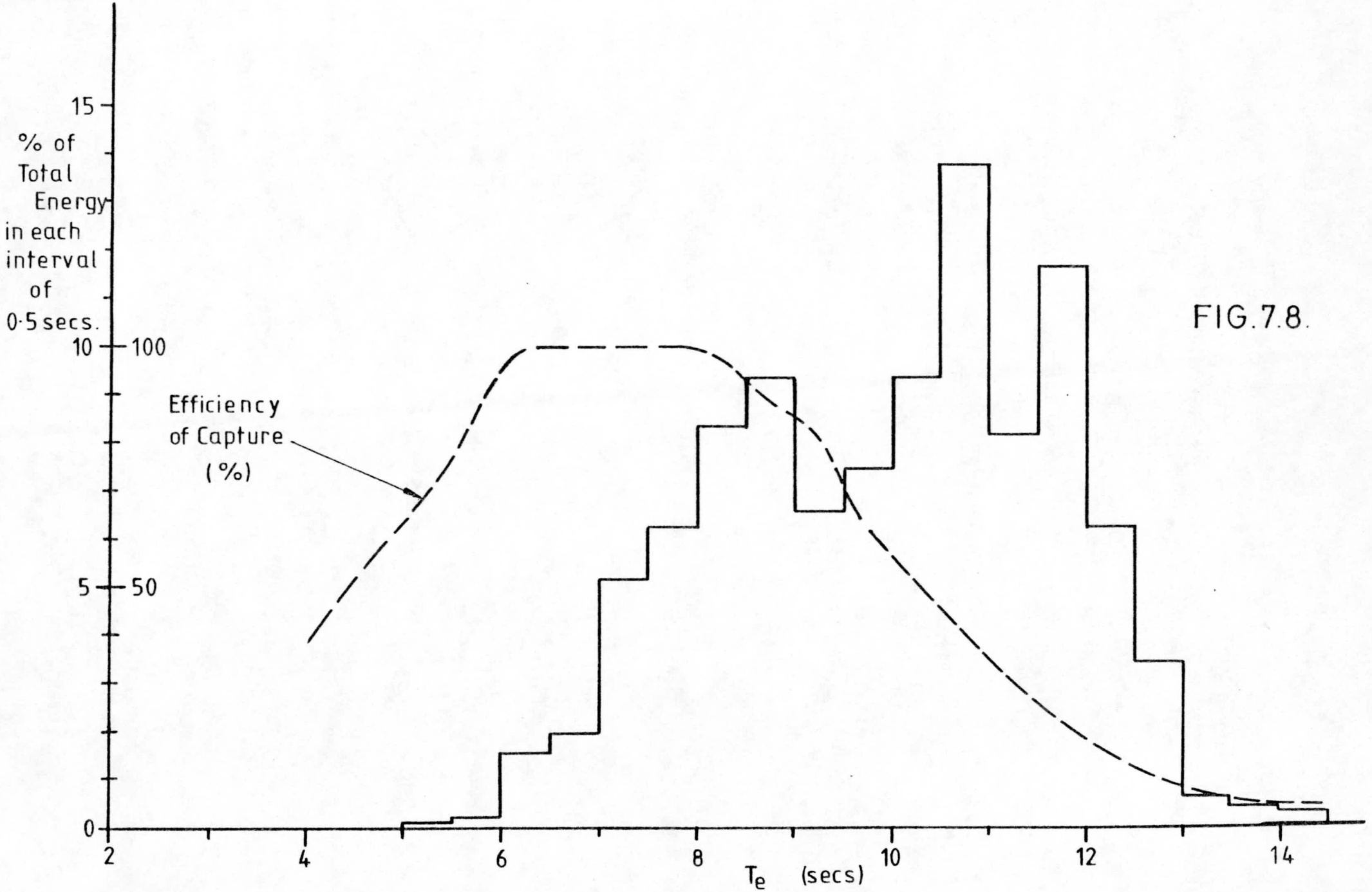
15
% of
Total
Energy
in each
interval
of
0·5 secs.
10
100
Efficiency
of Capture
(%)
5
50
0
2
4
6
8
10
12
14
T_e (secs)

FIG. 7.8.

4. The performance curves for H = 3, 4, 5, 7 and 10m have been drawn in Fig. 7.6 from data for H = 2.4, 4.8 and 7.2m (Fig. 2.5) on the basis that the efficiency and power output characteristics are continuous within the domain of wave steepness up to the limit of 1:10. This fully encloses the 1976/77 S. Uist data record (Fig. 7.5), and gives the energy density and efficiency relationships in the H_s-T_e plot shown by Fig. 7.9. A constant relationship of $H_s = \sqrt{2}H$ has been assumed, though the directional content of these will vary in some uncertain way with wave period.

5. Related experimental work at Bristol University suggests (Fig. 2.2) that the orbit of the cylinder has a value of about 3.0m when H = 9m (or H_s = 12.7m). This is well beyond the scatter of occurrences reported in the S. Uist spectrum. It has been used in the mechanical design of the cylinder device as a limit beyond which the orbit of the cylinder need not continue to increase with increasing wave height, even slowly, because of the cost of allowing for this in design (Section 5). Indeed there may be value in reducing this limit to, say, H_s = 7m (cylinder orbit = 2.5m), lowering mechanical costs with little loss of resource capture because the orbital motion of the cylinder would still continue though at reduced amplitude, the losses being very small until the wave height greatly exceeds the threshold selected. (The distribution of cylinder efficiency with wave height through the S. Uist 1976/77 wave spectrum is shown in Fig. 7.7).

6. The distribution of incident energy in the 1976/77 S. Uist wave spectrum is shown in Fig. 7.8, together with the efficiency curve for energy captured from this spectrum by a 12m cylinder, 3m submergence, tuned to 8s. It appears that the tuned frequency is too low to make the best of the resource available at this location. Whether or not this is true must await further experimental tests with higher periods of tuning. In this connection it is instructive to compare the small-amplitude theoretical curves for 8s and 9.8s, both for 12m cylinders, 3m submergence (Fig. 7.10). Although the higher period gives a more peaked curve and only increases by about 1 second the location of the efficiency curve for periods greater than the peak, the energy captured has been estimated to increase from 49.8% of the total resource to 61.7%. Fig. 7.10 also shows the theoretical curve for a 15m diameter cylinder tuned to 9.8s, and indicates that a further increase of 0.5-1.0 second in the position of the low frequency end of the curve may be achieved this way. This is equivalent to gains in efficiency of resource capture of about 10-20%.

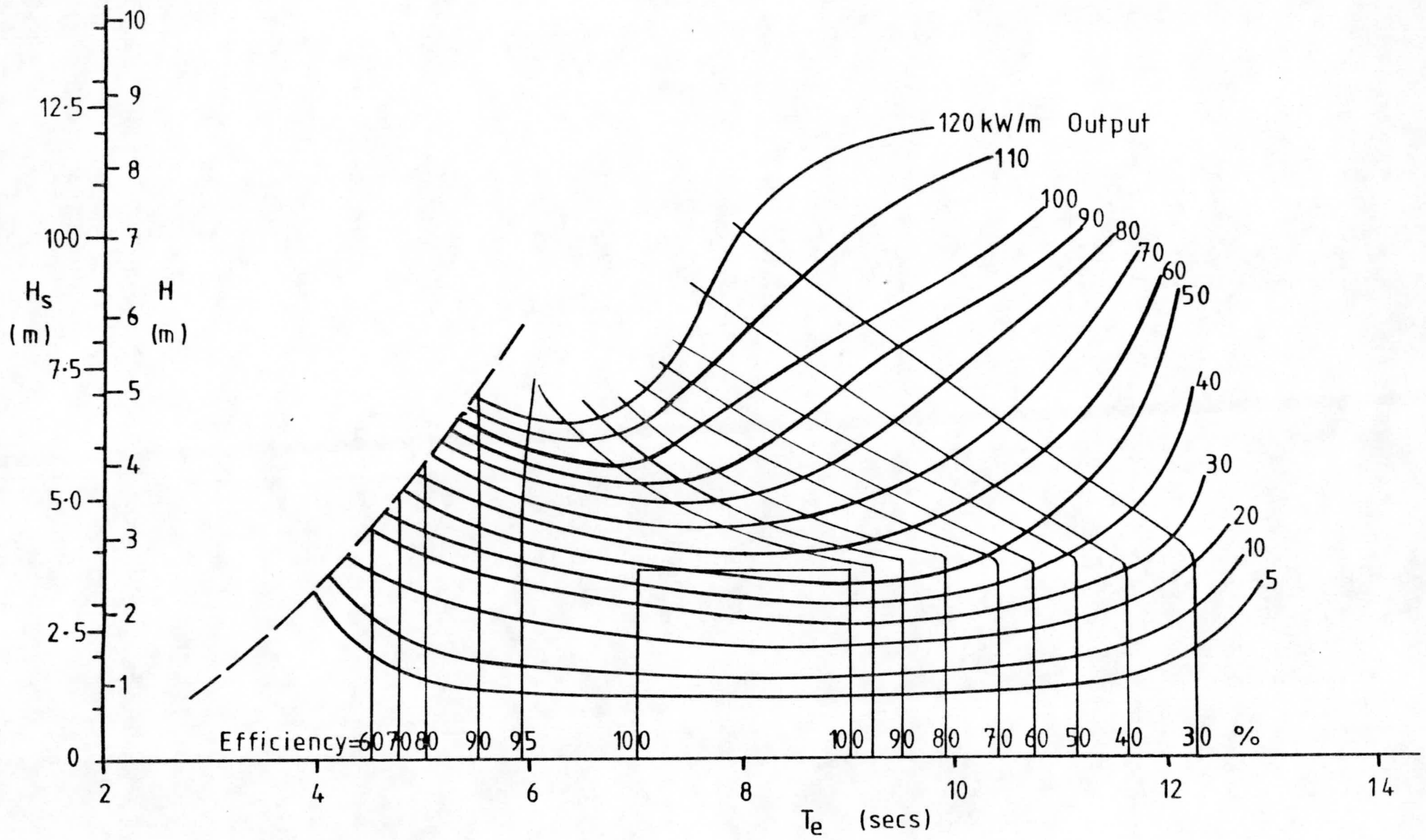
120 kW/m Output
110
100
90
80
70
60
50
40
30
20
10
5
H_s (m)
H (m)
10
9
12·5
8
10·0
7
6
7·5
5
4
5·0
3
2
2·5
1
0
Efficiency=60 70 80 90 95 100 100 90 80 70 60 50 40 30 %
2
4
6
8
10
12
14
T_e (secs)

FIG. 7.9.

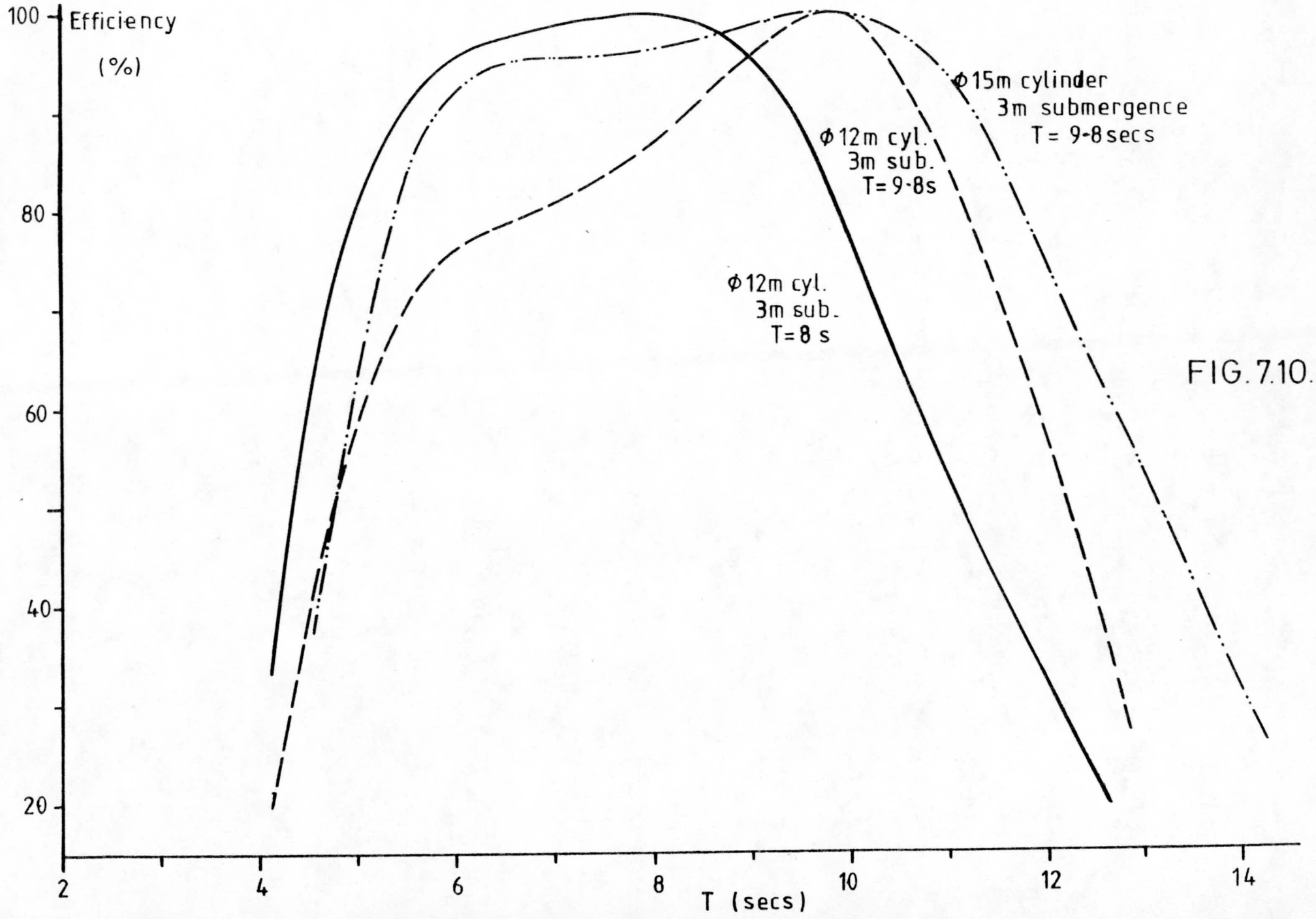
100
Efficiency
(%)
80
60
40
20
2
4
6
8
10
12
14
T (secs)
φ15m cylinder
3m submergence
T = 9-8secs
φ12m cyl.
3m sub.
T=9-8s
φ12m cyl.
3m sub.
T=8 s

FIG. 7.10.

7. The largest loss of resource with the "9.8s" cylinder is in the range $10.5 < T < 13.0$. This suggests that tuned periods of up to 11s should be considered, together with the alternatives of increasing the diameter of the cylinder and reducing the submergence (Fig. 7.11). On the basis of the limited evidence available it should therefore be possible to design a cylinder device capable of capturing up to 70% of the incident energy resource. Note that all efficiency values quoted here have been determined on the basis of :

   (a) Regular wave data, for normal and 45° seas;
   (b) 50m cylinders spaced along a line with 10m gaps.

8. The significance of mixed seas on overall annual capture efficiencies cannot yet be judged with any precision. The data for T = 8 seconds from Fig. 2.5 are shown on Fig. 2.7 against the only available mixed sea information, for T_e = 8 seconds. The divergence between the efficiency relationships must be interpreted against the distribution of energy in natural seas having the same energy period. Thus Fig. 7.5 for S. Uist shows that, at this period, most of the available resource has $H_s < 4m$, or $H_{rms} < 1m$ for mixed sea conditions. The bulk of this energy lies in the range $2 < H_s < 4m$, or $0.5 < H_{rms} < 1.0m$, where, for example, the long-crested mixed sea efficiency is on average about 10% less than for regular waves. For short-crested waves, however, it appears to be only about half that for regular waves. But Fig.7.8 confirms that the relative energy levels at $T_e < 8$ seconds are small. Hence although some reduction in capture efficiency from that quoted in Para.6 above is necessary, the size of this is dubious because:

   (a) The available mixed sea data is limited to one period;
   (b) The degree to which real seas contain directionality at each period within their spectra does not appear to be known, yet it is clearly very important when determining overall capture efficiency (the fact that the regular and short-crested efficiencies tend to a common value in Fig. 2.7 applies at a value of H_s well in excess of that for the data recorded with T_e = 8 seconds - Fig. 7.5).

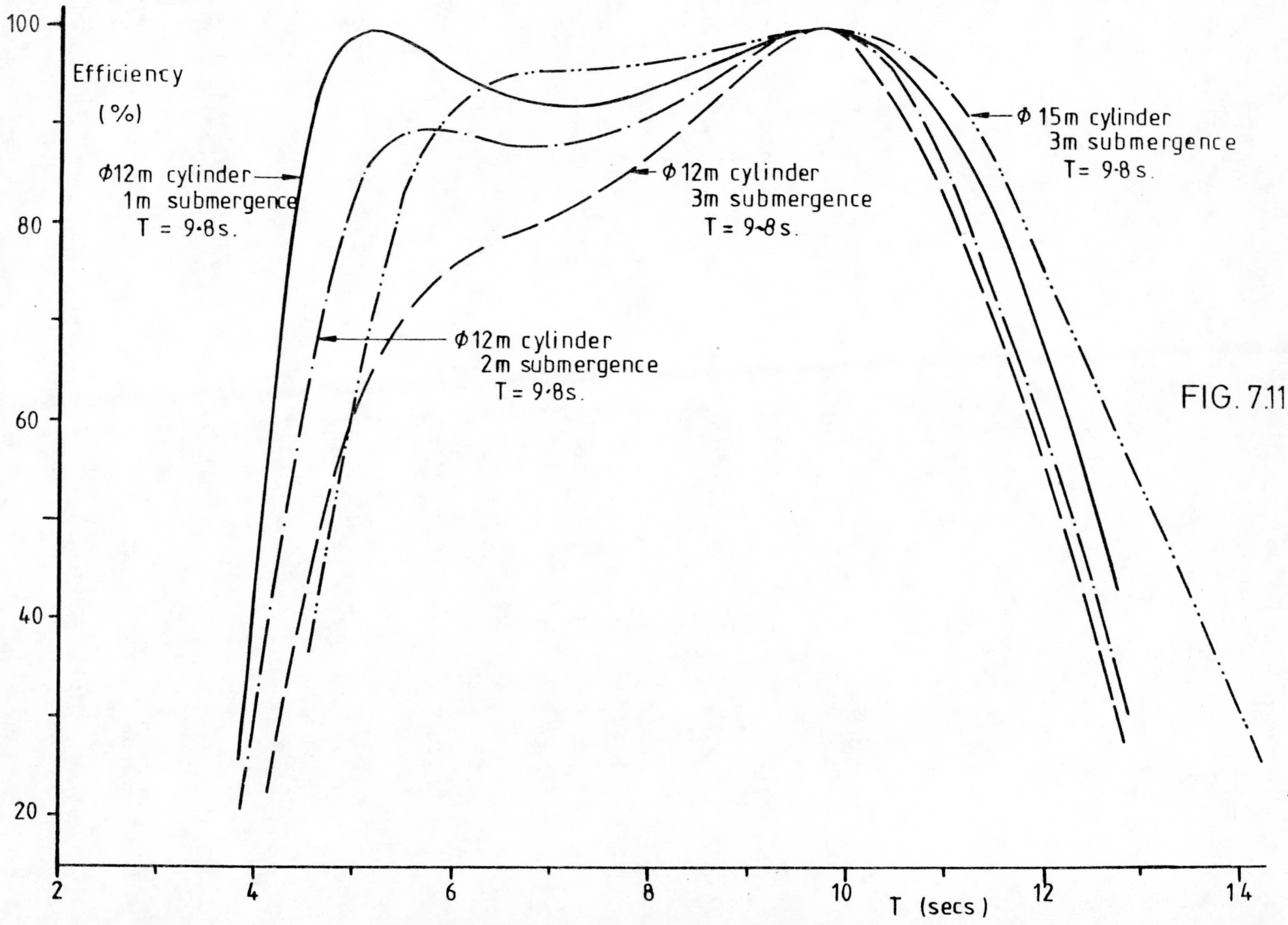
100
80
60
40
20
Efficiency
(%)
Φ12m cylinder
1m submergence
T = 9·8s.
Φ12m cylinder
2m submergence
T = 9·8s.
Φ12m cylinder
3m submergence
T = 9·8s.
Φ15m cylinder
3m submergence
T= 9·8s.
2
4
6
8
10
12
14
T (secs)

FIG. 7.11

On the basis of these arguments it is proposed that the annual capture efficiency calculated using regular wave data should be reduced by 5%, from 49.8% to, say. 47%, and that with the modifications to the tuning and diameter of the cylinder proposed in Para.6 above, the estimated maximum capture efficiency should be reduced to about 60%. In both cases extra tests are needed before accurate predictions may be made.

9. In calculating the above capture efficiencies the available resource was reduced by 5/6 to allow for the gaps between cylinders. The effect of lateral energy capture has already been built into the efficiency data (it could not be isolated from it). With inclinations of the waves up to 45° the observed gap between the cylinders progressively reduces. On the very limited data available (45° and normal only) it seems that the decrease in efficiency with inclination is to a significant extent offset by this increase in effective length. In any case, Ref. 2 suggests that over 50% of incident swell at S. Uist lies within ±15° of the direction of peak energy (Fig. 7.12) and over 95% within ±40°. Using the data in Fig. 7.12, together with the assumption that performance drops off as the cosine of the wave direction to 260°, and allowing for the reduction in gap width with increasing skew to 260°, the % of the energy distribution implied by Fig. 7.12 (i.e., assuming any one storm could come from any direction) intercepted by the cylinder decreases by 4% from the value given by assuming that all energy approaches normal to the line of devices.

10. The available resource at S. Uist for the year 1976/77 (Fig. 7.5) has been estimated to be 421 MWh/m. 45% and 58% of this, when captured by a cylinder 50m long, give 9.5 and 12.3 GWh. The lower figure applies to the cylinder as tested, designed and costed.

Bearing in mind the above evidence it is estimated that each overall efficiency value quoted is accurate to within ±10° of its value.

Distribution of selected set swell directions.

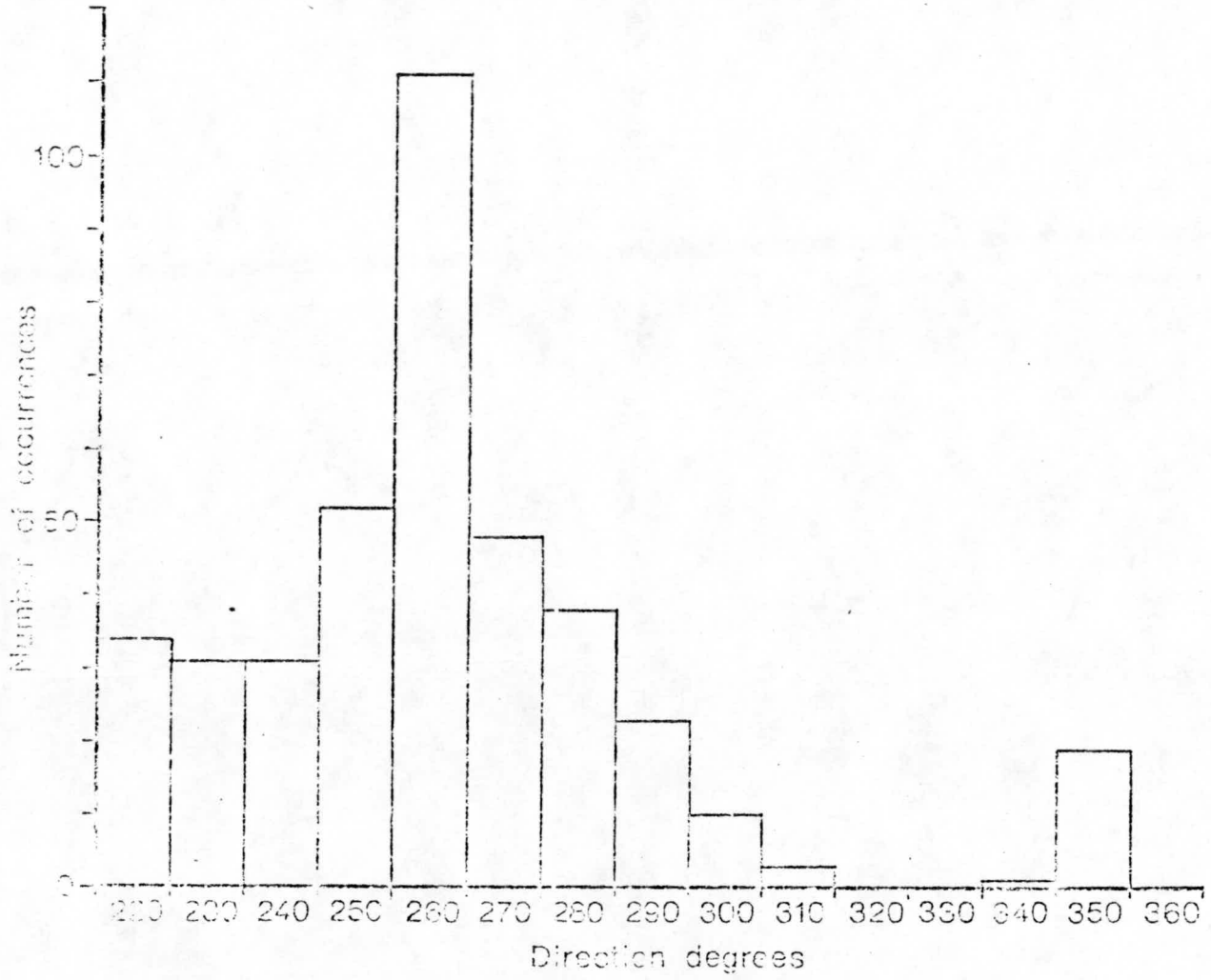

FIG. 7.12 - Ref. 2

7.4 Unit Costs

The following data have been used as a basis for the initial calculations:

1. Costs

From Table 7.1 the capital cost of each 50m cylinder device, including its moorings, power takeoff units and a proportional share in the common pipelines and 200MW turbo-generator unit, including its platform is £5.25M. The construction, installation and commissioning of each 200MW string has been estimated to take about 3 years, and it is assumed that capital will be spent at a uniform rate throughout. An interest rate of 12% is assumed.

The maintenance charge is equivalent to £0.2M/yr per cylinder (Section 7.2).

Transmission cost onward from the turbo-generator to the grid has, on the advice of Dr. R. Taylor (ETSU), been taken to be equivalent to adding 1p/kWh to unit costs.

2. Benefits

In Section 7.2 the capture efficiency of the cylinder as designed was estimated to be 45%. The following further efficiencies have been estimated:

Transmission to the Sea Bed (fluid turbulence)	= 95%
Pump/accumulator combination	= 85%
Pipeline transmission	= 90%
Turbo-generator	= 90%

The total efficiency is therefore = 29.4%

The S.Uist scatter diagram for 1976/77 has an annual energy of 421 MWh/m, or 21.05 GWh/50m cylinder.

Hence energy delivered to the National network = 6.19 GWh/cylinder.

3. Benefit/Cost comparisons

The benefit/cost ratio may be quoted in two ways, either as the ratio given by attaching a particular value to each unit of electrical output, or by determining the unit value needed to give a benefit/cost ratio of 1.0. The latter approach is preferable in the present context.

The lifetime of each 200MW installation will be taken as 20 years, and a discount rate of 5% will be assumed.

The benefit/cost ratio is determined by discounting back to the present day the value of the energy produced during the 20 year lifetime, less the annual cost of operation and maintenance, and dividing by the present value of the construction cost including interest.

On the basis of the above figures, the unit cost

is 11.4 p/kWh

This conclusion is the pessimistic upper limit.

As explained in Section 7.2, redesign of cylinder tuning, a small decrease in submergence, and perhaps a small increase in its diameter (rode and anchor forces increase linearly) should give an annual capture efficiency of at least 58%.

We believe that the power-train efficiency values quoted above are low, as follows:

Transmission to Sea Bed - raise to 98% if pto frame fixed:
Pump/accumulator - raise to 88% by optimising design;
Pipeline - typical average efficiency = 97%
Turbo-generator - perhaps 92% if duty not too variable;

The total efficiency is now = 44.5%

Assuming the same distribution of energy with wave height as for the 1976/77 data, the energy delivered to grid = 9.36 GWh/cylinder.

In this case, unit cost of electricity = 7.9 p/kWh

It should also be possible to improve unit costs by reducing capital expenditure per cylinder. A first estimate of this implies a saving of 25%. The unit cost would then be 6.7 p/kWh

If the lifetime of the scheme is taken to be 30 years rather than 20 years, and assuming the same average rate of expenditure on maintenance, these three calculations respectively give unit costs of :

10.1 p/kWh, 7.0 p/kWh, 6.1 p/kWh

Another method of comparing costs with benefits is to relate the annual value of the energy produced, less the operation and maintenance costs, to the total capital committed on each 200 MW installation. Again, either the annual value has to be specified in order to make this comparison, or the % return on capital indicated by this ratio may be specified in order to show what annual value (or aggregated unit cost) is needed to achieve it. The latter basis will be used here as being more directly informative for present purposes, with 5% return on capital.

For the above three cases with 20 year lifetime, the unit costs respectively are :

9.5 p/kWh, 6.6 p/kWh, 5.7 p/kWh

Finally, for some purposes it may be helpful to quote the ratio of capital expenditure at commissioning of an installation to the power then available. The comparable three figures, ignoring transmission line costs, are :

3260 £/kW, 3260 £/kW, 2440 £/kW

These last ratios give a simple means of comparing different types of power station. However, they make no reference to relative fuel prices, conversion efficiency characteristics, annual operation and maintenance charges, lifetime, and the relative values of the energy produced. The latter topic is particularly important for resources like wave energy that have yet to be harnessed and integrated into an electrical network based on thermal plant. Some comments on this are given in the Appendix.

SECTION 8

CONCLUSIONS AND RECOMMENDATIONS

This first design study of the submerged cylinder device has confirmed that its simple method of operation persists in all sea states and that its motion can be harnessed by proven technology. The forces imposed on the moorings in severe waves have been determined experimentally and theoretically and good agreement has been reached. An overall design for the structure and its foundations has been prepared, including the principal features of all elements of the power train through to the on-shore transmission link.

The cost estimates suggest that the unit price of electricity delivered to the grid will not exceed 10 p/kWh, and initial improvements to the basic design indicate that prices of 5-6 p/kWh may be achieved. This range is only 2-3 times the probable present day value of electrical units. The study has only lasted six months, has not been aimed at producing an optimum design and therefore there is the clear prospect that the device is capable of development to an economic level. The rising price of all fuels, in real terms, will help this trend.

We recommend that development of this device should be continued and the following studies should now be put in hand:

(a) Carry out laboratory work in a wide tank using representative waves to test a model cylinder with simulation of the power takeoff and anchorages proposed in this study or any modifications of such as are deemed desirable.

(b) Optimise the cylinder design and construction methods.

(c) Optimise the power takeoff proposals.

(d) Test components of the power takeoff system, particularly the pneumatic spring, in sea water at a suitable scale. It is considered that early verification of the performance of this spring is important.

(e) Develop the anchorage design having regard to the results from the laboratory tank tests.

(f) Take note of results of generic studies within the wave power programme on subjects such as sea bed power transmission, electrical conversion and transmission to shore and to incorporate applicable results into the design.

(g) Optimise the whole system.

(h) Prepare more accurate estimates of cost of electricity generated.

APPENDIX

SOME CONSIDERATIONS OF THE VALUE OF WAVE ENERGY

A.1 Relevant Features of Electrical Grid

The output of wave energy devices is characterised by:

1. Balancing short-term ouput variations (i.e. over minutes or less) from each device due to the hydraulic collection system into which many devices feed;

2. Medium-term variations (e.g. days) as storms occur, both at a distance and locally;

3. Long-term variations (e.g. months) at a mean (medium-term) output level, linked with the seasons of the year.

Together, these variations will be accepted to greater or lesser extent by the electrical network which the devices supply, bearing in mind that:

1. The network experiences relatively regular demand variations each day, though the levels change slowly from winter to summer (as Fig. A.1 shows for the CEGB network - not all networks have the same seasonal variation, and the demands on some go up in summer).

2. Taking the CEGB system, there is already a bias of installed capacity towards large thermal plant (Fig. A.2), a trend that is likely to continue in future. The nuclear component is expected to grow most quickly. This will demand extra provision for storage, whether by pumped water as at Dinorwic/Ffestiniog/Cruachan/Foyers/ Craigroyston?/Tintwistle?/etc., or in other ways. Such plant will be provided according to the operating costs of thermal sets best geared to base load. It is not immediately apparent how well 'excess' wave energy could fit into this scheme. The answers will relate to its persistence over periods of hours and days. It is clearly helpful that higher energy outputs occur in the winter when demand is high, though it is by no means unusual for difficulties of supply also to occur in the summer, due to the high level of plant outage at that time for maintenance (routine and major).

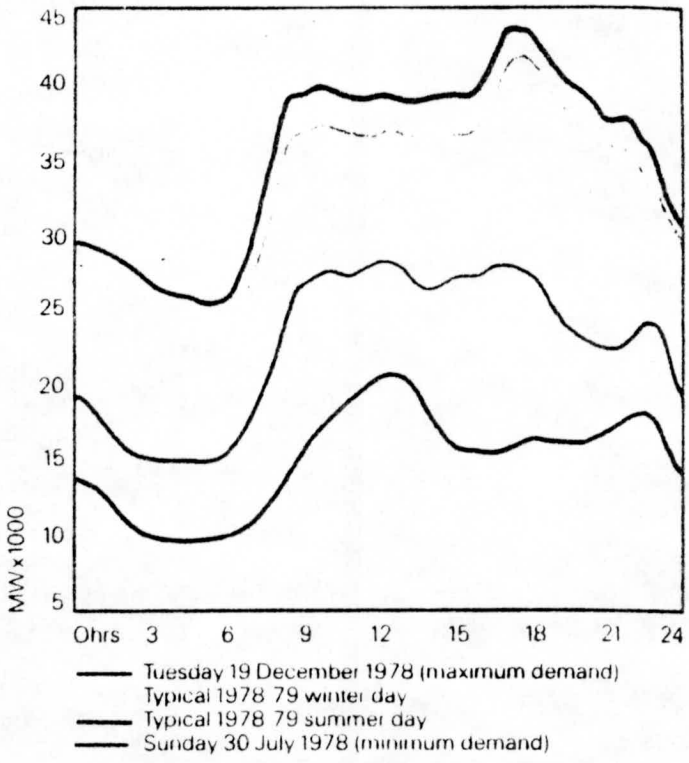

Summer and winter demands on the CEGB system in 1978-79 including days of maximum and minimum demand

FIG. A.1

Ref. C.E.G.B. Annual Report & Accounts 1978-79

FIG. A. 2

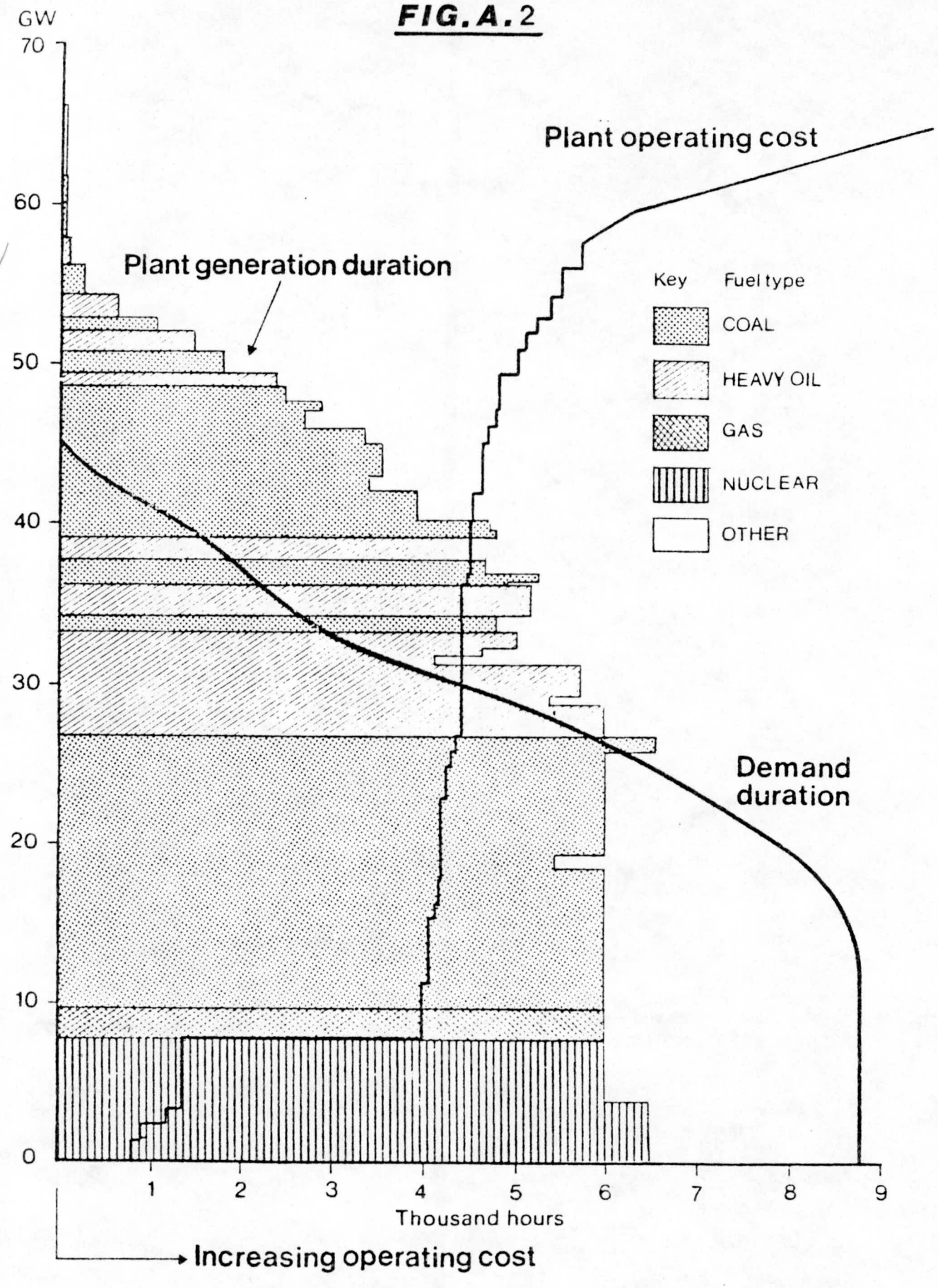

Fig. 5 Estimated mean system characteristics in 1982/83
(Source: S. Catchpole (CEGB), IAEA Salzburg Conference, May, 1977)

3. Following from this, the wave energy available during the high load, daytime period would either totally remove the need for a corresponding capacity of thermal plant if it is available at a roughly steady level throughout that period (i.e. firm at, say, 2 GW for that daytime period, and credited accordingly if sufficient warning can be given that it will be firm during that period - hence the displaced plant need not be available), or it would be supplied but at a variable or discontinuous rate. In the latter case other plant would have to remain at a corresponding state or readiness. The periods of warning associated with the arrival and decay of swell and storm seas must therefore be specified if this aspect of its value is to be judged.

4. On the other hand, the wave energy harnessed when the load is less than the daytime 'plateau' must either:

   (a) be rejected.

   (b) be supplied in preference to thermal, which in turn will not be generated.

   (c) be stored in preference to thermal, which in turn will not be generated, or;

   (d) be fed to storage facilities allocated for this purpose.

   It is unlikely that option (d) will be economically viable, and option (a) is improbable because once the capital for the wave devices is committed, and plant maintenance costs may be less related to the period of electrical output accepted than to the duration for which the devices are on location (or exposed to storms), it will be preferable to use the output for some purpose. The distinction between options (b) and (c) depends upon the fuel costs applying at any time as well as upon the levels of large thermal, and especially nuclear, planting and the pumped-storage capacity available; this will determine which course is best followed. An evaluation based simply on 'coal equivalent saved' may be preferable in the present circumstances, though the timescale for development of wave energy to the 'power station' scale may make this inappropriate.

5. The value of wave energy depends in part on the number of electrical units supplied per annum, and also on the certainty with which units will become available at any time of the day. Clearly there is an important statistical exercise to be done here that will need to call upon both real and hindcast wave data for a period of at least 10 years.

6. The output level of each wave energy device depends both on the efficiency with which the sensor responds to each incident level of sea energy (bearing in mind also the relative orientation of energy spectrum and device axis, the short-crestedness of the waves, currents, etc), and any internal restraints that may, for mechanical and safety reasons, need to be applied to its motion. For example, to design the power takeoff arrangements to accept a proportion of an incident energy level of 50 kW/m (the proportion being related to the conversion efficiency of the device in those waves) gives a system that will operate at an output level no higher than this for a large part of a year (20% of all waves in Fig. 7.5 are higher than 3.5m or about 65 kW/m). As long as the absolute level of the output from the device in higher waves is not less than this design value, it remains to be decided whether provision should be made for it to be more. Depending on the device in question, it may be possible to limit its motion and/or build in energy absorbers to ensure that the power takeoff system is not exposed to (i.e. has to be designed for) much higher throughput levels. In practice it will almost certainly be necessary to seek a compromise between absorbing all and none of the incident energy above a 'design' threshold. There are various possible mechanisms for 'shedding' excess inputs, which in the case of extreme energy levels will be economically preferable to attempting to capture these (20% of the energy from waves for which H_s = 8m, T_e = 12 seconds still gives nearly 4 MW from a 50m cylinder). Quite apart from the physical problem of achieving more, the arrival of such 'spikes' into the grid is unlikely to be matched by similarly high economic values, i.e. their value to the grid would be either very small or zero. The most economic arrangement for transmitted energy levels above the design threshold of, say, 2 GW will, as before, depend on the persistence of these levels and the ease with which they can be integrated into the grid alongside all other plant then preferably in use. For example, Fig. 7.5 shows that only 7.25% of waves have H_s > 5m (135 kW/m), and only 3% lie above 6m (200 kW/m). Absorbing up to 1/2 and 1/3 respectively of these levels into the power chain leading to the power takeoff

system is probably ample, if not too much. For the purposes of energy calculations, if these levels were both taken as 50 kW/m, the energy output would be underestimated by less than 2%. This is small enough to be ignored.

7. The rates of capital investment in wave energy plant and return on that investment will be important to determining the viability of the source. There appear to be two relevant limits here:

   (a) What minimum transmission capacity that must be installed to convey plant output to the main grid? This may not have to be up to the full 2 GW power level, but will probably be a substantial proportion of it (minimum number of lines in a multiple line connection).

   (b) The generating plant will probably comprise a number of device units, the outputs from which will be brought together to, say, a convertor/turbine of capacity, say, 250 MW.

   It will be necessary to expend the capital needed to establish a coherent device/transmission system before any return on capital is possible, and the size of this may at minimum be 200 MW of plant at sea and 1000 MW transmission capacity. This suggests the need for a major construction programme once a system has been adequately proven at the scale of, perhaps, 20 MW, this to involve a series of full size units supplying a converter station of corresponding capacity and on-shore load (e.g. displacing local oil-fired plant during the experimental period when the level of incident wave energy is sufficient). Some first estimates of initial capital costs for a 200 MW station plus transmission are given in Section 7.2.

8. It may be possible to generate from this 'minimum' installation when the transmission system, converter station (for 200 MW) and several wave energy devices are coupled up, though it is premature to estimate what the installed capacity would then be. It could, perhaps, initially involve no more than completing the transmission when the pilot 20 MW scheme is well proven, to absorb this output (though the 'locals' may by then have come to like saving oil).

9. The maintenance/replacement/outage costs for wave energy devices could clearly be severe, which suggests the preference for fully separate modular devices supplying a collecting main (electricity, high pressure oil or seawater) from which each may be disconnected at any time without jeopardising the performance of any others similarly connected. Servicing under winter conditions might almost be ruled out as impossible, though it may well be necessary to have stand-by arrangements in case on-site works are unavoidable. The cost of providing and using these will be high. Thus although the 'fuel' is free, the annual running cost of the station could be much higher than for thermal plant, fuel costs excluded. This aspect of system cost evaluation must not be overlooked. However, while it will be difficult to do this in advance of testing full scale units in full scale seas, it would be philosophically wrong to assume the need for a major back-up maintenance effort in support of a wave energy station, which will persist as a heavy drain on revenue. While the alternative of seeking a foolproof design may demand that capital expenditure is pitched at such a high level as to make wave energy unreasonably expensive on capital considerations alone, such an attitude is also applied to nuclear power stations with considerable financial success.

A.2 The Nature of Wave Energy

Figs. A.3a-c show the mean 3-hourly values of H_s through 1977 at S.Uist. The record is characterised by relatively short periods of high waves and longer periods of low waves, especially in the period June-September inclusive (the record for February is unusually low for that time of year). Figs. A.4-A.6 show some characteristics of this sequence. Clearly the peak values occur over relatively short periods, and the rates of increase in H_s, averaged over 6 hours, are often about twice as great as the subsequent rates of decay. From Section 7.3, however, these extreme levels coincide with lower capture efficiency, and their likelihood of recurrence is small (Fig. A.7).

In energy terms, the 'average H_s' values shown in Fig. A.7 represent much lower levels of output than are available from higher waves, so that even though the latter occur much less frequently (H_s < 3m for about 70% of the year - Fig.A.7), their energy contribution is important up to $H_s \simeq$ 6m - Fig.A.8 (20% of annual energy lies above this value).

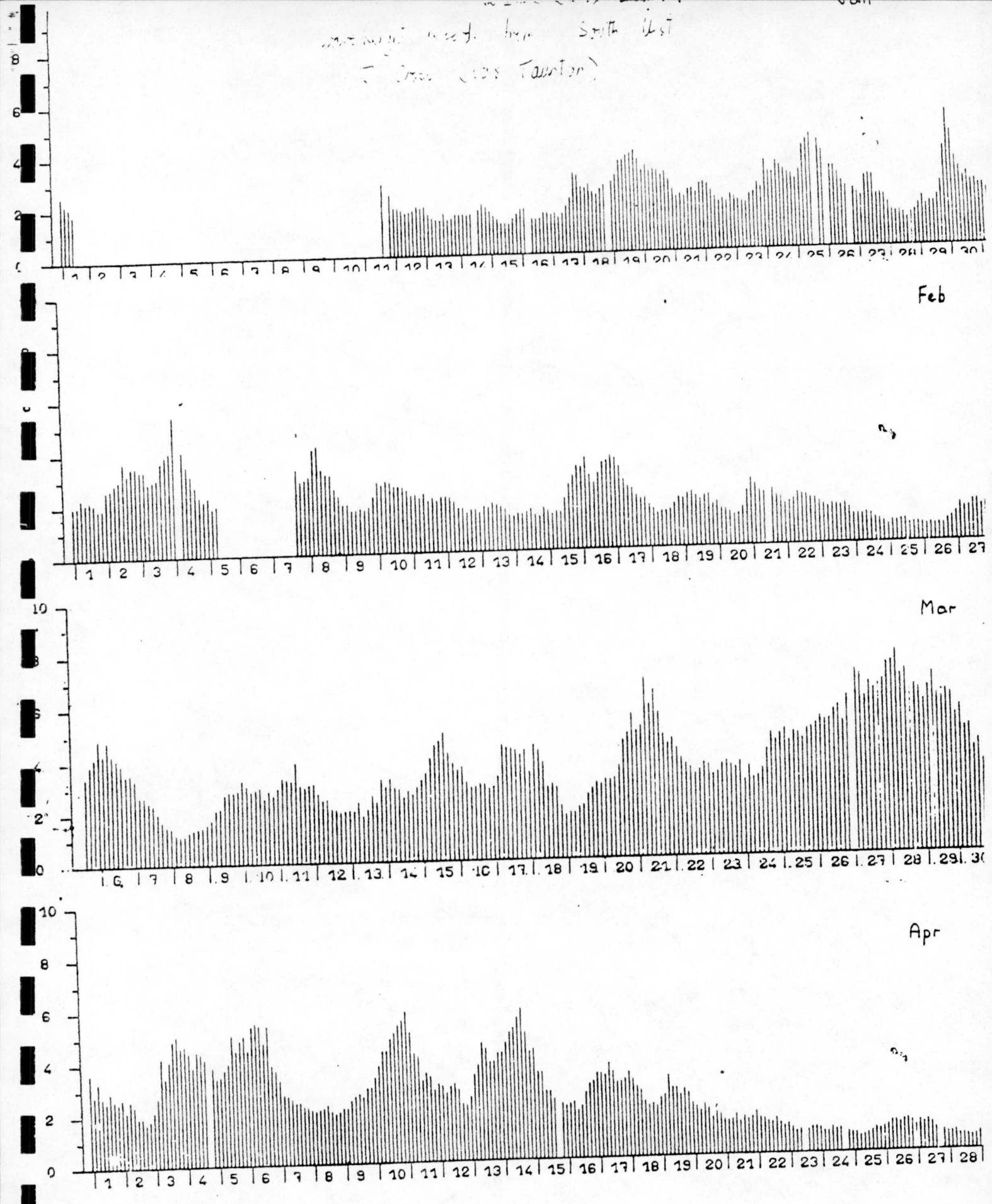

SOUTH UIST WAVERIDER

YEAR NO. 76 MONTH NO. 4 HS(METRES)

FIG. A.3a

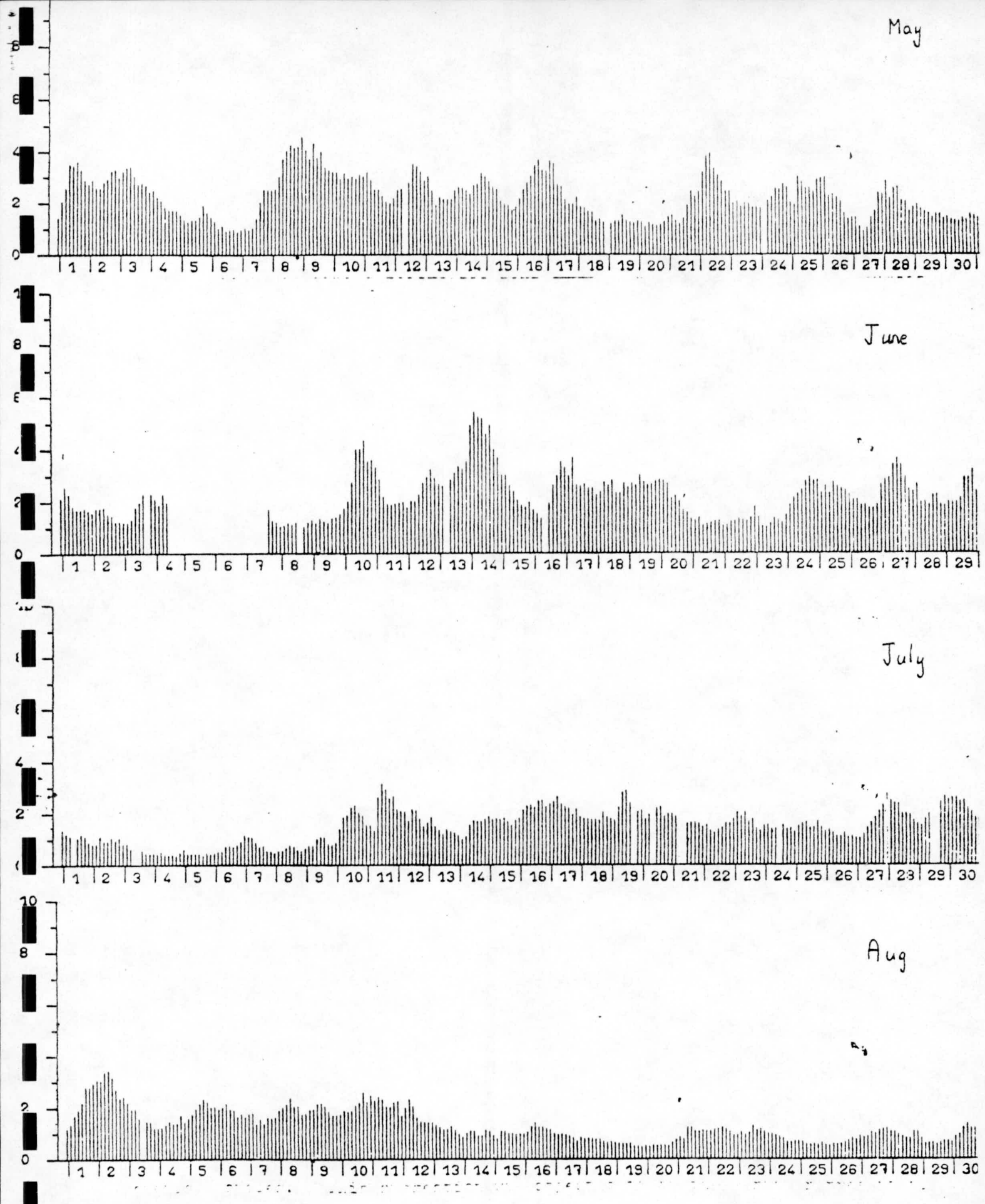

FIG. A.3b

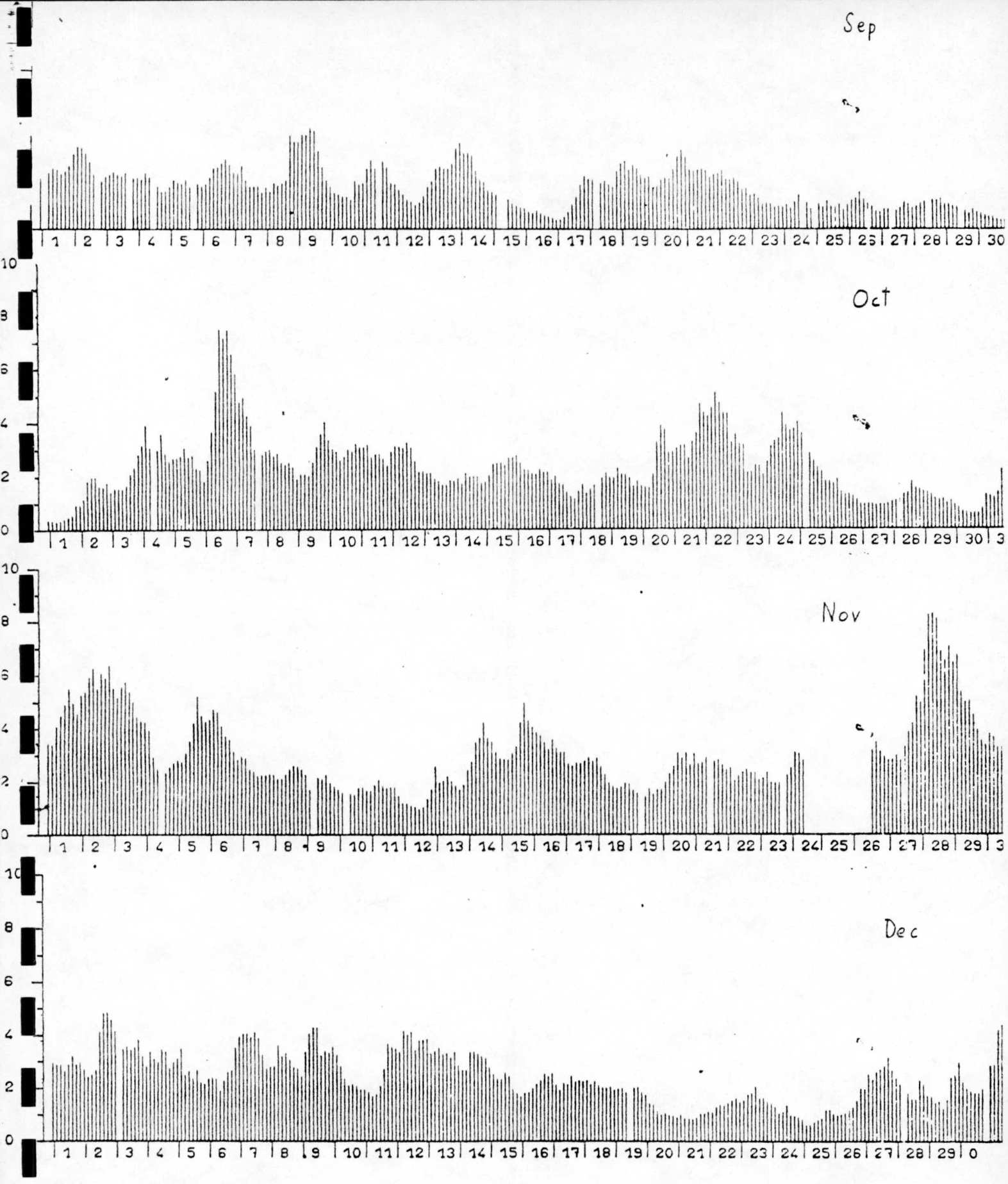

SOUTH UIST WAVERIDER

YEAR NO. 76 MONTH NO. 12 HS(METRES)

FIG. A.3c

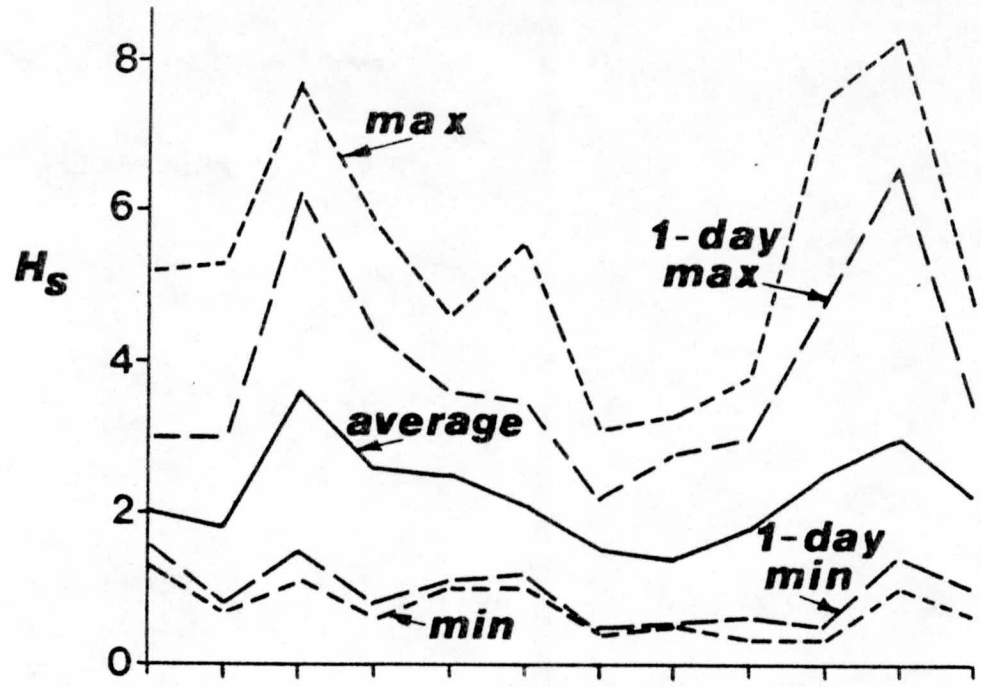

FIG. A.4

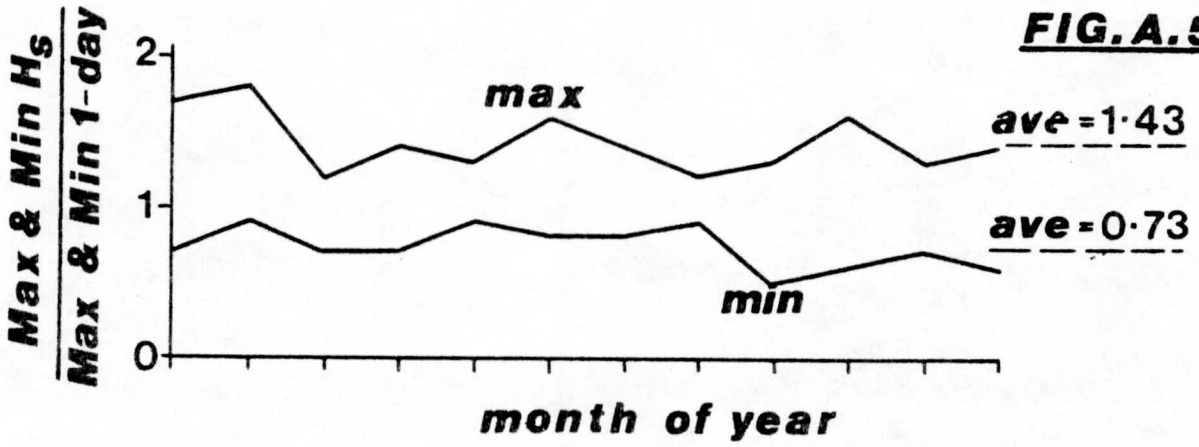

FIG. A.5

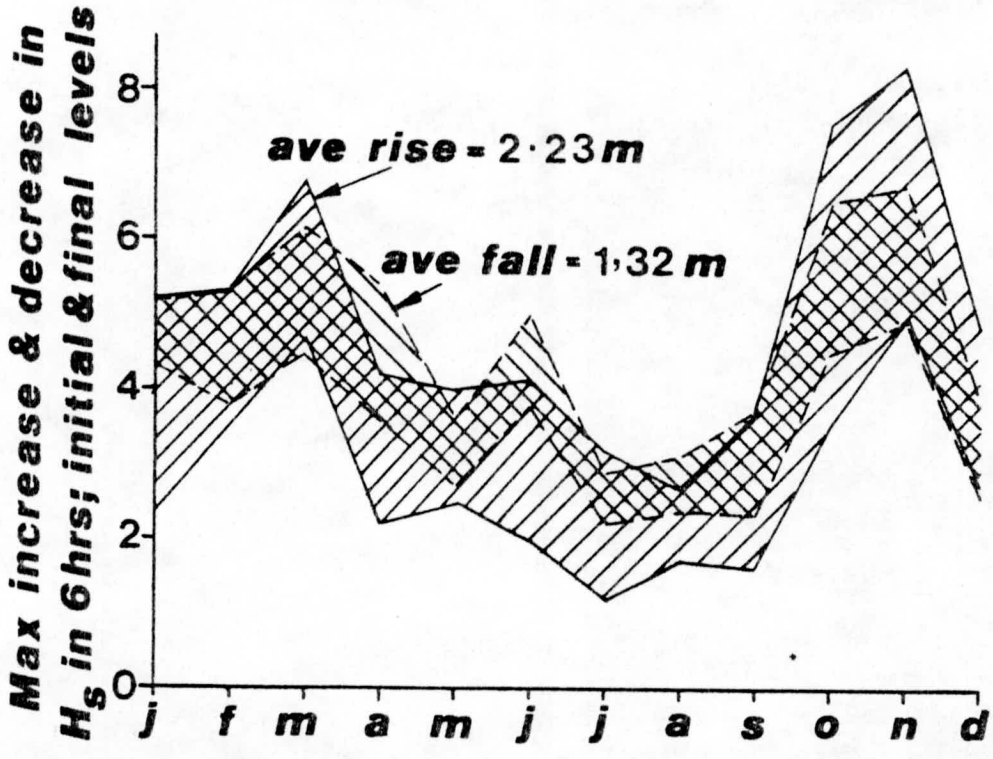

FIG. A.6

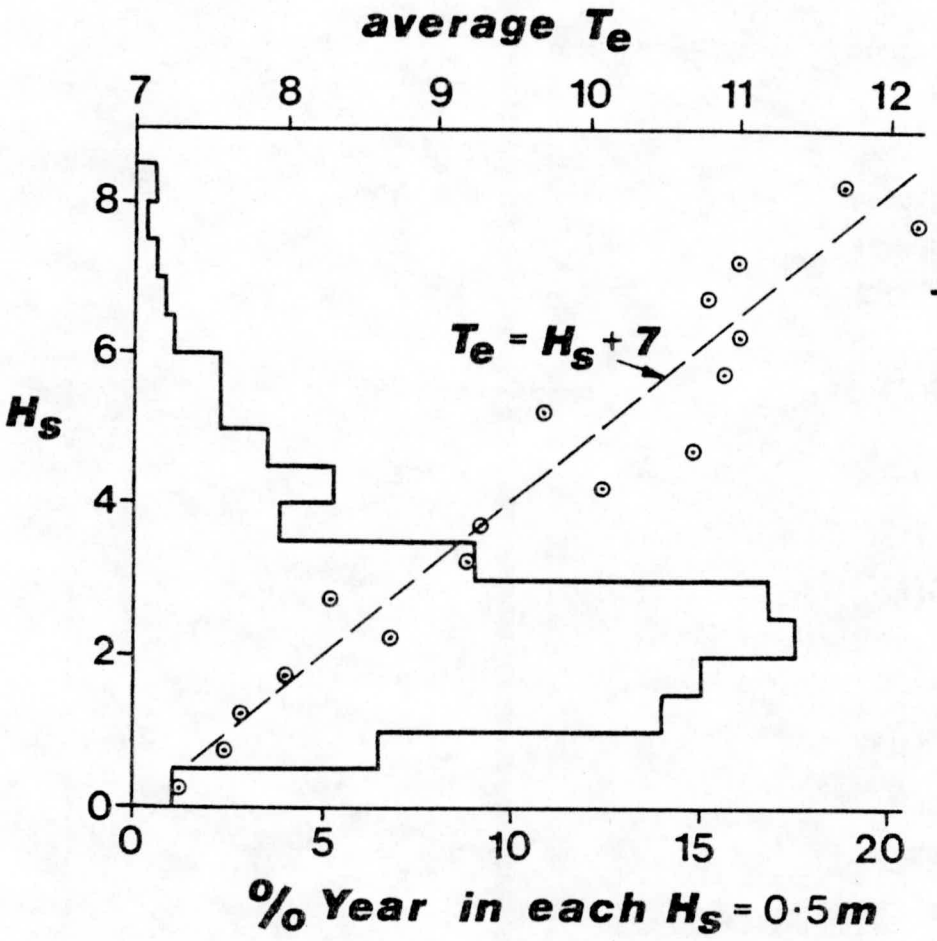
average T_e
7
8
9
10
11
12
8
6
4
2
0
H_s
$T_e = H_s + 7$
0
5
10
15
20
% Year in each H_s = 0·5 m

FIG. A.7

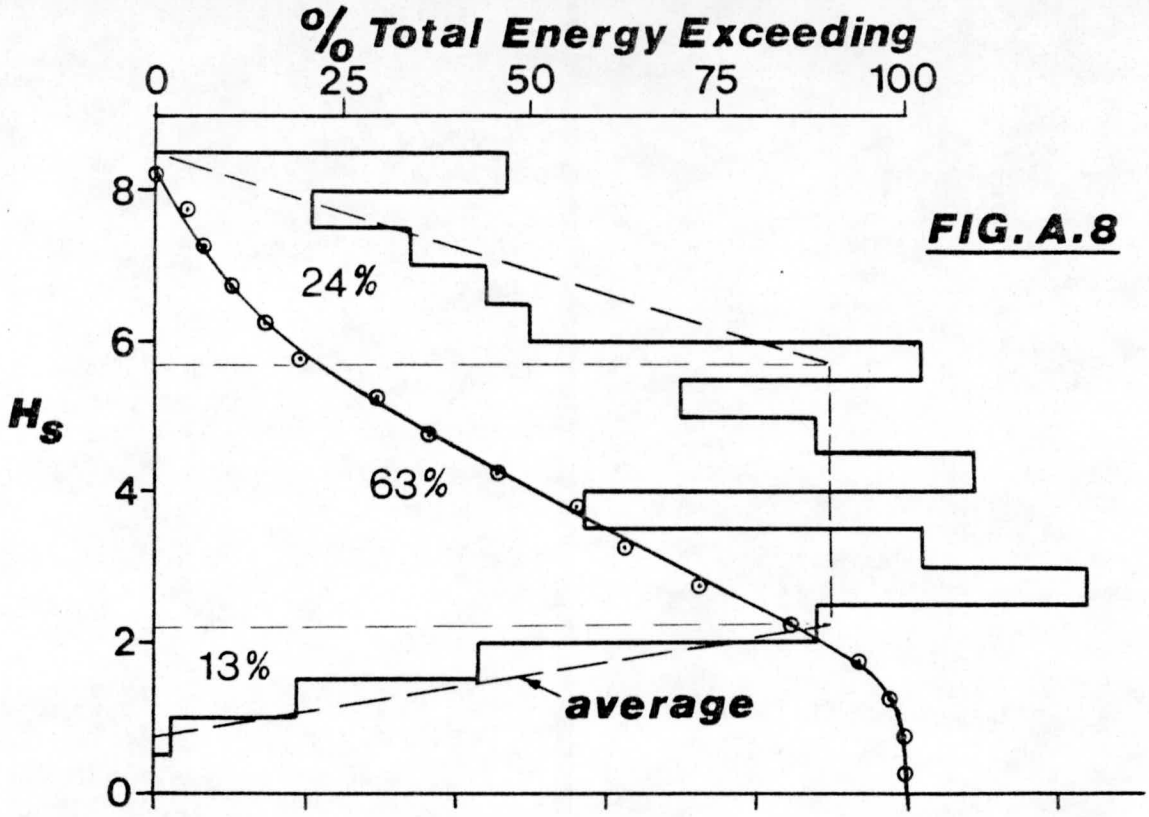
% Total Energy Exceeding
0
25
50
75
100
8
6
4
2
0
H_s
24%
63%
13%
average

FIG. A.8

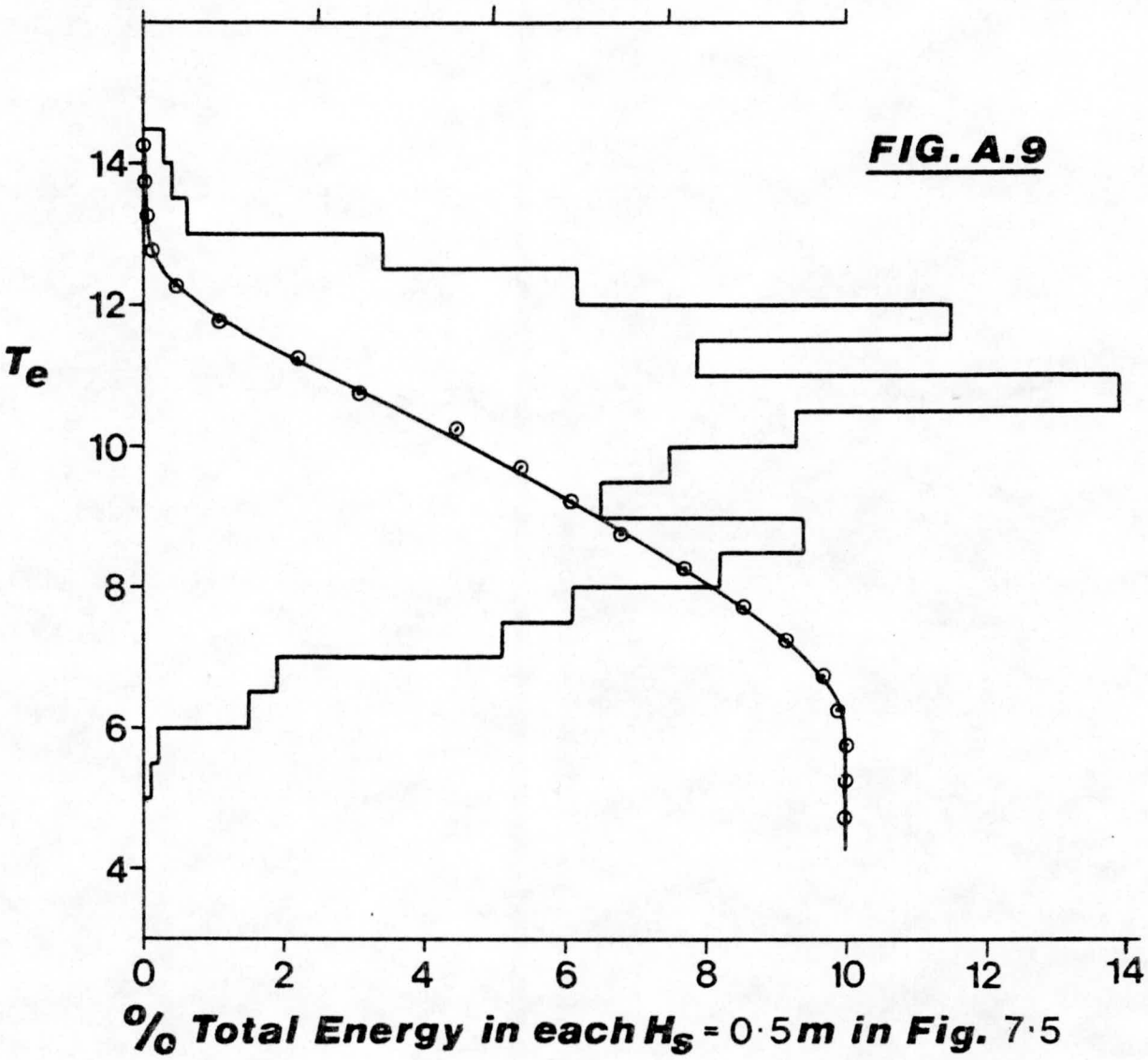
14
12
10
8
6
4
T_e
0
2
4
6
8
10
12
14
% Total Energy in each H_s = 0·5m in Fig. 7·5

FIG. A.9

Fig. A.9 interprets the S. Uist spectrum in a similar way to Fig.A.8, reflecting the approximate relationship between H_s and T_e shown in Fig.A.7. (Most of the energy at any level of H_s lies within ± 1.5 seconds of this relationship).

Wave energy therefore has two principal features:

1. A 'background' level, which in any month can be expected to persist through much of that month;

2. A variation, that at times will lead to much lower energy levels for a few successive days, and at times much more though for shorter periods. However, all but the extreme peaks extend over periods of more than about 12 hours (Fig.A.6).

A.3 Value of Wave Energy

It is generally felt that the value of each unit of electricity generated by a non-nuclear source depends on the proportion of all electricity supplied by nuclear plant at that time. It is strongly held in many quarters that this proportion must increase substantially over the next two decades, corresponding to the period during which wave energy devices may also be installed. In this case, the value of wave energy will depend on its usefulness alongside a preponderance of nuclear plant.

Fig. A.1 shows that the daily period of higher electrical demand extends over about 12-14 hours, whereas low demand covers about 6-8 hours. It is presumably the case that variations in wave climate do not relate to the time of day. Hence throughout each day, the 'background' output of the wave power station would act as quasi-base load plant, with higher level by winter than summer (Fig. A.4), though strictly speaking only 'firm' at a very low output level. The bulk of the output would correspond to the timescale of one or more days, during which time it would also be 'firm'. Because these periods can be predicted one or more days in advance of their occurrence, standby plant of equivalent capacity would not have to be maintained on short-term readiness.

Substantial fuel saving would therefore occur, especially during the daytime period (about 60% of the day). The base load saving is additional to this, though its energy content is less. By 1979 values, the return from this resource will probably lie in the range 2-2.5 p/kWh for the daytime 60% of output.

At night the resource would be more valuable in a coal-based network, when its output would displace this plant (as in the daytime, even in a nuclear-based system). If nuclear plant occupies the base load zone, it may be more prudent to store the wave energy generated at night if this can be released during the day in such a way as to displace the need for a capital (and fuel) commitment on equivalent thermal plant.

If a high value for wave energy is to be achieved, it is important to transfer the output at night into the daytime period. Depending on how this can be done, it seems possible that, in current terms, the average value of wave energy will exceed 2p/kWh.

REFERENCES

1. Ogilvie, T.F., 1963, J. Fluid Mechanics, 16, 451.
(see also Evans, D.V., 1976, J. Fluid Mechanics, 77, 1-25.

2. Crabb, J.A., 1979, "South Uist Wave Climate - a Summary of Recent Results", WESC(79) DA 89.

ACKNOWLEDGEMENTS

We have appreciated the continuing guidance of Mr. Malcolm Cloke and his colleagues at ETSU throughout the study.

We wish to record the importance to our findings of funding from the Marine Technology Directorate of the Science Research Council for fundamental studies of the submerged cylinder device at the University of Bristol, under the supervision of Dr. David Evans. The help of Mr. John Davis and Mr. Richard Finney, who are supported by their SRC grant, has emphasised the mutual value of collaboration in this way.